TECHNISCHE UNIVERSITÄT MÜNCHEN

Chirurgische Klinik und Poliklinik des Klinikums rechts der Isar

Functional relevance of the extracellular matrix protein Periostin in pancreatitis, pancreatic carcinogenesis and metastatic spread

Simone Christine Hausmann

Vollständiger Abdruck der von der Fakultät für Medizin der Technischen Universität München zur Erlangung des akademischen Grades eines

Doktors der Naturwissenschaften

genehmigten Dissertation.

Vorsitzender: Univ.-Prof. Dr. Radu Roland Rad

Prüfer der Dissertation: 1. apl. Prof. Dr. Jörg Hermann Kleeff

2. Univ.-Prof. Dr. Bernhard Küster

Die Dissertation wurde am 30.07.2015 bei der Technischen Universität München eingereicht und durch die Fakultät für Medizin am 16.12.2015 angenommen.

To my family

Zusammenfassung

In dieser Arbeit wurde die Funktion des extrazellulären Matrix Proteins Periostin während akuter Pankreatitis und nachfolgender Geweberegeneration sowie in der Pankreaskrebsentstehung und Metastasierung untersucht. Das exokrine Pankreas, welches hauptsächlich aus α-Amylase produzierenden Azinuszellen besteht, weist nach einer akuten Pankreatitis eine enorme Regenerationsfähigkeit auf. Dabei transdifferenzieren die Azinuszellen vorübergehend in duktal-ähnliche Strukturen und exprimieren pankreatische Progenitormarker um Zellproliferation zu induzieren. Auf diese Weise kann das geschädigte Gewebe ersetzt und die Organintegrität wiederhergestellt werden. Während gezeigt werden konnte, dass intrinsische Faktoren eine wichtige Rolle in der korrekten Ausführung des Regenerationsprogramms spielen, wurde der Einfluss von extrazellulären Matrixproteinen in dieser Hinsicht bisher noch nicht untersucht. Daten dieser Studie konnten zeigen, dass der Verlust von Periostin keine Auswirkung auf den Schweregrad der Pankreatitis hat, jedoch die nachfolgende Regeneration des exokrinen Pankreas stark beeinflusst. Das Fehlen von Periostin führte zu einer beeinträchtigten Regeneration, was sich durch eine anhaltende Entzündung des Gewebes sowie durch Pankreasatrophie und einer Differenzierung von Azinuszellen zu Adipozyten bemerkbar machte. Zudem wiesen Periostin defiziente Mäuse eine signifikant erhöhte Expression von Progenitorgenen auf wobei gleichzeitig die Expression von Differenzierungsgenen stark vermindert war. Dies deutet darauf hin, dass der Verlust von Periostin Azinuszellen in einem undifferenzierten Zellstatus hält. Zusammengefasst, weisen die Ergebnisse des ersten Teils dieser Arbeit darauf hin, dass die Kommunikation zwischen epithelialen und mesenchymalen Zellen unabdingbar für eine erfolgreiche Regeneration des exokrinen Pankreas ist.

Im zweiten Teil dieser Arbeit konnte gezeigt werden, dass Periostin und nachgeschaltete Signalwege die Tumorentstehung und Metastasierung begünstigen. *In vitro* Experimente belegten, dass Periostin die Transformation von Zellen fördert und das invasive Verhalten von Pankreaskrebszellen erhöht. Mit Hilfe eines genetisch veränderten Mausmodells des duktalen Pankreasadenokarzinoms mit zusätzlicher Deletion von Periostin konnte die Tumor-fördernde Rolle dieses ECM Proteins bestätigt werden. In frühen Stadien der Krebsentstehung, wiesen Periostin defiziente Mäuse weniger Vorläuferläsionen sowie weniger proliferierende Zellen und einen geringeren Grad an Metaplasie auf. Experimente, welche die Metastasierung untersuchten offenbarten, dass Periostin essentiell für das Überleben und die Proliferation von Krebszellen im Sekundärorgan ist. Zusätzlich konnte gezeigt werden, dass die Inhibierung des nachgeschalteten Signalwegs Periostins, durch die Verwendung eines Inhibitors der fokalen Adhäsionskinase, das Überleben von Pankreaskrebsmäusen signifikant verlängern und die Metastasenbildung in der Lunge signifikant reduzieren konnte. Somit zeigen diese Daten, dass Periostin eine Tumor-

fördernde Rolle in der Pankreaskrebsentstehung spielt, was durch die Aktivierung des Integrin-Signalweges vermittelt wird. Darüber hinaus, unterstützt Periostin die Metastasenbildung durch die Ausbildung einer Tumor-freundlichen Umgebung im Sekundärorgan, welche das Überleben und Wachstum von Pankreaskrebszellen fördert. Der Einsatz von FAK Inhibitoren stellt deshalb einen vielversprechenden Ansatz dar die Pankreaskrebsentstehung sowie Metastasierung zu inhibieren.

Parts of this thesis were submitted for publication:

Hausmann S., Regel I., Steiger K., Wagner N., Thorwirth M., Schlitter AM., Esposito I., Michalski CW., Friess H., Kleeff J., Erkan M. *Loss of Periostin results in impaired regeneration and pancreatic atrophy after cerulein-induced pancreatitis.* Am J Pathol. 2016 Jan;186(1):24-31.

Table of contents

List of abbreviations

ACC	Acinar cell carcinoma
ADM	Acinar-to ductal metaplasia
AFL	Atypical flat lesion
AKT → *PKB*	Protein kinase B
APS	Ammonium persulfate
ASI	Activated stroma index
α-Sma	α-smooth muscle actin
bp(s)	Base pair(s)
BMP	Bone morphogenetic protein
BrdU	5-bromo-2'-deoxyuridine
BSA	Bovine serum albumin
bw	Body weight
CCK	Cholecystokinin
CK19	Cytokeratin 19
CP	Chronic pancreatitis
CT	Computer tomography
CTGF	Connective tissue growth factor
D	Days
Da	Dalton
DAB	3,3'-diaminpbenzidine
DAPI	4',6'-Diamidino-2-phenylindole
ddH_2O	Double distilled water
DMEM	Dulbecco's Modified Eagle's Medium
DMSO	Dimethylsulfoxid
DNA	Desoxyribonucleic acid
dNTP	Desoxyribonucleosidtriphosphate
DPC4	Deleted in pancreatic cancer 4
DTT	Dithiothreitol
E-cadherin	Epithelial-Cadherin
E.coli	Escherichia coli
ECM	Extracellular Matrix
EDTA	Ethylenediaminetetraacetic acid
EMI	EMILIN family
EMT	Epithelial-mesenchymal transition
ERK	Extracellular signal-regulated kinase

FAK	Focal adhesion kinase
FAKi	Focal adhesion kinase inhibitor
FBS	Fetal bovine serum
GAPDH	Glyceraldehyde 3-phosphate dehydrogenase
GAP	GTPase activating protein
GDP	Guanosine diphosphate
GEF	Guanine nucleotide exchange factor
GEMM	Genetically engineered mouse model
GTP	Guanosine-5’-triphosphate
H	Hour
Hes1	Hes family bHLH transcription factor 1
IHC	Immunohistochemistry
IL	Interleukin
IPMN	Intraductal papillary mucinous neoplasm
kDa	Kilo Dalton
MAPK	Mitogen-activated protein kinase
MCN	Mucinous cystic neoplasm
mg	Milligram
min	Minute
ml	Milliliter
Mist1	Basic helix-loop-helix family, member a15
MRT	Magnetic resonance tomography
MTC	Mucin producing ductal structure
MUC5AC	Mucin 5AC
NaCl	Sodium chloride
NaF	Sodium fluoride
NaOH	Sodium hydroxide
$Na_4P_2O_7$	Sodium pyrophosphate
nM	Nanomolar
nm	Nanometer
NP-40	Nonidet™ P40
Na_3VO_4	Sodium orthovanadate
OSF-2	Osteoblast specific factor-2
PanIN	Pancreatic intraepithelial neoplasia
PBS	Phosphate buffered saline
PCR	Polymerase chain reaction
PDAC	Pancreatic ductal adenocarcinoma

Pdx1	Pancreatic and duodenal homeobox 1
Pen	Penicillin
PFA	Paraformaldehyde
PKB	Protein kinase B
PMSF	Phenylmethanesulfonylfluoride
PNET	Pancreatic neuroendocrine tumor
Postn	Periostin
Pparγ	Peroxisome proliferator-activated receptor gamma
Ppib	Peptidylprolyl isomerase B
PSC	Pancreatic stellate cell
Rb	Retinobblastoma
Rbpjl	Recombination signal binding protein for immunoglobulin kappa J region-like
Rcf	Relative centrifugal force
RNA	Ribonucleic acid
rpm	Rounds per minute
RPMI-1640	Roswell Park Memorial Institute-1640 Medium
SDS	Sodium dodecyl sulfate
SEM	Standard error of the mean
Smad	Sma-and Mad-related protein
Sox9	Sry (sex determining region Y)-box 9
SPARC	Secreted protein acidic and rich in cysteine
Strep	Streptomycin
TBS	Tris-buffered saline
TBS-T	Tris-buffered saline with Tween-20
TC	Tubular complexes
TM	Melting Temperature
TP53	Tumor protein p53
U	Unit
V	Volt
VEGF	Vascular endothelial growth factor
WT	Wild type
5-FU	5-fluorourcil

Introduction

1.1 The pancreas

1.1.1 Anatomy and physiology

The pancreas is located in the abdominal cavity between the duodenum and the spleen (Figure 1.1 A) and consists of two compartments that differ morphologically and functionally. The exocrine compartment is comprised of acinar cells and ductal epithelium and constitutes up to 90% of the pancreas (Swift et al. 1998). Acinar cells, which are organized in grape-like clusters called acini, are located at the end of the duct and produce and secrete digestive enzymes such as α-Amylase and lipases (Figure 1.1 C). The ductal epithelium secretes bicarbonate and mucins and transports the digestive enzymes from the acini in this bicarbonate-rich fluid to the duodenum (Edlund 2002, Pan and Wright 2011). The endocrine compartment makes up only 1-2% of the pancreas and consists of five different cell types that are located in the islets of Langerhans: the glucagon secreting α-cells, the insulin producing β-cells, the somatostatin expressing δ-cells, the ghrelin releasing ε-cells and the pancreatic polypeptide secreting PP-cells (Figure 1.1 D). Once released these hormones play an important role in regulating blood glucose homeostasis and energy metabolism (Cano, Hebrok, and Zenker 2007, Edlund 2002, Pan and Wright 2011).

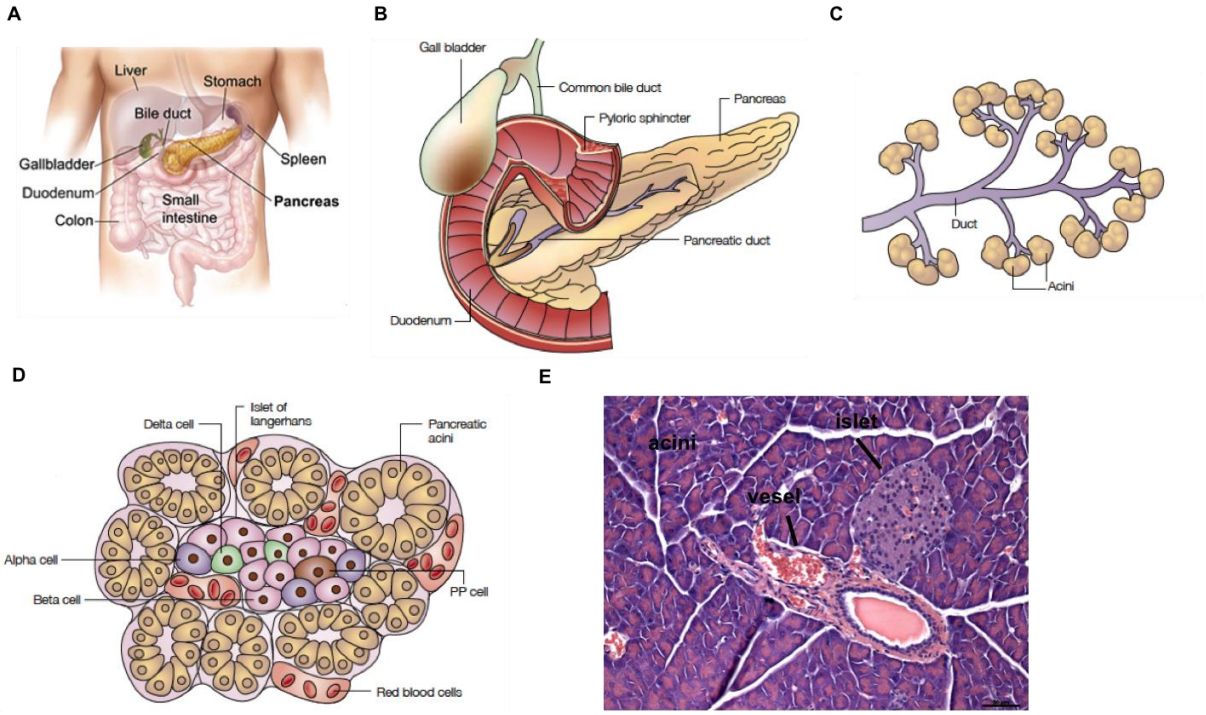

Figure 1.1: Localization and morphology of the pancreas. A) Localization of the pancreas in the human body (National Cancer Institute). **B)** Gross anatomy of the pancreas (adapted from Bardeesy 2002). **C)** Acini organized in grape-like structures. **D)** Different pancreatic endocrine cell types (adapted from Bardeesy 2002 (Bardeesy and DePinho 2002)). **E)** Microscopic structure of a murine wild type pancreas.

1.1.2 Development of the pancreas

The pancreas arises from a dorsal and ventral protrusion of the gut endoderm in vertebrates (Edlund 2002). Morphologically obvious becomes the development of the pancreas on embryonic day (E) 8.75 in mice because that is when the epithelial buds are formed independently in different locations in the foregut endoderm (Figure 1.2). During the following branching morphogenesis process, the cells of the pancreatic buds show a strong proliferation leading to an increase of size and a simultaneously change in shape evident by the formation of branched tubular structures and finally fusion of the buds at E12.5 (Shih, Wang, and Sander 2013). This phase, which is referred to as 'primary transition phase' occurs until E12.5 and is characterized by the expression of the key transcription factors pancreatic and duodenal homeobox 1 (Pdx1; E8.5), pancreas specific transcription factor 1a (Ptf1a; E9.5), hes family bHLH transcription factor 1 (Hes1; E9.5), hepatocyte nuclear factor 1-alpha (Hnf1a; E8.0), neurogenin 3 (Ngn3; E9.5) and sex determining region Y-box 9 (Sox9; E9.0) by most of the progenitor cells. Additionally, signaling molecules are secreted by the mesoderm such as members of the Wnt, Hedgehog and Notch pathway as well as the growth factors bone morphogenetic protein and fibroblast growth factor (Cano, Hebrok, and Zenker 2007, Pan and Wright 2011). However, the pancreas is not differentiated yet and mesenchymal cells surround the pancreatic epithelium (Shih, Wang, and Sander 2013). The 'secondary transition phase' ranging from E12.5 until birth is characterized by further branching and development of a complex tubular network as well as differentiation into the three major pancreatic cells, acinar, ductal and endocrine cells, at E13.5. However, coalescence of endocrine cells and maturation of islets does not occur until after birth (Cano, Hebrok, and Zenker 2007, Pan and Wright 2011).

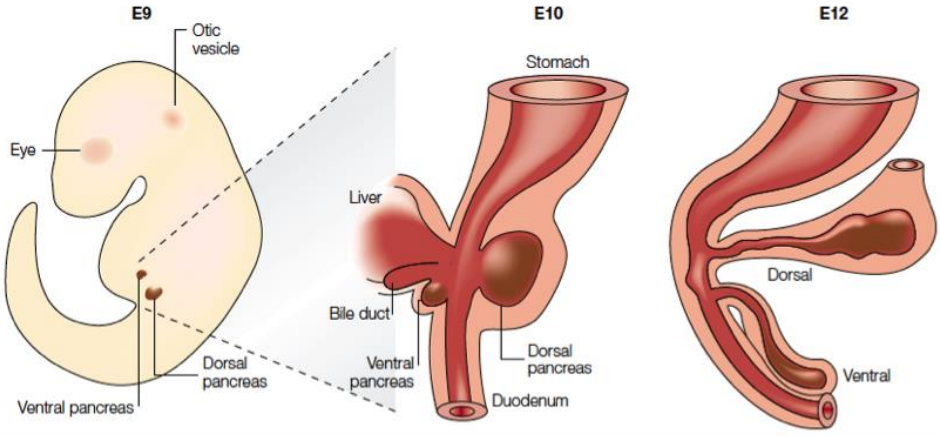

Figure 1.2 Schematic representation of the pancreas development at embryonic day (E)9, E10 and E12 (adapted from (Edlund 2002)).

1.2 Acute and chronic pancreatitis

The pancreas can suffer from two different forms of exocrine inflammation. The acute pancreatitis occurs suddenly and when treated only for a few days with subsequent complete regeneration of the pancreas. Whereas chronic pancreatitis persists for a longer period of time, usually even years, and creates permanent damage of the pancreas.

1.2.1 Acute pancreatitis

The acute pancreatitis is an inflammatory disease of the exocrine compartment of the pancreas, which occurs mainly due to obstruction of the distal bile-pancreatic duct by gallstones. The obstruction elevates the duct pressure resulting in activation of trypsinogen into active trypsin and consecutively activation of other digestive enzymes, which as a consequence leads to autodigestion and inflammation of the pancreas (Wang et al. 2009, Frossard, Steer, and Pastor 2008). Another common risk factor causing acute pancreatitis is increased alcohol abuse whereas metabolic diseases, autoimmune pancreatitis and drug-induced pancreatitis are rather scarce. In most of the cases the pancreatitis resolves and the patients do not have any complications. However, in around 20% of cases the pancreatitis can lead to serious consequences including organ failure and mortality (Lund et al. 2006). Currently, there are different models to study acute pancreatitis in mice. The most common experimental model is the caerulein-based acute pancreatitis model in which pancreatitis is induced in mice by hourly repetitive intraperitoneal injections of the cholecystokinin (CCK) analogue caerulein at supraphysiological doses (50 µg/kg body weight to 100 µg/kg body weight). Through binding of caerulein to the high affinity CCK receptor zymogen granules are released in vesicles and digestive enzymes are secreted. As soon as the high affinity CCK receptors are saturated caerulein binds to the low affinity CCK receptor that leads to an inhibition of exocytosis of the zymogen granules. As a consequence digestive enzymes accumulate within acinar cells resulting in a severe damage of the exocrine compartment. Islets and ducts however are not affected (Hyun and Lee 2014). In acute pancreatitis the caerulein-induced damages of the exocrine compartment are reversible upon withdrawal of caerulein administration.

1.2.2 Chronic pancreatitis

Chronic pancreatitis (CP) is an irreversible inflammation of the exocrine compartment of the pancreas that is accompanied with morphological changes such as abundant fibrosis and eventually loss of endocrine and exocrine function of the pancreas and development of diabetes. In the western world chronic pancreatitis is most commonly associated with elevated alcohol abuse (Witt et al. 2007). Though, cystic fibrosis, autoimmune diseases, hyperglycemia and hyperlipidemia are also established but rather rare risk factors for

developing chronic pancreatitis (Etemad and Whitcomb 2001, Ahmed et al. 2006). In a minority of patients diagnosed with CP no underlying cause can be identified and therefore the pancreatitis is classified as idiopathic pancreatitis. A major morphological feature of CP is a strong desmoplastic reaction characterized by an excessive production of extracellular matrix (ECM) proteins and pancreatic stellate cell (PSC) activation. In response to cytokines released by damaged acinar cells and infiltrated immune cells, PSCs get activated, proliferate exponentially and produce an abundant amount of ECM proteins that replace the pancreatic parenchyma and consequently lead to pancreas insufficiency (Apte et al. 1999, Michalski et al. 2007). The therapy options for CP are still only symptomatic and aim at relieving pain and treating pancreas insufficiency by the administration of digestive enzymes or by insulin injections when diabetes has developed (Witt et al. 2007). Chronic pancreatitis has also been described as a strong risk factor for developing pancreatic cancer. However, only a small subset of chronic pancreatitis patients (5% of patients) develops pancreatic cancer (Raimondi et al. 2010). To study CP into more detail, different experimental models of chronic pancreatitis have been established. Apart from genetic models using among others SPINK3-deficient (Ohmuraya et al. 2006) or CFTR-deficient mice (Snouwaert et al. 1992) there are caerulein-induced pancreatitis models inducing CP by repetitive caerulein injections over several weeks (Neuschwander-Tetri et al. 2000) and experimental models using combinations of caerulein-induced pancreatitis with other agents such as ethanol and cyclosporine (Gukovsky et al. 2008). Additionally, pancreatic duct ligation can be performed to recapitulate duct obstruction in mice. In this model the pancreatic duct from the splenic lobe is ligated and mice show a strong inflammatory stromal response (Watanabe et al. 1995).

1.3 Pancreatic cancer

Pancreatic cancers are neoplasms of the pancreas, which can arise from the exocrine as well as the endocrine compartment. Exocrine cancers account for 95% of all pancreatic cancers with pancreatic ductal adenocarcinoma (PDAC) being the most common type (Li et al. 2004). Other exocrine pancreatic cancers include acinar cell carcinoma (ACC), intraductal papillary mucinous neoplasm and mucinous cystadenocarcinoma. Cancers developing from endocrine cells are very rare and only make up for around 5% of all pancreatic cancers. In the following the most common pancreatic cancers will be described.

1.3.1 Pancreatic ductal adenocarcinoma (PDAC)

Pancreatic ductal adenocarcinoma is the fourth leading cause of cancer-related deaths in the United States both in men and women with an incidence rate (48,960 new estimated cases) almost equaling its mortality rate (40,560 estimated deaths). The median survival is only 4- 6 months and despite intensive research using animal models and developing targeted therapies the five-year survival rate of only 7% has not been dramatically improved over the last 30 years (Siegel, Miller, and Jemal 2015). The main problems contributing to this poor survival are the lack of early detection methods and absence of therapy options. Most patients present already at advanced stages of pancreatic cancer when the tumor cannot be removed by surgical means and often metastases to distant organs have already occurred. Histologically, most PDACs are well-differentiated, highly infiltrative cancers with neoplastic cells forming glands. Additionally, PDAC is characterized by an excessive fibrotic reaction consisting of stromal, endothelial, nerve and inflammatory cells, called desmoplasia (Maitra and Hruban 2008).

The etiology for developing pancreatic cancer has not been elucidated yet. However, so far different risk factors have been identified. Around 10% of pancreatic cancers have a familial basis and the risk of developing PDAC for people having a first-degree relative suffering from pancreatic cancer is 2.3-fold elevated (Shi, Hruban, and Klein 2009, Amundadottir et al. 2004). Tobacco use has been shown to increase the risk of developing pancreatic cancer up to 3.6-fold (Hassan et al. 2007) and multiple studies are demonstrating that next to chronic pancreatitis an advanced age, obesity, as well as diabetes mellitus is associated with an increased risk of PDAC development (Everhart and Wright 1995, Shikata, Ninomiya, and Kiyohara 2013, Arslan et al. 2010, Lowenfels et al. 1993).

Up to now, the cell of origin of PDAC is still under investigation and has not yet been identified. However, due to their duct-like appearances there are three different precancerous lesions, pancreatic intraepithelial neoplasms (PanINs), mucinous cystic neoplasms (MCNs) and intraductal papillary mucinous neoplasms (IPMNs) that are longly discussed to give rise to PDAC (Maitra et al. 2005). However, recent studies using engineered mouse models and lineage tracing approaches for instance indicate that PDAC might also arise from centroacinar or acinar cells in the pancreas through a process called acinar-to-ductal metaplasia (ADM) (Stanger et al. 2005, Habbe et al. 2008, Guerra et al. 2007, Morris et al. 2010). More recently another potential precursor lesion called atypical flat lesion (AFL) has been identified. This lesion was mostly found in areas where ADMs occurred and is characterized by its flat appearance and the very strong stromal response surrounding the lesion. The stroma was described as loose and highly cellular and α-Sma expression was found in almost 100% of the stroma around atypical flat lesions in murine as well as human

pancreatic tissue. Further analysis of the stromal compartment revealed that AFLs exhibited a strong proliferative phenotype and a high immune cell infiltration (Aichler et al. 2012).

1.3.2 Precancerous lesions

In order to better understand the development of PDAC and helping to find early detection methods as well as therapeutic approaches much effort has been undertaken to characterize non-invasive precancerous lesions of PDAC.

PanINs are by far the best classified lesions and can be found in elderly people (around 30% specimen show PanIN lesions) as well as in chronic pancreatitis patients and in pancreata showing invasive cancer (Hezel et al. 2006). They are only millimetric in size (<5 mm), produce mucinous substances and according to their morphology they are subdivided into PanIN-I (PanIN-IA and PanIN-IB), PanIN-II and PanIN-III lesions with an increase of nuclear atypia and architectural abnormality from grade I to III (Maitra and Hruban 2008). PanIN-IA lesions are characterized by a flat appearance, having cells of columnar epithelial shape and round nuclei with basal orientation. PanIN-IB lesions only differ from PanIN-IA lesions by a papillary appearance. PanIN-II lesions display nuclei of different sizes often accompanied by loss of nuclear polarity. In PanIN-III lesions the morphology changes to a papillae-like appearance, the nuclei are disoriented, show a complete loss of polarity and are enlarged (Hruban et al. 2001). Lesions with these features are often termed carcinoma-in-situ by pathologists (Hingorani et al. 2003). In line with the increasing architectural disorganization, proliferation increases from PanIN-I to PanIN-III and genetic mutations accumulate (Kanda et al. 2012, Klein et al. 2002). While early PanIN-I lesions only show mutations in the Kirsten rat sarcoma viral oncogene (Kras) as well as telomerase shortening, PanIN-II lesions already display additional inactivation of p16 followed by inactivation of TP53 and DPC4 in PanIN-III lesions (Yamano et al. 2000, Wilentz et al. 1998, Wilentz, Iacobuzio-Donahue, et al. 2000, Moskaluk, Hruban, and Kern 1997).

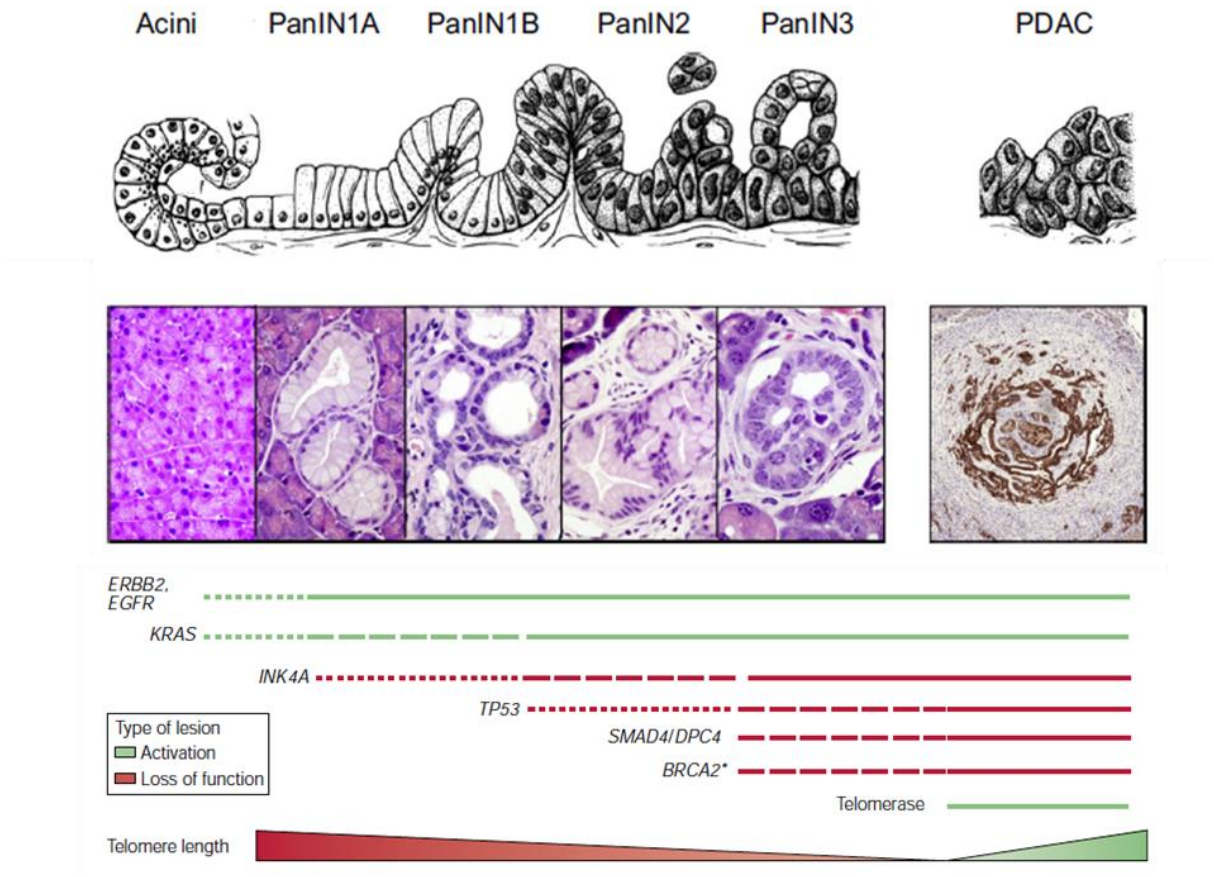

Figure 1.3 Accumulation of mutations during progression of precancerous lesions. During the course PDAC development mutations accumulate as PanINs progress (adapted and modified from (Bardeesy and DePinho 2002, Guerra and Barbacid 2013, Hruban, Wilentz, and Maitra 2005, Hruban et al. 2000).

IPMNs are larger in size (>1 cm) than PanINs and can therefore be detected by imaging modalities (Canto et al. 2006). They can arise in different parts of the pancreas whereby the occurrence of IPMNs in the main duct has been associated with invasive PDAC (Sohn et al. 2004). IPMNs are characterized by Mucin 2 expression and a papillary structure and can be classified into intestinal, gastric-foveolar, pancreatobiliary and oncocytic subtypes. *KRAS* mutations can be detected in 80% of cases. Other frequent aberrations are *GNAS* mutations and inactivation of *RNF43* (Wu et al. 2011, Amato et al. 2014).

MCNs are rare mucin-secreting epithelial cystic lesions that mostly occur in women and show an ovarian-like stroma expressing progesterone and estrogen receptors (Masia et al. 2011). Most of the times they can be found in the tail of the pancreas. Sequencing analysis found *KRAS* mutations in around 80% of MCN lesions as well as *TP53* and *SMAD4* mutations (Jimenez et al. 1999).

ADMs are duct-like structures that emerge from acinar or centroacinar cells that undergo transdifferentiation upon cell damage. During this process acinar cells loose typical differentiation markers such as amylase and trypsin and start to express ductal markers like

CK19. ADMs can further be classified into mucin producing ductal structures (MTC) and tubular complexes (TC) without showing mucin secretion. ADMs often occur in areas close to PanIN lesions but also arise in areas without any PanINs present suggesting that ADMs emerge independently and further promotes the assumption of an acinar origin of PDAC (Aichler et al. 2012).

AFLs usually occur in areas close to ADMs and also show a ductal phenotype. Additionally, nuclear atypia (enlarged nuclei), presence of mitoses and high proliferation rates up to 80% are characteristic for these lesions. AFLs can be easily recognized due to a strong stromal reaction high in cell content surrounding the lesions. As ADMs the expression of acinar markers is strongly reduced (Aichler et al. 2012).

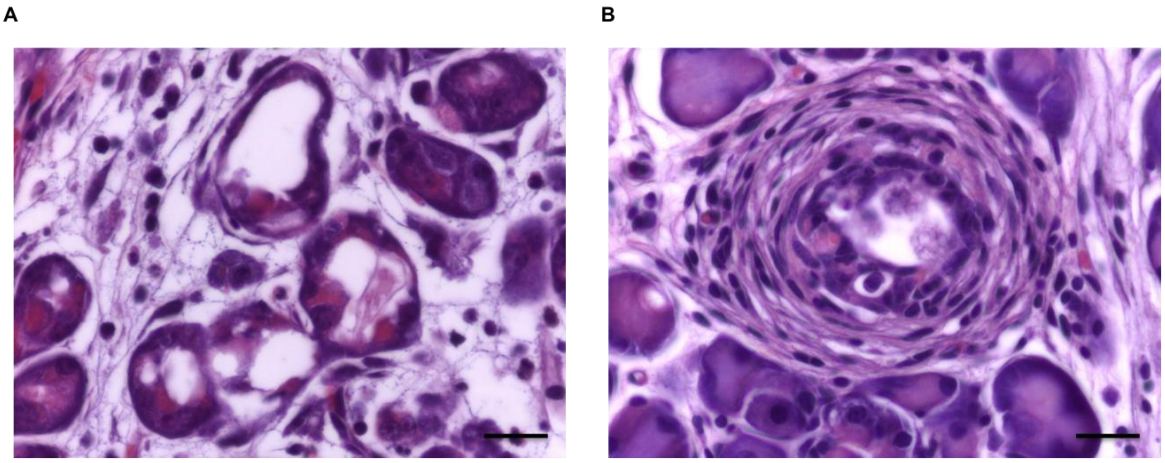

Figure 1.4 HE staining showing acinar-to-ductal metaplasia and an atypical flat lesion. A) Acinar-to-ductal metaplasia in a caerulein-induced WT mouse. **B)** A murine AFL with the characteristic strong stromal reaction surrounding the lesion.

1.3.3 Endocrine cancer

Endocrine tumors of the pancreas also referred to as pancreatic neuroendocrine tumors (PNET), are very rare tumors of the pancreas. Only up to 2% of pancreatic cancers arise in the endocrine compartment. The classification of tumors is based on the hormones produced and includes: insulinomas, gastrinomas, VIPomas, glucagonomas, somatostatinomas, adrenocorticotropic hormone producing tumors and growth hormone releasing factor secreting tumors. Insulinomas are the most common functional endocrine tumors and can occur throughout the whole pancreas. Around 15-30% of PNETs are non-functional meaning they only secrete small amounts of hormones or they produce hormones that do not cause any symptoms. These tumors are usually larger and highly metastatic. With 40-60 months the median survival is much longer compared to PDAC (Mulkeen, Yoo, and Cha 2006).

1.3.4 Acinar cell carcinoma (ACC)

With only 1% of all pancreatic neoplasms, acinar cancers also represent a very infrequent form of pancreatic tumors. They are characterized by the expression of following pancreatic enzymes: trypsin, lipase, chymotrypsin and amylase and show hardly any stroma compared to PDAC. Different subtypes of cancers with acinar differentiation can be distinguished due to their expression profile. Acinar-endocrine tumors for example show acinar and endocrine cell differentiation. In contrast to PDAC, *KRAS*, *TP53* and *SMAD4* mutations are not very common in ACC whereas mutations in adenomatous polyposis coli-β –catenin pathway as well as chromosomal instability are often found. The median survival of acinar cell carcinomas is also very poor (ca. 18 months) and approximately 15% of patients show metastatic fat necrosis (Mulkeen, Yoo, and Cha 2006, Matthaei, Semaan, and Hruban 2015).

1.3.4 Therapy options for PDAC

With a 5-year survival rate of only 7% pancreatic cancer is still one of the most deadliest diseases (Siegel, Miller, and Jemal 2015). So far resection of pancreatic tumors is the only curative method. However, only around 20% of pancreatic cancer patients qualify for pancreatic cancer resection and the 5-year survival rate increases merely up to 15-20% in these patients (Kuhlmann et al. 2004). Administration of postoperative chemotherapy with fluorouracil and leucovorin or fluorouracil and gemcitabine as well as administration of neoadjuvant preoperative chemotherapy has shown to prolong overall survival of patients (Neoptolemos et al. 2004, Evans et al. 2008). Yet, the rate of pancreatic cancer recurrence is very high and risk factors such as large tumor size, lymph node involvement and well-differentiated tumors have been identified. Most of pancreatic cancers are diagnosed at advanced stages when palliative therapy is the only option left. For a long time monotherapy with 5-fluorourcil (5-FU) was the chemotherapy of choice in PDAC patients although the overall survival with less than 6 months was rather disappointing. The combination of 5-FU with other substances such as doxorubicin or mitomycin improved the toxicity but did not show an effect regarding the survival of patients (Cullinan et al. 1985, Moertel 1978). In 1997 a major breakthrough in therapy of PDAC was achieved with the drug gemcitabine, which was not only able to increase the median survival (4.41 versus 5.65 months) and one-year overall survival rate of patients (18% versus 2%) but also improved the well-being of patients compared to those receiving 5-FU treatment (Burris et al. 1997). Gemcitabine combination therapies (gemcitabine with either cisplatin, oxaliplatin, irinotecan or pemetrexed) followed but did not show an additional advantage compared to gemcitabine monotherapy (Colucci et al. 2002, Heinemann et al. 2006, Louvet et al. 2005, Poplin et al. 2009, Stathopoulos et al. 2006, Oettle et al. 2005). In 2011 Folfirinox, consisting of 5-FU, leucovorin, irinotecan and oxaliplatin, was the first combination therapy showing a better median overall survival (6.8 versus 11.1 month) in metastatic pancreatic cancer patients (Conroy et al. 2011). In the

following years molecular targeted therapies have been developed and showed promising effects in *in vitro* and *in vivo* experiments but were not very successful in clinical trials. The EGFR inhibitor Erlotinib for instance only increased the median overall survival from 5.91 to 6.24 months in locally advanced or metastatic patients (Moore et al. 2007). Since PDAC is characterized through a dense fibrotic stroma and the assumption that it forms a barrier for chemotherapy delivery, several anti-fibrotic therapies have been developed to reduce the tumor microenvironment. The recently approved therapy consisting of nanoparticle albumin-bound paclitaxel (nab-paclitaxel) in combination with gemcitabine has shown promising effects in increasing the median overall survival of PDAC patients to 12.2 months. Nab-paclitaxel can bind to the albumin binding protein secreted protein acidic and rich in cysteine (SPARC) that is overexpressed in PDAC and thereby uptake of paclitaxel in pancreatic stromal cells is achieved. The stroma is consequently depleted and the delivery of gemcitabine is enhanced. In fact, in clinical trials a 2.3-fold intratumoral increase of gemcitabine could be detected (Von Hoff et al. 2011). Long-term survival data from of a phase III clinical trial has additionally demonstrated the efficacy of nab-paclitaxel treatment in combination with gemcitabine in metastatic pancreatic cancer patients. The median overall survival was significantly increased (8.7 versus 6.6 months) compared to the gemcitabine monotherapy group and 4% of long-term survivors could be identified in the combination treatment group (Goldstein et al. 2015). Another study showed that the administration of the hedgehog inhibitor IPI-926 successfully depleted the stroma in genetically engineered mice and that in combination with gemcitabine survival of the mice was increased (Olive et al. 2009). However, in a clinical phase II trial metastatic pancreatic cancer patients displayed an increased mortality in this treatment group and the study had to be stopped. Though, a current phase II trial testing the hedgehog inhibitor vismogedib (GDC-0449) in combination with gemcitabine and nab-paclitaxel in metastatic cancer patients has promising preliminary results so far. The treatment is tolerated and 80% of patients have a stable disease (De Jesus-Acosta 2014).

However, further studies utilizing genetically engineered mouse models recently demonstrated that stromal ablation in mice resulted in a higher mortality (Rhim et al. 2014, Ozdemir et al. 2014). Due to controversial roles of the pancreatic tumor microenvironment further studies are needed to analyze the role of stromal elements in pancreatic cancer to find new therapeutic treatment options.

1.4 Model systems for pancreatic cancer

To study the molecular biology of pancreatic cancer and to get a better insight into the interaction of key signaling pathways, the role of the microenvironment and to identify new biomarkers as well as to test potentially new treatment options different models in pancreatic cancer research are used.

1.4.1 Pancreatic cancer cell lines

Pancreatic cancer cell lines are often used in *in vitro* and *in vivo* experiments to study adhesion, migration, invasion, proliferation and response to therapeutic drugs. There are a variety of pancreatic cancer cell lines available with different phenotypic and genotypic properties consistent with the human tumor they were derived from (Deer et al. 2010). This huge diversity of cell lines allows the appropriate choice to study particular signaling pathways or the influence of different mutations on new chemotherapeutic drugs. However, studying pancreatic cancer by using cell lines also has some restrictions since cell lines can change their morphology and expression profile when kept in culture. Furthermore, pancreatic cancer cell lines are mostly isolated from patients with advanced tumors and thus signaling pathways playing a role in tumor initiation cannot be studied *in vitro*.

1.4.2 Subcutaneous and orthotopic xenograft models

Subcutaneous and orthotopic xenografts are often utilized as preclinical models to study treatment response of new drugs *in vivo.* In the subcutaneous model, established human cell lines are subcutaneously injected into immunodeficient mice. A big advantage of this model is that it allows to study angiogenesis as well as tumor growth in a time dependent manner. However, metastasis formation and more importantly the interaction with the microenvironment, which plays an important role in development and treatment of PDAC, cannot be investigated properly. In the orthotopic model, pancreatic cancer cells are transplanted directly into the murine pancreas whereby tumor development, angiogenesis and metastasis can be analyzed more in detail. Due to the lack of an intact immune system in the immunodeficient mice the microenvironment is altered and hence tumorigenesis and metastasis might not accurately reflect the situations in humans. A big disadvantage of both methods is the use of human cell lines that might have changed while culturing them for many passages and consequently might not reflect the original characteristics of the primary tumor anymore (Daniel et al. 2009). Due to these limitations clinical efficacy of the tested drugs often fails (Ellis and Fidler 2010). To partially overcome these problems, fresh pieces of human tumor tissue are directly implanted subcutaneously or orthotopically (patient-derived xenografts) into immunodeficient mice (Tentler et al. 2012). This model imitates more

precisely the tumor heterogeneity and tumor-stroma interaction as it still has the molecular characteristics of the original tumor.

To prevent the use of immunodeficient mice with an altered microenvironment, cell lines from genetically engineered mouse models harboring Kras and p53 mutations are used for orthotopically transplantation into immunocompetent mice. The tumors of this model develop a microenvironment that resembles the one in the human disease and the tumors are histologically similar to human PDAC (Tseng et al. 2010). Therefore, this model might be more appropriate for evaluating novel therapeutic agents.

1.4.3 Genetically engineered mouse models

Establishment of genetically engineered mouse models (GEMMs) that recapitulate all steps of the human disease are crucial to elucidate the molecular biology of pancreatic tumor initiation, progression and metastatic spread as well as the interaction of tumor cells with the microenvironment.

To generate mouse models with pancreas-specific mutations or gene deletions predominantly the Cre/loxP system is applied (Sauer and Henderson 1988). This system uses the bacteriophage-P1-derived Cre recombinase, which recognizes specific 34 bp sequences (loxP sites) that flank the gene of interest. Upon Cre expression under the control of a tissue specific promoter, the flanked DNA fragment can be excised in the specific tissue by the Cre enzyme and the DNA ends recombine. The first successful mouse model of pancreatic cancer was generated in 2003 by Hingorani et al. (Hingorani et al. 2003) utilizing this Cre/loxP system. In this model an oncogenic form of the *Kras* gene (G → A transition in codon 12 results in substitution of glycine (G) with aspartic acid (A); KrasG12D) is silenced by a floxed transcriptional STOP cassette (Lox-Stop-Lox) upstream of exon 1 of the *Kras* gene. The Lox-Stop-Lox cassette however can be deleted specifically in the pancreas when the mice are bred to transgenic mice expressing a Cre recombinase under the pancreas specific promoter *Pdx1* or *Pft1a*. The Pdx1-Cre model is a transgenic model and mutant Kras expression starts during embryonic development in pancreatic progenitor cells as well as in the developing foregut and recent research also showed *Pdx1* expression in the epidermis (Mazur, Gruner, et al. 2010). The $Ptf1a^{Cre/+}$ model is a knock-in mouse model in which one allele of the *Ptf1a* gene is replaced by the Cre sequence. Ptf1a expression can be found in all cells with pancreatic fate during pancreas development as well as in extrapancreatic organs such as the brain, spine and the retina (Obata et al. 2001). Mice expressing mutant Kras under the control of either *Pdx1* or *Ptf1a* promoter develop the full spectrum of pancreatic intraepithelial neoplasms starting with PanIN-I lesions at the age of four weeks in the small intralobular ducts (Aichler et al. 2012). In older mice a very strong inflammatory fibrotic response can be detected as it is described in human PDAC. At the age of 12-15 months a small subset of mice shows invasive pancreatic and metastatic cancer (Hingorani

et al. 2003). The late occurrence of invasive PDAC in these mice however, suggests that other mutations are needed to drive PDAC development. As a consequence various GEMMs were established with additional mutations in tumor suppressor genes or oncogenes such as inactivation of the tumor suppressor p53 or p16. Furthermore, GEMMs with temporally inducible gene expression have been established which enable the activation of mutant *Kras* gene expression in adult mice which resembles more the situation in humans. Therefore, estrogen receptor-Cre fusion genes (CreERT) and cycline-responsive Cre expression alleles (TRECre) have been generated (Gidekel Friedlander et al. 2009, Habbe et al. 2008).

1.5 Signaling pathways in pancreatic cancer

Pancreatic tumorigenesis is driven by the gradually accumulation of mutations in genes responsible for cell cycle regulation, DNA damage repair, cell differentiation and survival of cells. Alterations in these key genes result in uncontrolled proliferation, malignant transformation as well as resistance to apoptosis of cells. In recent years the most frequently altered genes in pancreatic tumorigenesis comprising *KRAS*, *TP53*, *CDKN2A* (*p16*) and *SMAD4*, have been identified and well characterized. Additionally, global genomic analyses revealed modifications in developmental pathways such as Notch, Hedgehog and Wnt signaling to contribute to pancreatic carcinogenesis.

1.5.1 The oncogene Kras

The *KRAS* proto-oncogene belongs to the RAS family of Guanosine-5'-triphosphate (GTP)-binding proteins and mediates cell proliferation, differentiation and survival of cells upon activation through extracellular signals such as growth factors (Campbell et al. 1998, Malumbres and Barbacid 2003). When KRAS gets activated guanine nucleotide exchange factors (GEFs) exchange GDP through GTP whereas inactivation of KRAS is mediated by GTPase activating proteins (GAP) that catalyze the hydrolysis of GTP. KRAS is the most common and earliest genetic mutation in pancreatic cancer. Already 30% of early PanIN lesions harbor this mutation and the frequency increases to 95% with disease progression (Hruban et al. 1993, Rozenblum et al. 1997). Indeed, the genetically engineered mouse model established by Hingorani and colleagues has impressively shown that a single mutation in the Kras gene is sufficient to induce transformation of normal pancreatic tissue to precancerous lesions and infiltrating pancreatic adenocarcinoma (Hingorani et al. 2003). One single point mutation in the *Kras* gene at codon 12 leads to the substitution of glycine (G**G**T) with aspartate (G**A**T), valine (G**T**T) or rather rarely arginine (**C**GT). This exchange in amino acid results in the inhibition of the intrinsic GTP autolytic activity and consequently results in a constitutively active Kras protein expression. Point mutations in codon 13 and 61 have also

been described but are less frequent. Activated Kras leads to the subsequent activation of several downstream pathways (Raf-Mapk, PI3K) influencing proliferation, migration, differentiation and survival of cells thus promoting tumor development.

1.5.2 Tumor suppressor genes

The most frequent mutated tumor suppressor gene in pancreatic cancer is ***p16/CDKN2A***, which is inactivated in approximately 95% of PDAC patients, followed by *TP53* inactivation and mutation in *Smad4/DPC4* that can be found in around 50-75% and 55% of cancers, respectively (Caldas et al. 1994, Redston et al. 1994, Wilentz, Su, et al. 2000). The *p16* (*Ink4)* gene is located on the Ink4a-ARF locus, which encodes for the tumor suppressors *p16* and *p19*, both playing important roles in cell division. Since some parts of these two genes overlap, deletion of one gene often leads to the simultaneous (in 40% of PDAC cases) loss of the other. In pancreatic cancer, *p16* inactivation can be found due to homozygous deletion (40%), promoter hypermethylation (15%) or intragenic mutations (40%). Already 30% of early PanINs show an inactivation of *p16* and loss of p16 protein function increases in more advanced precancerous lesions (55% PanIN-II and 70% PanIN-III) (Caldas et al. 1994, Schutte et al. 1997, Ueki et al. 2000, Wilentz et al. 1998). The physiological role of p16 is to inhibit cyclinD1-dependent kinases 4 and 6, which results in inhibited phosphorylation of the G1 checkpoint retinoblastoma (Rb) protein and thus to a blocked entry into the S-phase of the cell cycle. P19 also plays an important role in cell cycle arrest through inhibition of Mdm2-induced degradation of p53, which leads to p53 stabilization and consequent cell growth inhibition (Hezel et al. 2006). Hence, loss of p16 and p19 is affecting the two most important pathways controlling cell proliferation and apoptosis. The second most frequently mutated tumor suppressor in pancreatic cancer is ***p53*** itself, which shows missense mutations in the DNA binding domain in most cases (Rozenblum et al. 1997). As loss of p16, inactivation of p53 predominantly occurs in high-grade PanIN lesions and invasive PDAC (Maitra et al. 2003). Under normal conditions low cellular p53 levels can be found since p53 is bound to Mdm2, which promotes p53 degradation via the ubiquitin pathway. However, upon cell stress or cell damage p53 gets upregulated and cell cycle arrest, DNA repair and apoptosis are induced. Loss of a functional p53 protein therefore results in increased proliferation and an accelerated development of PDAC (Hingorani et al. 2005). Another common inactivated tumor suppressor in PDAC is ***SMAD4/DPC4***, which plays an important role in the TGFβ signaling pathway. Deletion of SMAD4/DPC4 is a late event in PDAC tumorigenesis with SMAD4/DPC4 inactivation being the result of either homozygous deletion or intragenic mutation (Hahn et al. 1996, Wilentz, Iacobuzio-Donahue, et al. 2000). Upon ligand binding, the TGFβII receptor becomes activated and heterodimerizes with the TGFβI receptor. Subsequently, SMAD proteins are phosphorylated, translocate to the nucleus and induce expression of target genes, mostly cycline kinase inhibitors that control growth, differentiation

and apoptosis. In case of SMAD4 loss, TGFβ signaling is impaired and the expression of anti-proliferative genes such as p21 and p27 is inhibited leading to increased cell proliferation and migration (Datto et al. 1995, Polyak et al. 1994, Levy and Hill 2005). Moreover, TGFβ signaling has been shown to directly repress *c-MYC* gene expression, which additionally keeps the cells in cell cycle arrest. However, upon SMAD4/DPC4 deletion, c-MYC gets re-expressed and promotes cell growth and proliferation (Pietenpol et al. 1990).

1.5.3 Developmental pathways

Developmental pathways are usually quiescent in adult organisms, however during pancreatic tumorigenesis these pathways get re-activated and contribute to cell proliferation and tumor progression.

The **Hedgehog** family comprises Sonic, Indian and Desert Hedgehog secreted proteins that control pancreas growth as well as growth of other organs during embryogenesis by binding to receptors expressed by neighboring cells. Upon ligand binding the negative regulator of Hedgehog signaling, Patched receptor, dissociates from Smoothened, which then activates Gli that translocates to the nucleus and induces transcription of target genes (Rhim and Stanger 2010). For proper pancreas development Hedgehog signaling has to be inactivated after E9.5; however, re-activated hedgehog signaling can be observed in early PanIN lesions as well as in more advanced lesions and PDAC suggesting a crucial role for the Hedgehog in tumor initiation and progression. Evidence from recent studies highlights that the Hedgehog signaling has an important function in the epithelial-mesenchymal crosstalk since activation of the pathway could be found in the tumor stroma (Tian et al. 2009). Further studies even showed that paracrine Hedgehog signaling increases the stromal reaction in GEMMs and treatment of mice with a Hedgehog inhibitor resulted in depletion of the stroma (Olive et al. 2009, Bailey et al. 2008).

The **Notch** signaling plays an important role in controlling cell proliferation, cell fate decisions and differentiation during organogenesis. The pathway gets activated when one of the Notch ligands (Delta-like 1, 3, 4, Jagged1, 2) binds to a membrane-bound Notch receptor (Notch 1-4) of an adjacent cell. Through proteolysis the intracellular domain of the Notch receptor (NICD) is released and can translocate to the nucleus building a complex with RBPJκ. Subsequently, the expression of Notch target genes such as *Hes1* is induced. In the adult pancreas a very low activity of the Notch pathway is seen, whereas in PanIN lesions and PDAC Notch ligands and receptors are strongly expressed (Miyamoto et al. 2003). Studies with GEMMs showed that expression of a constitutively active NICD is not sufficient to induce pancreatic carcinogenesis, only in the context with $Kras^{G12D}$, mice showed accelerated PanIN development indicating that Notch1 interacts with oncogenic Kras thus promoting tumor development (De La et al. 2008). However, other studies could show that only deficiency of Notch2 and not Notch1 was able to reduce PanIN development and delay

PDAC onset (Mazur, Einwachter, et al. 2010). Therefore, Notch seems to have context-dependent effects on pancreatic cancer development.

Another developmental pathway regulating morphogenesis, proliferation and differentiation during pancreatic organogenesis is the **Wnt** signaling. In the canonical Wnt signaling pathway, ligand binding to the Frizzled family of receptors and co-receptors leads to the inactivation of the β-catenin destruction complex. This complex, which consists of the cytoplasmic proteins Axin, GSK and APC, phosphorylates β-catenin and thereby promotes degradation of β-catenin. Upon destruction of this complex, β-catenin accumulates in the cytoplasm and can translocate to the nucleus where it induces gene expression. In the non-canonical Wnt signaling pathway, the signal transduction upon Wnt ligand binding to Frizzled receptors and co-receptors is independent on β-catenin. In pancreatic cancer a variety of Wnt ligands activating the canonical as well as the non-canonical Wnt pathway are deregulated implicating a tumor- supporting role of Wnt signaling in pancreatic tumorigenesis (Pilarsky et al. 2008, Al-Aynati et al. 2004, Zeng et al. 2006, Pasca di Magliano et al. 2007).

1.6. Tumor-stroma interaction

Pancreatic cancer is characterized by its abundant tumor-associated stroma consisting of activated pancreatic stellate cells and fibroblasts, secreted extracellular matrix proteins, nerve cells, endothelial cells as well as infiltrating immune cells and up to 80% of the pancreatic tumor mass is made up of this fibrotic stroma (Mollenhauer, Roether, and Kern 1987, Erkan et al. 2008). For many years desmoplasia has been considered as passive byproduct. However, recent research has revealed that fibrogenesis is an active process in which tumor cells interact with the stroma thereby influencing angiogenesis, tumorigenesis, therapy resistance and even metastatic spread (Erkan et al. 2009, Hwang et al. 2008, Vonlaufen et al. 2008).

1.6.1 Pancreatic stellate cells

Pancreatic stellate cells (PSCs) are stellate-shaped cells that are located in the periacinar spaces in the healthy pancreas and their long cytoplasmic processes reach and surround the base of adjacent acinar cells. Around 4-7% of all cells in the pancreas are PSCs and in their inactivated (quiescent) state they are characterized by the storage of vitamin A containing lipid droplets in the cytoplasm as well as by expression of glial fibrillary acidic protein and desmin (Apte et al. 1998, Bachem et al. 1998). Though, upon pancreatic injury, PSCs change their morphology from a quiescent state into a myofibroblast-like phenotype with coincident loss of the lipid droplets. Additionally, they start to secrete huge amounts of extracellular matrix proteins and hence contribute to fibrosis. The activated state of PSCs is characterized by the expression of α-smooth muscle actin (α-Sma). The activation of PSCs is

induced through a hypoxic environment or the release of cytokines from damaged acinar or tumor cells (Apte and Wilson 2012, Masamune et al. 2008). Furthermore, PSC activity can be maintained through an autonomous feedback loop (Erkan et al. 2007).

Although already detected in 1982 by Watari and colleagues, methods for the isolation and characterization of PSCs were not developed until 1998 (Watari, Hotta, and Mabuchi 1982, Bachem et al. 1998, Apte et al. 1998). Isolation and cultivation of these cells was a major breakthrough since the biology of PSCs could be analyzed now.

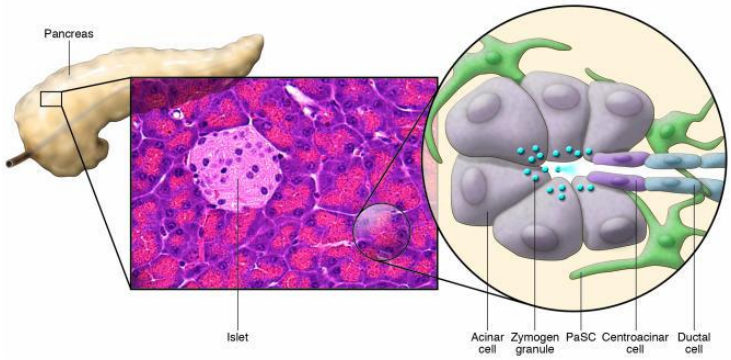

Figure 1.5: Localization of pancreatic stellate cells. Pancreatic stellate cells, illustrated in green, are located in the periacinar spaces. (Adapted from Omary et al 2007 (Omary et al. 2007)).

1.6.2 Extracellular matrix (ECM)

The extracellular matrix consists of several proteins with collagen being the most abundant. Other components of the ECM are Fibronectin, laminins as well as hyaluronic acid, proteoglycans and metalloproteinases (Frantz, Stewart, and Weaver 2010). Its physiological function is on the one hand providing mechanical and structural support since without being attached to the ECM cells undergo a process called anoikis, which means cell death due to lack of cell attachment to the ECM. On the other hand the ECM plays an important role in mediating extracellular signals (outside-in signaling) as it functions as reservoir of growth factors and other soluble factors. Hence, the ECM can influence processes such as proliferation, differentiation, migration as well as polarity of cells. Additionally, the ECM is important for the inside-out signaling that is crucial for the formation of focal adhesions and to control the affinity of ECM proteins to binding to integrins. That way, the cell can terminate existing contacts and bind to new ECM molecules (Hynes 2009).

Upon tissue injury such as pancreatitis, activated PSCs produce enormous amounts of ECM proteins, which are deposited in the extracellular space. One of the hallmarks of this acellular matrix is the abnormal vasculature. Due to the rigidity of the extracellular matrix blood vessels are compressed and therefore perfusion is disturbed. This phenomenon has been shown to reduce delivery of chemotherapeutic drugs to the cancer thereby contributing to therapy resistance (Olive et al. 2009). Moreover, for a long time the ECM has been

considered as an inactive entity, recent research however demonstrated that the ECM can promote carcinogenesis through activating oncogenic signaling pathways in epithelial cells (Comoglio and Trusolino 2005). However, recent literature showing that depletion of the tumor microenvironment results in more aggressive tumors and a shorter survival of animals implies that the role of the tumor microenvironment is more complex (Rhim et al. 2014, Ozdemir et al. 2014).

1.6.3 The ECM protein Periostin

Periostin, also known as osteoblast-specific factor 2 (OSF-2), is a secreted 90 kDa matricellular protein that was initially identified in the periodontal ligament and periosteum of mice (Horiuchi et al. 1999, Takeshita et al. 1993). In humans it is located on chromosome 13q and in mice on chromosome 3, respectively. It consists of an N-terminal secretory signal sequence and an EMILIN (EMI) domain, four repeated fasciclin I (FASI) domains and a carboxyl-terminal domain where splicing and proteolytic cleavage occurs. The EMI domain is a cysteine residue-rich sequence through which Periostin interacts with other proteins such as Notch1, type I Collagen and Fibronectin (Tanabe et al. 2010, Norris et al. 2007, Kii et al. 2010). Binding to Tenascin-C and Bone morphogenetic protein-1 (BMP-1) as well as to different subunits of the integrin receptors takes place in the FASI domain (Horiuchi et al. 1999, Kii et al. 2010, Maruhashi et al. 2010). Periostin protein expression can be induced through TGFβ, BMP, vascular endothelial growth factor (VEGF), connective tissue growth factor 2 (CTGF2), vitamin K, as well as different interleukins such as IL-4 and IL-13 (Norris et al. 2007). Many different tissue-dependent functions have been described for Periostin so far. In heart, bone and tooth it plays an important role in tissue development and regeneration and studies have shown important functions of Periostin in inflammatory allergic and respiratory diseases (Masuoka et al. 2012, Li et al. 2015). Furthermore, in a variety of cancers Periostin is dysregulated and mostly associated with pro-tumorigenic functions. Only a few studies reported tumor-suppressive functions so far. In bladder cancer for instance downregulation of Periostin was shown to result in a more aggressive tumor phenotype and forced overexpression lead to reduced invasiveness and metastasis (Kim et al. 2005). However, upregulation of *Periostin* gene expression has been reported for most of cancers such as non-small lung cell cancer (NSCLC), renal cell carcinoma (RCC), colon cancer, malignant pleural mesothelioma, breast cancer, head and neck as well as ovarian and pancreatic cancer (Soltermann et al. 2008, Bao et al. 2004, Baril et al. 2007, Gillan et al. 2002, Schramm et al. 2010, Dahinden et al. 2010, Erkan et al. 2007, Shao et al. 2004, Kudo et al. 2006). Periostin mediates its functions through binding to the integrin receptors $\alpha_v\beta_3$, $\alpha_v\beta_5$ and $\alpha_6\beta_4$ thereby activating intracellular downstream signaling pathways such as AKT and FAK. Activation of these pathways promotes survival, angiogenesis, invasiveness, resistance to apoptosis and metastasis (Siriwardena et al. 2006, Kudo et al. 2006, Bao et al.

2004). Additionally, Periostin has been implicated in epithelial-to-mesenchymal transition (EMT) and in remodeling the tumor microenvironment thus supporting the above-mentioned pro-tumorigenic functions (Liu and Liu 2011, Kanno et al. 2008, Fukushima et al. 2008, Erkan et al. 2007). Moreover, recent studies highlight the importance of Periostin in enabling metastatic spread. Malanchi et al. for example showed that in breast cancer, Periostin facilitates metastasis formation in the secondary target organ by creating a metastatic niche in which tumor cells can survive and proliferate (Malanchi et al. 2012).

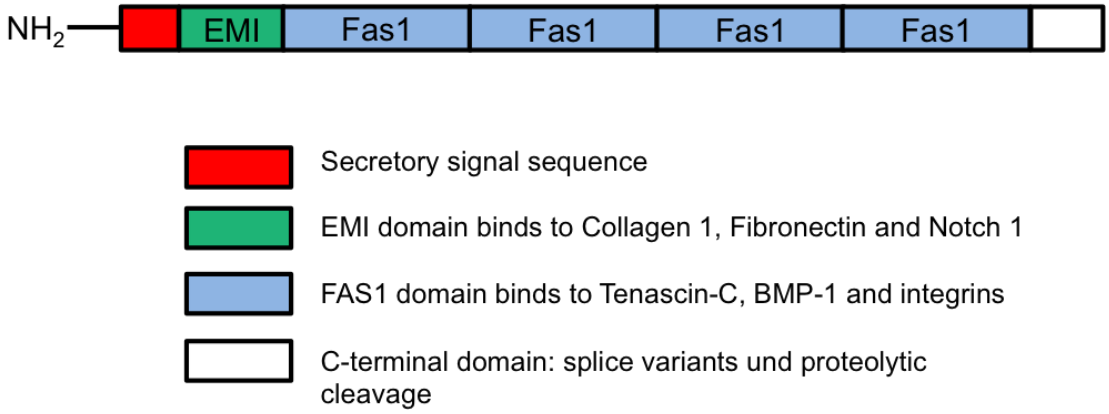

Figure 1.6: Structure of Periostin. The protein structure of Periostin includes an amino-terminal secretory signal sequence followed by an EMI domain and four repeated Fas1 domains.

1.6.4 Periostin in pancreatic cancer

In pancreatic cancer, Periostin is exclusively expressed by stromal cells such as PSCs whereas cancer cells show no or only little Periostin expression. Compared to normal pancreatic and chronic pancreatic tissue, Periostin is highly overexpressed in pancreatic cancer as well as in serum of cancer patients and a high gene expression correlates with a shorter survival of pancreatic cancer patients. *In vivo* Periostin expression can be detected in the stroma surrounding precancerous lesions such as ADMs and PanINs (Erkan et al. 2009). Also in non-invasive IPMNs a strong Periostin deposition can be observed whereas the pre-neoplastic MCNs do not show Periostin expression (Fukushima et al. 2008). *In vitro* studies demonstrated that Periostin supports proliferation and invasion of pancreatic cancer cells under stress conditions such as nutrient deprivation and that these effects are mediated by activation of AKT and FAK signaling pathways (Erkan et al. 2007, Baril et al. 2007). Further studies revealed that pancreatic cancer cells stably overexpressing Periostin had an increased ability to form anchorage-independent colonies in soft agar (Ben et al. 2011). So far no *in vivo* studies analyzing the function of Periostin in pancreatic cancer initiation, progression and metastatic spread have been performed.

1.6.5 Periostin as therapeutic target

Since Periostin expression has been identified to precede α-Sma expression in PSCs, it is a suitable marker to detect cancer-induced activation of PSCs (Erkan et al. 2007). Due to the fact that Periostin is a secretory ECM protein that accumulates during pancreatic carcinogenesis it provides properties as a suitable target for new diagnostic approaches. Additionally, tumor-promoting effects during pancreatic carcinogenesis qualify Periostin and member of its downstream signaling pathway as promising targets to inhibit pancreatic carcinogenesis and metastatic spread. Studies using a DNA aptamer that binds to Periostin and inhibits its functions demonstrated blocked adhesion, migration and invasion of breast cancer cells *in vitro* and *in vivo* confirming the potential as therapeutic drug target (Lee et al. 2013).

1.7 Aim of the study

In this study the function of the ECM protein Periostin in different pathological conditions will be analyzed. In the first part of the thesis the role of Periostin in severe acute pancreatitis and following regeneration of the pancreas parenchyma will be investigated. Therefore, Periostin global knock out mice and wild type control mice will be treated with repetitive caerulein injections and pancreatic tissue will be harvested after different time points. Immunohistochemical as well as RNA-based analyses will be performed to elucidate the role of Periostin in the acute phase of pancreatitis as well as during the regenerative period/course of regeneration.

In the second part of the thesis, the influence of Periostin on pancreatic carcinogenesis will be studied. To analyze the effect of Periostin ablation *in vivo* Periostin global knock out mice will be crossed with mice expressing a constitutive active form of oncogenic Kras under a pancreas specific promoter. Alternatively, different pancreatic cancer mouse models will be treated with an inhibitor directed against a downstream target of Periostin. The different mouse models will then be characterized and the results of these experiments will reveal if Periostin plays a role in early time points of cancer initiation as well as if inhibition of Periostin signaling delays cancer progression and prolongs survival of mice.

In the last part of the project the function of Periostin in metastatic spread will be examined. *In vitro* and *in vivo* studies will be performed to analyze if Periostin promotes invasion of cancer cells and fosters metastasis formation in the secondary target organ. Additionally, the use of an FAK inhibitor in these experiments will further elucidate if a pharmacological inhibition of downstream pathways of Periostin inhibits metastatic spread.

2 Material and Methods

2.1 Mice

2.1.1 Mouse models

B6;129-*Postn*^{tm1Jmol}/J (Jackson Laboratory, Bar Harbor, ME, USA, order number 009067):

In these mice exons 4-10 of the *Periostin* gene are replaced by a neomycin resistance cassette, which leads to a global loss of *Periostin* gene expression in these mice.

Ptf1a$^{Cre/+}$; LSL-Kras$^{G12D/+}$:

This mouse line is generated by breeding Ptf1aCre mice, (B6.129S6(Cg)Ptf1a$^{tm2(cre/ESR1)Cvw}$/J, which were kindly provided by PD Dr. Dieter Saur, Klinikum rechts der Isar, TU Munich) and LSL-Kras$^{G12D/+}$ mice (B6.129S4-Kras^{tm4Tyj}/J), Jackson Laboratory, Bar Harbor, ME, USA (order number 008179). The Ptf1a$^{Cre/+}$; LSL-Kras$^{G12D/+}$ mice express the Cre recombinase under the control of the pancreas specific *Ptf1a* promoter which leads to the cleavage of the stop cassette (LSL) in front of the oncogenic *Kras^{G12D}* in exocrine pancreas cells and the subsequent expression of this activated Kras gene. The mutation in the Kras gene is located at codon 12. The amino acid glycine is exchanged through aspartic acid, which leads to a constitutive expression of the GTPase and a permanent activation of the Ras/Erk signaling pathway.

Ptf1a$^{Cre/+}$; LSL-Kras$^{G12D/+}$;Postn:

Ptf1aCre$^{+/-}$; LSL-Kras$^{G12D/+}$ mice were crossed with Postn$^{-/-}$ or Postn$^{+/-}$ mice, respectively, leading to mice expressing oncogenic Kras in the exocrine compartment and additionally lacking homozygous (Kras^{G12D};Postn$^{-/-}$) or heterozygous (Kras^{G12D};Postn$^{+/-}$) *Periostin* gene expression.

Ptf1a$^{Cre/+}$; LSL-Kras$^{G12D/+}$; p53$^{lox/+}$

This mouse line is based on the Kras^{G12D} mouse line and was bred with the B6.129P2-Trp53^{tm1Brn}/J mouse (Jackson Laboratory, order number 008462). In this mouse model additionally one allele of the tumor suppressor gene *Tp53* is silenced due to flanking LoxP sites in exons 2-10 of the *Tp53* gene.

Following abbreviations for the above mentioned mice are used from now on:

B6;129-*Postn*^{tm1Jmol}/J	Postn$^{-/-}$
Ptf1a$^{Cre/+}$; LSL-Kras$^{G12D/+}$	Kras^{G12D}

Ptf1a$^{Cre/+}$;LSL-Kras$^{G12D/+}$;Postn$^{+/-}$	Kras^{G12D};Postn$^{+/-}$
Ptf1a$^{Cre/+}$;LSL-Kras$^{G12D/+}$;Postn$^{-/-}$	Kras^{G12D};Postn$^{-/-}$
Ptf1a$^{Cre/+}$; LSL-Kras$^{G12D/+}$; p53$^{lox/+}$	Kras^{G12D};p53$^{lox/+}$
Ptf1a$^{Cre/+}$; LSL-Kras$^{G12D/+}$; p53$^{lox/lox}$	Kras^{G12D};p53$^{lox/lox}$

2.1.2 Treatment of mice

2.1.2.1 Caerulein-induced acute pancreatitis

Postn$^{-/-}$, Postn$^{+/-}$ and wild type mice as well as Kras^{G12D};Postn$^{-/-}$ and Kras^{G12D} mice at the age of 8 to 9 weeks (sex matched) received eight hourly intraperitoneal (i.p.) injections of 100 µg/kg body weight caerulein (Sigma, Steinheim, Germany) diluted in 0.9% NaCl (Braun, Melsungen, Germany) on two consecutive days. Mice were sacrificed after one, two, four, seven and twenty-one days. Animals without any treatment were referred as day zero controls.

2.1.2.2 Caerulein-induced chronic pancreatitis

Kras^{G12D}, Kras^{G12D};Postn$^{+/-}$ and Kras^{G12D};Postn$^{-/-}$ at the age of 8 to 9 weeks (sex matched) received 6 hourly i.p. injections of 50 µg/kg body weight caerulein on three days a week (Monday, Wednesday, Friday) over a period of 6 weeks. Mice were sacrificed 8 weeks after the last caerulein injection.

2.1.2.3 Orthotopic injection of pancreatic tumor cells

Transgenic (Postn$^{-/-}$, Postn$^{+/-}$) as well as age and sex matched wild type mice were injected with 1x10^{6} pancreatic tumor cells (termed 1050-KPC) of the genotype Kras^{G12D};p53$^{lox/+}$ in 50 µl PBS (Sigma, Steinheim, Germany) to the head of the pancreas using a 30-gauge needle and a 1 ml disposable insulin syringe (BD, Biosciences, Heidelberg, Germany). Three weeks after orthotopic implantation of cells, mice were sacrificed and the tumor volume was assessed. Operations were performed by Tao Cheng.

2.1.2.4 FAKi treatment of Kras^{G12D} mice

Kras^{G12D} mice at the age of 8 to 9 weeks (sex matched) received eight hourly intraperitoneal (i.p.) injections of 100 µg/kg body weight caerulein on two consecutive days. Mice were sacrificed seven days after the last caerulein injection. To analyze the effect of the FAK inhibitor PF 573228 (R&D Systems, Wiesbaden-Nordenstadt, Germany), one group of Kras^{G12D} mice additionally received twice daily 30 mg/kg body weight FAK inhibitor on the days of caerulein injection as well as on the seven consecutive days. The FAK inhibitor was therefore dissolved in DMSO (Roth, Karlsruhe, Germany) to reach a concentration of 100

mM. This stock solution was then further diluted in 2-Hydroxypropyl-β-cyclodextrin (Sigma, Steinheim, Germany) to 12 mM. Mice were then injected intraperitoneally with 100 µl of this 12 mM solution twice daily. Control treatment group received 100 µl of the dissolvent 2-Hydroxypropyl-β-cyclodextrin. For all further treatments with the FAK inhibitor this concentration was used.

2.1.2.5 Survival of FAK inhibitor treated $Kras^{G12D};p53^{lox/lox}$ mice

$Kras^{G12D};p53^{lox/lox}$ mice received twice daily 30 mg/kg body weight FAK inhibitor starting at the age of four weeks until death or severe signs of morbidity. One group of $Kras^{G12D};p53^{lox/lox}$ mice received twice daily 30 mg/kg body weight FAK inhibitor as well as one i.p. injection of 100 mg/kg body weight gemcitabine every third day for four cycles. As control $Kras^{G12D};p53^{lox/lox}$ mice treated with dissolvent were used as well as gemcitabine (R&D Systems, Wiesbaden-Nordenstadt, Germany) treated $Kras^{G12D};p53^{lox/lox}$ mice. Gemcitabine was diluted in water to 100 mM and then further diluted in 0.9% saline to 66.7 mM. Mice were injected with 100 µl of this 66.7 mM solution every third day for four cycles.

2.1.2.6 Injections of tumor cells to the tail vein

Transgenic ($Postn^{-/-}$, $Postn^{+/-}$) as well as age and sex matched wild type mice were injected intravenously with $1x10^6$ pancreatic tumor cells of the genotype $Kras^{G12D};p53^{lox/+}$ (termed as 1050-KPC) in 150 µl PBS to the lateral tail vein. Five weeks after the tail vein injection mice were sacrificed.

To analyze the effect of FAK inhibition in these mice, one group of wild type mice additionally received a daily i.p. injection of 30 mg/kg body weight of the FAK inhibitor over the period of five weeks.

2.1.2.7 Treatment of $Kras;p53^{lox/+}$ mice with FAK inhibitor

10 week old $Kras;p53^{lox/+}$ mice were treated for one week with one daily i.p. injection of 30 mg/kg body weight of the FAK inhibitor. After seven days mice were sacrificed and blood was taken from the vena cava inferior for subsequent analysis of circulating tumor cells. To avoid clotting, the blood was given into a 2 ml eppendorf tube containing 100 µl of heparin-sodium (25,000 I.E./5ml; Brau, Melsungen, Germany). Subsequently, red blood cells were lysed by adding 8 ml of red blood cell lysing buffer (Sigma, Steinheim, Germany) and incubating cells for 10 min at room temperature. Afterwards, the lysed blood was transferred to a 50 ml tube and 30 ml of PBS containing 3% FBS (Sigma, Steinheim, Germany) was added. After repeating this washing step twice, cells were cultured in DMEM (Sigma, Steinheim, Germany) supplemented with 1% Pen/Strep (PAA, Coelbe, Germany) and 10% FBS. After 10 days medium was aspirated, cells were washed with PBS and fixed with ice-cold

methanol (Roth, Karlsruhe, Germany) und eventually stained with 0.05% crystal violet (Roth, Karlsruhe, Germany) for 30 min followed by several H_2O washing steps. Pictures of stained cells were taken under the microscope, counted and presented per blood volume. Vehicle treated Kras; $p53^{lox/+}$ mice served as control.

2.1.2.8 BrdU injection of mice

At the day of analysis all mice were intraperitoneally injected with 12.5 mg/kg body weight 5-Bromo-2-deoxyuridine (BrdU) dissolved in 0.9% NaCl. Two hours later mice were anesthetized with isoflurane (Abbott, Chicago, IL, USA) and sacrificed by cervical dislocation.

2.2 Histological analyses

2.2.1 Hematoxylin and Eosin (H&E) staining

Eosin solution: 1.5 g Eosin Y (Sigma, Steinheim, Germany); 300 ml 96% ethanol; 6 drops of 100% acetic acid (Roth, Karlsruhe, Germany)

Paraffin embedded sections (2-3 µM) were deparaffinized by incubating the sections in Roticlear (Roth, Karlsruhe, Germany) three times for 10 min each. Afterwards, the tissue sections were rehydrated by incubation in decreasing ethanol concentrations (three times 100%, 96%, 70%, 50% for 2 minutes each) and finally washed in distilled water for 5 minutes. Staining of sections with hematoxylin solution (Merck-Millipore, Darmstadt, Germany) followed for 15 seconds in order to visualize acidic structures such as the nuclei in dark violet. Tissue slides were blued by washing the sections under tap water for 15 minutes and subsequently stained with eosin solution for 2 seconds to mark basophilic structures such as connective tissue and extracellular matrix in pink. Subsequently the slides were dehydrated by incubation in solutions of increasing ethanol concentrations (5 seconds in 70% ethanol, 30 seconds in 96% ethanol and three times for 2 minutes each in 100% ethanol) and cleared in Roticlear (three times 5 minutes each). Finally, slides were mounted with one drop of Vecta Mount Permanent Mounting Media (Vector Laboratories, Burlingame, CA, USA) and coverslips (Thermo Scientific, Dreieich, Germany).

2.2.2 Immunohistochemistry

Deparaffinization and rehydration of tissue sections was carried out as described in 2.2.1. For antigen retrieval, slides were sub-boiled in 10 mM citrate buffer pH 6 (Roth, Karlsruhe, Germany) for 10 minutes at 600 Watt in a microwave or in case of CD45 immunohistochemistry by sub-boiling the sections in BD Pharmingen™ Retrievagen A solution (BD Biosciences, Heidelberg, Germany) for 20 min, respectively. After cooling down

at room temperature (RT) for 20 minutes, slides were washed in TBS-T once. In case of nuclear staining the cell membrane was permeabilized by incubation of slides in PBS containing 0.3%Triton-X100 (Roth, Karlsruhe, Germany) for 5 minutes at RT. After washing the sections three times in TBS-T for 5 minutes each endogenous peroxidase activity was blocked by incubating the slides with 3% hydrogen peroxide for 5 min. After washing the slides for 5 minutes in distilled water, unspecific binding sites were blocked by applying TBS containing 1% BSA (Roth, Karlsruhe, Germany) and 5% serum from the species in which the secondary antibody was derived. After one hour of incubation at room temperature blocking solution was dripped off and primary antibody solutions were applied (see dilutions in table 2.1). Slides were then incubated in a humid chamber at 4°C overnight.

Non-bound primary antibody was removed by two washes with TBS-T and HRP-labeled secondary antibody (Dako, Hamburg, Germany) was applied for one hour at room temperature. After two washing steps with TBS-T (5 minutes each), the color reaction was performed with the DAB+ Chromagen Solution (Dako, Hamburg, Germany) according to the manufacturer's instructions. Placing the slides into distilled water stopped the color reaction. Subsequently slides were counter stained with hematoxylin solution for 10 seconds. Afterwards, sections were blued under tap water, rehydrated, cleared and mounted as described in 2.2.1.

Table 2.1 Primary antibodies for immunohistochemistry

Antibody	Dilution	Host	Company	Order number
BrdU	1:300	mouse	Cell signaling	5292
α-Sma	1:1000	mouse	Dako	M0851
p-p44/42$^{Thr202/Tyr204}$	1:300	rabbit	Cell signaling	4376
α-Amylase	1:5000	mouse	Santa Cruz	sc-46657
CK19	1:200	rat	Developmental Studies Hybridoma Bank	
CD45	1:10	rat	BD Pharmingen	550539
Ki67	1:500	rabbit	Novus	NB110-89717
Periostin	1:500	rabbit	Acris	AP08724AF-N
MUC5AC	1:500	mouse	Thermo Scientific	MS-145
Cleaved Caspase 3	1:100	rabbit	Cell signaling	9661
p-FAK^{Y397}	1:100	rabbit	Abcam	4803
Insulin	1:200	rabbit	Santa Cruz	sc-9168
F4/80	1:160	rat	Abcam	ab16911

2.2.3 Immunofluorescence

Paraffin embedded tissue sections were treated as described in 2.2.2 except the quenching of endogenous peroxidase. Primary antibodies are listed below (Table 2.2).

Table 2.2 Primary antibodies for immunofluorescence

Antibody	Dilution	Host	Company	Order number
α-Amylase	1:5000	mouse	Santa Cruz	sc-46657
CK19 (Troma-III)	1:20	rat	Developmental Studies Hybridoma Bank	

Various fluorochrome-labeled secondary antibodies (Table 2.3) were used and slides were mounted with DAPI containing mounting medium (Dianova, Hamburg, Germany).

Table 2.3 Secondary antibodies for immunofluorescence

Antibody	Dilution	Host	Company	Order number
anti-mouse IgG, Alexa Fluor® 488 conjugate	1:500	donkey	Life Technologies	A-21202
anti-rat IgG, Alexa Fluor® 594 conjugate	1:500	goat	Life Technologies	A-11007

2.2.4 Alcian blue staining

Deparaffinization and rehydration was performed as described in 2.2.1. Subsequently tissue sections were stained for 30 min with an alcian blue solution (3% Alcian Blue 8GX (Sigma, Steinheim, Germany); acetic acid (Roth, Karlsruhe, Germany) pH 2.5) to visualize acidic sulfated mucosubstances as they can be detected in PanINs. Excessive color was removed by washing under running tap water for 15 min. Sections were then counter stained with nuclear fast red solution (Vector Laboratories, Burlingame, CA, USA) for 5 min to label the nuclei in red. Afterwards slides were washed in running tap water again followed by a wash in distilled water, dehydrated, cleared and mounted as described in 2.2.1.

2.2.5 Histological scoring and quantification

With the help of a pathologist, HE staining of mice were scored regarding ADM formation, pancreatic atrophy, lipomatosis, mesenchymal activation and immune cell infiltration. Scores ranging from 0 - 3 with 0.5 steps were given to describe the severity of the phenotype (no phenotype: 0, minor: 1, moderate: 2 and severe: 3). In case of ADM formation the proportion

of normal pancreas and acinar-to-ductal metaplasia were specified in percent of the whole pancreatic tissue.
For quantification of BrdU positive and CD45 positive cells as well as alcian blue positive lesions 3 mice per genotype and time point were chosen and at least 3 pictures per slide were taken under the microscope and evaluated manually or using the Axiovision software (Zeiss, Oberkochen, Germany).

2.2.6 Activated stroma index (ASI)

The activated stroma index of at least three mice per group and time point was assessed. Therefore, tissue sections were stained for α-Sma (Dako, Hamburg, Germany) as described in 2.2.2 except for the counterstaining with hematoxylin. Consecutive sections were stained with aniline (Sigma, Steinheim, Germany) to detect collagen deposition. Slides were scanned using a Nikon coolscan V (Nikon Corp., Tokyo, Japan) scanner. The ratio of α-Sma stained area to aniline stained area of scanned images was then calculated in Photoshop as described in (Erkan et al. 2008).

2.3 Proteinbiochemistry

2.3.1 Protein isolation from cells and murine tissue

Modified RIPA Buffer for protein isolation from tissue:

50 mM Tris-HCl pH 8.0 (Sigma, Steinheim, Germany); 150 mM NaCl (Roth, Karlsruhe, Germany); 2 mM EDTA (Roth, Karlsruhe, Germany); 1% Nonidet NP40 (Sigma, Steinheim, Germany); 0.5% SDS (Sigma, Steinheim, Germany); 1% Na-deoxycholate (Sigma, Steinheim, Germany); 30 mM NaF (Sigma, Steinheim, Germany); 20 mM $Na_4P_2O_7$ (Sigma, Steinheim, Germany); 1mM $NaVO_3$ (Sigma, Steinheim, Germany); 1 mM DTT (Sigma, Steinheim, Germany)

RIPA Buffer for protein isolation from cells:

50 mM Tris-HCl pH 7.5; 1% NP-40; 0.25% Na-deoxycholate; 150 mM NaCl; 1 mM EDTA (Roth, Karlsruhe, Germany); 1 mM PMSF (Sigma, Steinheim, Germany); 5 mM NaF; 1 mM Na_3VO_4 (Sigma, Steinheim, Germany), 1 µg/ml Aprotinin (Sigma, Steinheim, Germany); 1 mM Leupeptin (Sigma, Steinheim, Germany); 1 µg/ml Pepstatin (Sigma, Steinheim, Germany)

Per 10 ml Ripa buffer 1 tablet Complete Mini Protease Inhibitor Cocktail and 1 tablet PhosSTOP Phosphatase Inhibitor Cocktail (both Roche, Penzberg, Germany) was added.

For protein isolation of the murine pancreas, mice were sacrificed and small pieces of pancreas were cut and immediately snap frozen in liquid nitrogen and afterwards stored at -80°C. For protein extraction the pancreas pieces were thawed in modified RIPA buffer containing Complete Mini Protease Inhibitor Cocktail and PhosSTOP Phosphatase Inhibitor Cocktail and homogenized using a mechanical TissueLyser (Qiagen, Hilden, Germany). After sonication using the ultrasonic processor UP100H at 20 kHz (Hielscher Ultrasonics GmbH, Teltow, Germany), samples were centrifuged at 16,100 rcf for 15 min at 4°C and supernatant was transferred to new tubes and stored at -80°C.

To isolate protein from cells, medium of approximately 90% confluent cells was removed and cells were washed with cold PBS. RIPA buffer was added to the confluent cells and cell lysates were harvested by using a cell scraper (Sarstedt, Nümbrecht, Germany). After sonication the cell lysate was centrifuged at 16,100 rcf for 15 min at 4°C and supernatant was transferred to new tubes and stored at -80°C.

2.3.2 Determination of protein concentration

Protein concentration was assessed using the BCA kit from Thermo Fisher, Waltham, MA, USA, according to the manufacturer's instructions. Absorbance was measured at 570 nm using a Multiskan EX Microplate Photometer (Thermo Fisher, Dreieich, Germany).

2.3.3 SDS polyacrylamide gel electrophoresis

5X Sample Loading Buffer:

62.5 mM Tris-HCl pH 10; 10% SDS; 50% Glycerol (Roth, Karlsruhe, Germany); 5% β-Mercaptoethanol (Sigma, Steinheim, Germany); 0.05% Bromphenol blue (Sigma, Steinheim, Germany)

Stacking Gel (4%)

3 ml ddH_2O; 750 µl 30% Acrylamide (Roth, Karlsruhe, Germany); 1.3 ml 0.5 M Tris-HCl pH 6.8; 50 µl 10% SDS; 25 µl 10% APS (Sigma, Steinheim, Germany); 10 µl TEMED (Roth, Karlsruhe, Germany)

Resolving Gel (10%)

4.1 ml ddH_2O; 3.3 ml 30% Acrylamide/Bis solution; 2.6 ml 1.5M Tris-HCl pH 8.8; 100 µl 10% SDS; 50 µl 10% APS; 15 µl TEMED

10X Running Buffer:

10 g SDS; 30 g Tris base (Sigma, Steinheim, Germany); 144 g Glycine (Roth, Karlsruhe, Germany); add 1000 ml dH_2O

Protein transfer to nitrocellulose blotting membranes (GE Healthcare, Chalfont St Giles, UK) was performed at 100 V for 1 hour in 1X transfer buffer under wet conditions using the BioRad wet tank blotting system (Mini Trans-Blot® Cell, BioRad, Munich, Germany).

10X Transfer Buffer:

30g Tris base; 144 g Glycine; add 1000 ml dH_2O

1X Transfer Buffer:

- 100 ml 10X Transfer buffer
- 200 ml methanol
- 700 ml dH_2O

To 20 µg total protein 5X sample loading buffer was added and proteins were denatured by incubating at 95°C for 10 minutes. Proteins were then separated on a SDS polyacrylamide gel in 1X running buffer at 30 mA in BioRad Mini Protean Gel System chambers (BioRad, Munich, Germany). The concentration of the SDS polyacrylamide gels was determined according to the size of the proteins of interest ranging from 10 to 15%. As reference for protein size 10 µl of a prestained protein ladder (Thermo Scientific, Waltham, MA, USA) was loaded onto the gel.

10X TBS:

12.1 g Tris base; 85.0 g NaCl; add 1000 ml dH_2O; pH 7.4

1X TBS-T:

- 100 ml 10X TBS
- 900 ml dH_2O
- 1 ml Tween 20 (Roth, Karlsruhe, Germany)

After transfer of the proteins to the nitrocellulose membrane unspecific binding sites were blocked by incubating the membrane in TBS-T containing either 5% BSA or 5% skim milk powder (Roth, Karlsruhe, Germany). After incubation for 1 hour at room temperature the blocking solution was removed and the membranes were incubated with the primary antibody diluted in TBS-T/5%BSA or TBS-T/5% skim milk at 4°C over night. The next day, primary antibody solutions were removed and membranes were washed with TBS-T three times for 10 minutes each. Subsequently, the according HRP-coupled secondary antibody was applied in TBS-T containing 5% skim milk for 1 hour at room temperature. After 3 washing steps with TBS-T (10 minutes each) the protein bands were visualized using the ECL Western Blotting Detection Reagents (GE Healthcare, Chalfont St Giles, UK) and

Amersham Hyperfilms (GE Healthcare, Chalfont St Giles, UK) in an Opti Max X-Ray Film Processor (Protec Processor Technology, Oberstenfeld, Germany).

Table 2.4 Primary antibodies for Western Blot

Antibody	Dilution	Host	Company	Order number
p44/42 MAPK	1:5000	rabbit	Cell signaling	9102
p-p44/42$^{Thr202/Tyr204}$	1:5000	rabbit	Cell signaling	9101
FAK	1:1000	rabbit	Cell signaling	3285
p-FAK^{Y397}	1:2000	rabbit	Cell signaling	3283
SRC	1:5000	rabbit	Cell signaling	2109
p-SRC^{Y416}	1:5000	rabbit	Cell signaling	6943
GAPDH	1:10000	rabbit	Santa Cruz	sc-25778
β-Actin	1:5000	rabbit	Santa Cruz	sc-69879

Table 2.5 Secondary antibodies for Western Blot

Antibody	Dilution	Host	Company	Order number
Anti-mouse IgG, HRP conjugate	1:5000	goat	Promega	W4021
Anti-rabbit IgG, HRP conjugate	1:5000	goat	Promega	W4011

2.3.3 Enzyme linked immunosorbent assay (ELISA)

To analyze the expression of 12 different cytokines in serum of mice the Mouse Inflammatory Cytokines Multi-Analyte ELISAarray™ Kit (Qiagen, Hilden, Germany) was used according to the manufacturer's instructions. To obtain serum, mice were sacrificed and blood was taken from the vena cava inferior using a 1 ml insulin syringe. Serum was isolated by centrifuging the blood for 10 min at 2,000 rcf.

2.4 RNA and DNA analyses

2.4.1 RNA isolation from tissue

Mice were sacrificed and a small part of the pancreas was immediately placed into RLT-buffer containing 1% β-Mercaptoethanol. The tissue was then homogenized using the TissueLyser (Qiagen, Hilden, Germany) and RNA isolation was performed with the Qiagen RNeasy Kit according to manufacturer's instructions. RNA concentration was measured with the NanoDrop 2000 spectrophotometer (Thermo Scientific, Dreieich, Germany). RNA was stored at -80°C.

2.4.2 cDNA synthesis

1 µg RNA was reverse transcribed during cDNA synthesis using the RevertAid First Strand cDNA Synthesis Kit (Thermo Fisher, Waltham, MA, USA) according to the manufacturer's protocol. cDNA concentration was adjusted with ddH_2O to 20 ng/µl. cDNA was stored at -20°C.

2.4.3 Quantitative real-time RT-PCR (qRT-PCR)

Quantitative real-time PCR (qRT-PCR) was performed using a LightCycler480 (Roche, Penzberg, Germany) and the SYBR Green master mix (Roche, Penzberg, Germany). As housekeeping gene Peptidylprolyl Isomerase B (*Ppib*) was used. The final concentration of primers was 0.5 µM and 40 ng of cDNA served as template for qRT-PCR. All samples were pipetted in doublets in a 96-well plate. Relative mRNA expression values were calculated with the following exponential equation: $2^{\Delta CT(Ppib)-\Delta CT(target\ gene)}$; normalized mRNA expression values were calculated as fold change compared to control. All primers were adjusted to a melting temperature of 60°C and the following PCR program was used for the analysis of all genes of interest.

Table 2.6 Genotyping PCR program

Step	Temperature [°C]	Time [sec]	Cycle
Pre Incubation	95	300	
Amplification	95	15	45
	55	15	
	68	15	
Melting	95	1	
	65	20	
	98	continuous 0.11°C/sec	5 Acquisitions/sec
Cooling	37	∞	1

The following primers were used for quantitative real-time RT-PCR.

Table 2.7 Primer sequences used for qRT-PCR

Name	Primer fwd (5'→3')	Primer rev (5'→3')
Postn	CTGCCCCGCAGTGATGCCTA	GCCTCGTTACTCGGCGCGAA
Hes1	AAAATTCCTCCTCCCCGGTG	TTTGGTTTGTCCGGTGTCG
Sox9	GCAAGCTGGCAAAGTTGATCT	GCTGCTCAGTTCACCGATG
Pdx1	TGCCACCATGAACAGTGAGG	GGAATGCGCACGGGTC
Mist1	TCCCCAGTTGGAAGGGCCTCA	TCCTGCATGGGTGTTCGGCG
Rbpjl	GTATCGAAGTCAGTGGCGGT	GCAGGCTCAGGTGAGTCAAA
Ppib	GGAGCGCAATATGAAGGTGC	CTTATCGTTGGCCACGGAGG

Pparγ	GAAAGACAACGGACAAATCACC	GGGGGTGATATGTTTGAACTTG

2.4.4 gDNA isolation from mouse tails

Tails were lysed in 500 µl STE buffer (50 mM Tris-HCl pH 8; 100 mM NaCl; 1% SDS; 1 mM EDTA pH 8) containing 25 µl of 20 mg/ml proteinase K (Peqlab, Erlangen, Germany) and incubated overnight at 55°C and 550 rpm. Afterwards the digested tails were centrifuged for 10 min at 13,400 rcf and 400 µl of the supernatant was transferred to a new tube. One volume 100% isopropanol was added to precipitate the DNA. After another centrifugation step (10 min, 13,400 rcf) the supernatant was discarded and the cell pellet was washed with 70% ethanol and centrifuged again at 13,400 rcf for 10 min. The supernatant was discarded and as soon as the DNA pellet was dried it was resuspended in 50 µl ddH_2O. 1 µl of gDNA was then used as template for genotyping PCR. All genotyping PCRs were run on a 2% agarose (Roth, Karlsruhe, Germany) gel.

2.4.5 Genotyping PCR

For all genotyping PCRs the REDTaq® Master Mix (Sigma) and 1 µl of gDNA was used. The final concentration of primers was 10 pM.

Table 2.8 Genotyping PCR program

Step	Temperature [°C]	Time [sec]	Cycle
Pre-Incubation	94	60	1
Amplification	94	90	40
	58	30	
	72	60	
Final Elongation	72	10	1
Cooling	4	∞	1

The following genotyping primers were used:

$Ptf1a^{Cre/+}$

5'-ACCAGCCAGCTATCAACTCG-3'

5'-TTACATTGGTCCAGCCACC-3' wt band: 324 bp

5'-CTAGGCCACAGAATTGAAAGATCT-3' lox band: 199 bp

5'-GTAGGTGGAAATTCTAGCATCATCC-3'

LSL-Kras$^{G12D/+}$

5'-CACCAGCTTCGGCTTCCTATT-3'	wt band: 272 bp
5’-AGCTAATGGCTCTCAAAGGAATGTA-3’	lox band: 192 bp
5'-CCATGGCTTGAGTAAGTCTGC-3'	

p53$^{lox/+}$

5’-CACAAAAAACAGGTTAAACCCA-3’	wt band: 300 bp
5’-AGCACATAGGAGGCAGAGAC-3’	lox band: 350 bp

Postn

5'-CCTTGCCAGTCTCAATGAAGG-3'	wt band: 691 bp
5'-TGACAGAGTGAACACATGCC-3'	knock out band: 500 bp
5'-GGAAGACAATAGCAGGCATGCTG-3'	

2.5 Cloning

2.5.1 Generating the Periostin promoter sequence

To obtain the Periostin promoter, a PCR with genomic DNA from a pancreatic stellate cell line isolated from healthy human pancreatic tissue was performed.

For this purpose the Q5 proof reading polymerase (NEB, Frankfurt, Germany) was used according to the manufacturer’s protocol and primers were designed to detect a 2.276 kb big sequence (chr13:38190844-38193120) around 7 kb upstream of the transcription start site containing open chromatin (DNAse I sensitive sites) and acetylated histones in the area indicating that this is an active region containing the Periostin promoter. Overhangs of the Kpn recognition sequence were added to the 5’ Periostin promoter forward primer and overhangs of the recognition sequence of the HindIII enzyme were added 5’ to the Periostin promoter reverse primer.

- Postn promoter fwd with **KpnI** recognition sequence:
  5’-AT**GGTACC**GGGAGAGTAGAAACTCTTAAGTGC-3’

- Postn promoter rev with **HindIII** recognition sequence:
  5’-AT**AAGCTT**CACTTCAAAAGGAAGGAGGAAAAG-3’

Table 2.9 PCR program to retrieve Periostin promoter

Step	Temperature [°C]	Time [sec]	Cycle
Pre-Incubation	98	30	1
Amplification	98	50	35
	60	30	
	72	90	
Final Elongation	72	10	1
Cooling	4	∞	1

After the amplification, 3'-A overhangs were added to the sequence. Therefore, directly after the PCR was finished, 1 unit of Taq Polymerase (Life Technologies, Carlsbad, CA, USA) was pipetted to each reaction and incubated for 10 min at 72°C. Afterwards the products resulting from the PCR amplification were separated on a 0.8% agarose gel. The 2.276 kb fragment was excised from the gel with a scalpel and the DNA was extracted using the QIAquick Gel extraction kit (Qiagen, Hilden, Germany) according to the manufacturer's instructions.

2.5.2 Subcloning of Periostin promoter in TOPO vector

Cloning of the purified Periostin promoter sequence into a TOPO subcloning vector was performed according to the manufacturer's protocol (Life Technologies, Carlsbad, CA, USA).

2.5.3 Transformation

50 µl of competent Top10 one shot E.colis (Life Technologies, Carlsbad, CA, USA) were thawed on ice. In the meantime 250 µl SOC medium (Life Technologies, Carlsbad, CA, USA) and agar plates containing 100 µg/ml Ampicillin (Roth, Karlsruhe, Germany) were pre-warmed to 37°C. 2 µl of the TOPO cloning reaction was mixed gently with 50 µl E.colis and incubated on ice for 30 min. After heat-shocking the bacteria for 30 seconds at 42°C they were immediately put back on ice. When cooled down 250 µl of pre-warmed SOC medium was added to the bacteria and an incubation step at 37°C for 1 hour at 225 rpm followed. Meanwhile 40 µl of 40 mg/ml X-gal dissolved in N,N-Dimethylformamide (both Sigma, Steinheim, Germany) were spread onto 100 µg/ml Ampicillin agar plates and incubated for 30 minutes at 37°C. Finally, 100 µl of the bacteria media was plated out on agar plates and spread evenly. The plates were then incubated at 37°C over night. The next day white colonies were picked and over night cultures were prepared. Therefore, one white colony was scratched away of the agar plate with a 10 µl tip and put to 3 ml of LB medium (Roth, Karlsruhe, Germany) containing 100 µg/ml Ampicillin and incubated at 37°C shaking over night.

2.5.4 Isolation of plasmid DNA

After over night incubation, bacteria culture was centrifuged at 6,000 rcf for 15 min and DNA plasmid Miniprep isolation was performed according to the manufacturer's instruction (Qiagen, Hilden, Germany). Isolated plasmid DNA was tested via restriction enzyme digestion with HindIII and KpnI.

2.5.5 Restriction enzyme digestion

1 µg of plasmid DNA was incubated with 1 µl HindIII and 1 µl KpnI in 5 µl buffer 4 (NEB, Frankfurt, Germany) and 42 µl dH_2O at 37°C for 8 h and heat inactivated at 60°C for 20 min. 5 µl of the digestion product was loaded on a 0.8% agarose gel. Successful cloning was indicated by retrieving two bands, one 2.276 kb band representing the Periostin promoter sequence and one 3.9 kb band representing the TOPO vector. The 2.276 kb band was carefully cut out under UV light and purified using the QIAquick Gel extraction kit.

2.5.6 Ligation of Periostin promoter and pGL3 vector

1 µg of the pGL3 vector (Promega, Madison, WI, USA) was also cut with HindIII and KpnI as described in 2.5.5. The linearized pGL3 vector was then ligated with the Periostin promoter sequence using an Instant Sticky-end Ligase Master Mix (NEB, Frankfurt, Germany). 100 ng of the linear pGL3 vector was mixed with a 3-fold molar excess of Periostin promoter and adjusted to a total volume of 15 µl with ddH_2O. Then 15 µl of Instant Sticky-end Ligase Master Mix were added and thoroughly mixed by pipetting up and down. After 10 min incubation on ice, the sample could be used for transformation as described in 2.5.3 except for the X-Gal treatment of plates since the pGL3 vector does not contain a lacZ gene. Colonies were picked, over night cultures were prepared and a plasmid Miniprep performed. To rule out that mutations have occurred in the Periostin promoter sequence, 50 ng/µl of plasmid DNA was sent to Eurofins for sequencing. The concentration of primers was 10 pmol/µl.

Table 2.10 Sequencing primer

Name	Primer Fwd (5'→3')	Primer Rev (5'→3')
RVprimer3	CTAGCAAAATAGGCTGTCCC	
Postn prom rev		CACTTCAAAAGGAAGGAGGAAAAG

2.6 Cell Culture

2.6.1 Isolation of murine acini

Culture medium: Waymouth's MB 752/1 (Life Technologies, Carlsbad, CA, USA); 10% FBS; 1% Pen/Strep; 0.1 mg/ml trypsin inhibitor (MP Biomedicals, LCC, Newport Beach, CA, USA);

2 mg/ml dexamethasone (Sigma, Steinheim, Germany); 5mM; HEPES (Life Technologies, Carlsbad, CA, USA); 0.13% $NaHCO_3$ (Roth, Karlsruhe, Germany).

The pancreas was minced into small pieces and digested for 15 min at 37°C in 5 ml of RPMI (Sigma, Steinheim, Germany) containing 0.5 mg/ml collagenase P (Roche, Penzberg, Germany). Afterwards, the cell suspension was washed with RPMI supplemented with 5% FBS, transferred to a 50 ml tube and centrifuged at 0.3 rcf for 5 min at room temperature. The supernatant was discarded and the cell pellet was resuspended in 10 ml RPMI containing 5% FBS and filtered through a 100 µm nylon cell strainer (BD, Heidelberg, Germany). In order not to lose any cells the cell strainer was washed with additional 10 ml of RPMI containing 5% FBS. The filtered cell suspension was centrifuged again at 0.3 rcf for 5 min at room temperature. The supernatant was discarded and the cell pellet was washed with 20 ml of RPMI containing 5% FBS. Another centrifugation step at 300 rpm for 5 min at room temperature followed. After discarding the supernatant the cell pellet was washed with 15 ml of Hanks balanced salt solution without phenol red (Biochrom, Berlin, Germany) in order to wash out collagenase P. The cell suspension was centrifuged again at 0.5 rcf for 5 min at room temperature. This washing step was repeated twice. Finally, the cells were resuspended in 10 ml culture medium and seeded into a 10 cm dish.

2.6.2 3D cell culture

3D culture medium (100 ml): Waymouth's MB 752/1; 20% FBS; 2% Pen/Strep,; 0.2 mg/ml trypsin inhibitor; 4 mg/ml dexamethasone (Sigma); 10 mM HEPES; 0.26% $NaHCO_3$.

Acini were isolated as described in 2.6.2 and incubated in culture medium overnight at 37°C. The next day, the 3D cell culture was prepared. First, a 12-well plate was coated with rat tail collagen (Corning, Corning, NY, USA) mixed with 3D medium. The desired final concentration of collagen was 1 mg/ml and the collagen-3D medium mixture was prepared according to the following formula:

10X PBS: final volume/10 = ml PBS
Collagen: (final volume x final collagen concentration [mg/ml])/collagen concentration
1 M NaOH: volume collagen x 0.023
3D medium: final volume – volume (collagen + 10X PBS + NaOH)
$NaHCO_3$: 10% of volume was added

After coating the wells of a 12-well plate with 400 µl of collagen-medium mixture the cell layer was prepared. Acinar cells were centrifuged for 5 min at 500 rpm. The supernatant was discarded and the cell pellet was resuspended in 3D cell culture medium. The collagen-cell

layer was prepared according to the above-described formula, instead of media cell suspension was used. Carefully, 1500 µl of collagen-cell suspension was pipetted on the coated 12-well plate and an incubation period of 1h at 37°C followed.
After polymerization of the collagen 1100 µl of 2D cell culture medium was added as well as 500 ng/ml mrPostn and 10 µM FAK inhibitor, respectively.

2.6.3 Invasion assay

0.05% crystal violet: 10 mg crystal violet in 20 ml methanol

To analyze the invasive behavior of two murine pancreatic cancer cell lines upon stimulation with recombinant Periostin (R&D Systems, Wiesbaden-Nordenstadt, Germany) Matrigel® Invasion Chambers (Corning, Corning, NY, USA) were used. Prior to use the invasion chambers had to be taken out from -20°C and when having reached room temperature the matrigel coated inserts needed to be rehydrated with serum free medium. In the meantime cells were trypsinized and counted. $1x10^5$ cells were seeded in a volume of 500 µl into the inserts. To determine the effect of Periostin on invasion different concentrations of recombinant Periostin protein were added (100 ng/ml; 500 ng/ml; 1 µg/ml) to the cells. As chemoattractant 500 µl DMEM containing 10% FBS was given into the wells of the 24-well plate. The plate was then incubated at 37°C. After 15 hours the medium of the inserts was aspirated and non-invaded cells were removed by using a cotton swab. Invaded cells were fixed in 500 µl ice-cold methanol for 20 minutes and subsequently stained in 0.05% crystal violet (Roth, Karlsruhe, Germany) dissolved in methanol for 30 minutes. Excessive color was removed by washing the inserts in distilled H_2O. The membrane of the inserts was dried, then carefully removed from the insert using a scalpel and mounted on a glass slide using vectamount mounting medium (Vector Laboratories, Burlingame, CA, USA) and 25x25 mm coverslips (Thermo Scientific, Dreieich, Germany). All invaded cells were counted under a Zeiss microscope.
When the effect of FAK or Periostin inhibition was analyzed, the assay was stopped after 20 hrs and analyzed as described above.

2.6.4 MTT assay

5 mg/ml MTT solution: 25 mg of 3-(4,5-dimethylthiazol-2-yl)-2,5-diphenyltetrazolium bromide (MTT) dissolved in 5 ml PBS

To analyze the effect of murine recombinant Periostin on cancer cell proliferation, murine pancreatic cancer cells were starved (DMEM containing 0.1% FBS) for 24 hrs before seeding 2,000 cells in 100 µl DMEM supplemented with 5% FBS and 1% Pen/Strep in a 96-well plate. After cells were attached 10% of volume (10 µl) MTT reagent was added and cells were

incubated for 4 hrs at 37°C. During this time, the yellow MTT is metabolized by the mitochondrial dehydrogenase of viable cells producing a violet water insoluble formazan. After 4 hrs of incubation the cells were lysed overnight by adding 100 µl lysis buffer (10% SDS containing 0.01 N HCl) in order to precipitate the formed formazan. The next day a colorimetric determination followed by measuring the intensity of metabolized MTT at a wavelength of 570 nm with the GloMax®-Multi Detection System (Promega, Madision, WI, USA) reader.

2.6.5 Colony formation assay

2X DMEM: DMEM containing 10% FBS, 2% Pen/Strep and L-Glutamine (Life Technologies, Carlsbad, CA, USA) diluted 1:100
0.05% crystal violet: 10 mg crystal violet in 20 ml methanol

To analyze the ability of cancer cell to grow anchorage independently upon Periostin stimulation, the colony formation assay was performed. Therefore, 12-well plates were coated with 500 µl sterile autoclaved 2% agar-agar (Roth, Steinheim, Germany) solution mixed with 2X DMEM in the ratio 1:1. While the base agar-agar –medium solution was cooling down the top layer was prepared. Cancer cells were trypsinized, counted and 5,000 cells were resuspended in 250 µl of 37°C warm 2X DMEM. Quickly, the same volume of 40°C pre-heated 1% agar-agar was added in case for the $p48^{Cre/+};Kras^{G12D};p53^{fl/+}$ cell line 950 and 250 µl of pre-warmed 0.7% agar in case for the $p48^{Cre/+};Kras^{G12D};p53^{fl/+}$ cell line 1050, respectively. The cell suspension was carefully mixed with the agar-agar solution and poured on top of the coated layer. Plates were incubated at 37°C and the next day 250 µl DMEM containing 5% FBS, 1% Pen/Strep and different Periostin concentrations (500 ng/ml and 1 µg/ml) were added. Medium was changed every two days. After two weeks, the medium was aspirated and the cells were incubated with 250 µl of a 0.05% crystal violet solution dissolved in methanol for 2 hrs. Purple stained cells were then counted under the microscope.

2.6.6 Dual Glo luciferase assay

150,000 HeLA cells were seeded in a 24 well plate. After attachment of cells, the medium was changed to DMEM containing 1% Pen/Strep and 0.1% FBS. The next day 500 ng of the pGL3-Periostin promoter construct was co-transfected with 100 ng of pRTLK plasmid (Promega, Madison, WI, USA) and 250 ng of either c-MYC or NFATc2 (both Origene Technologies, Rockville, MD, USA) expression plasmid using Lipofectamine 2000 (Life Technologies, Carlsbad, CA, USA) according to the manufacturer's instructions. As control the pGL3-Periostin promoter construct was co-transfected with 100 ng of RTLK plasmid and an empty vector. After 24 hours of incubation the cells were trypsinized and 50,000 cells per well were transferred into a 96-well luminescence plate. When all cells were attached the

Dual Glo Luciferase Assay (Promega, Madison, WI, USA) was performed according to the manufacturer's protocol.

2.7 Statistical analysis

All experiments were performed at least three times. Statistical analysis was performed using the GraphPad Prism 6 software (GraphPad Software Inc., San Diego, CA, USA) and statistical significance was determined by two-tailed unpaired t-test or Mann-Whitney U-test. Survival of mice was analyzed using Kaplan-Meier curves and the log-rank test was utilized to test for significant differences between the groups. Results are presented as means ± standard error of the mean (SEM). P values less than 0.05 were considered statistically significant (* $P< 0.05$; ** $P < 0.01$; *** $P<0.001$).

3 Results

3.1 Periostin is crucial for regeneration after caerulein-induced tissue damage

3.1.1 No morphological difference between untreated wild type and Postn$^{-/-}$ mice

Prior to performing experiments with Postn$^{-/-}$ mice the pancreatic compartment of 8-week old Postn$^{-/-}$ mice was analyzed morphologically and compared to corresponding wild type (WT) mice to determine whether the loss of Periostin influences the development of the pancreatic compartment. Histological assessment of the pancreatic compartment by HE staining as well as staining for the acinar marker α-Amylase and the islet specific marker Insulin revealed no differences between the two genotypes. In both mice functional acini and islet cells were detected (Figure 3.1 A). Also, the pancreas mass-to-body weight ratio and macroscopic examination of 8-week old pancreas from WT and Postn$^{-/-}$ mice did not show any differences (Figure 3.1 B and C). Thus, these results indicate that loss of Periostin does not influence pancreas development.

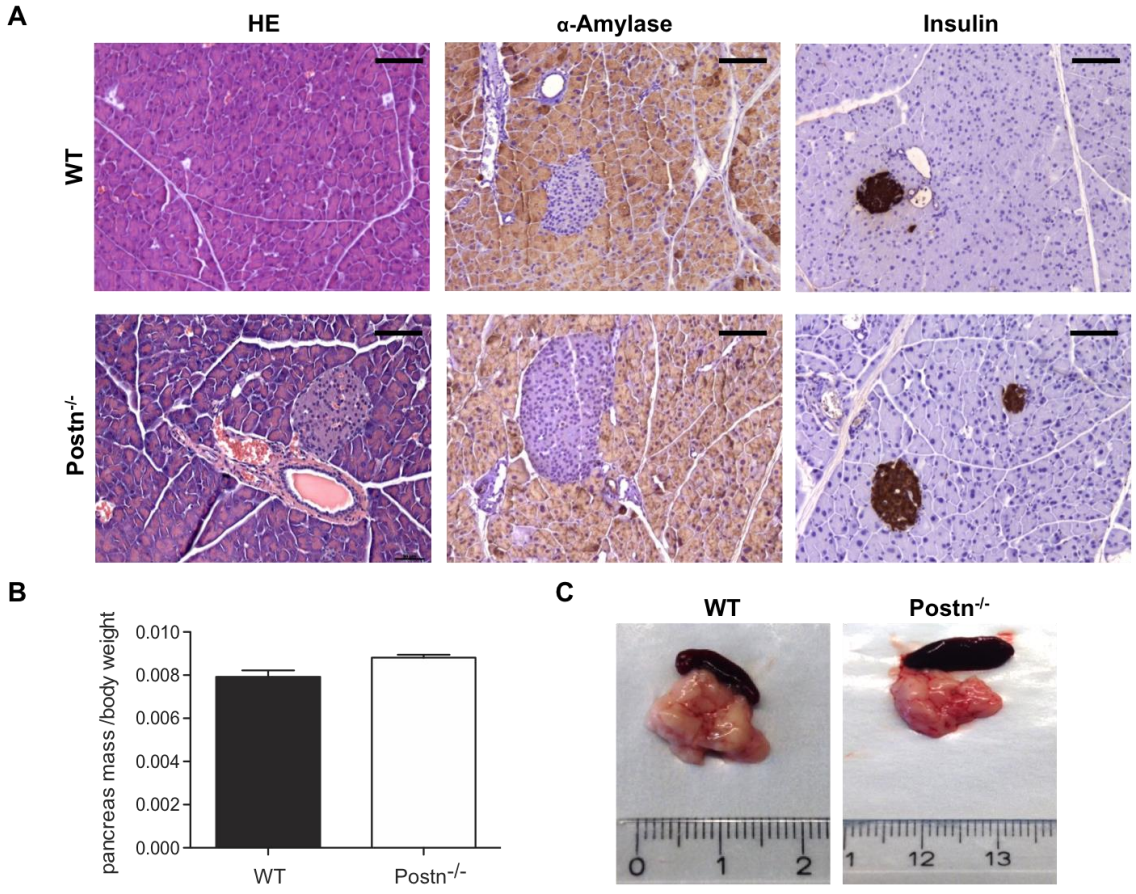

Figure 3.1 Characterization of the pancreatic compartment of WT and Postn$^{-/-}$ mice. A) Representative HE, α-Amylase and Insulin staining of WT and Postn$^{-/-}$ mice showing no differences in the exocrine and endocrine compartment. Scale bars represent 100 µm. **B)** Pancreas mass-to-body

weight ratio. Data are expressed as means ± SEM (n=3), unpaired two-tailed t-test. **C)** Representative pictures of the pancreas of 8-week old mice demonstrating that there is no observable difference between the two genotypes.

3.1.2 Periostin is upregulated during acute pancreatitis and recovery

To investigate the role of Periostin in acute pancreatitis and during pancreatic regeneration, tissue damage was induced by repetitive intraperitoneal (i.p.) injections of the cholecystokinin analogue caerulein in WT mice according to Figure 3.2.

Figure 3.2: Acute pancreatitis protocol.

Gene expression analysis (qRT-PCR) and immunohistochemical staining for Periostin of untreated 8-week old sex-matched WT mice sacrificed at the time points depicted in Figure 3.2 revealed that the Periostin expression level was very low in the healthy organ. However, upon caerulein-induced pancreatitis Periostin expression markedly increased on mRNA as well as protein level and continued to be highly expressed during the regeneration phase, but showed a decline to almost basal levels after twenty-one days (Figure 3.3 A). The staining of formalin-fixed paraffin embedded tissue sections for the ECM protein Periostin showed a similar picture (Figure 3.3 B). In untreated WT mice hardly any Periostin expression was detectable, whereas already one day after caerulein administration Periostin protein expression could be observed. The expression continued during the regeneration phase of WT mice and even after twenty-one days there was still Periostin expression detectable; however, at much lower intensity and abundance compared to the inflammatory and regenerative phase (Figure 3.3 B). As shown in Figure 3.3.C localization of Periostin was inter-and intralobular as well as around acinar complexes in the inflammatory phase. During recovery of the pancreas, Periostin expression was predominantly detected around ADMs and regenerative areas.

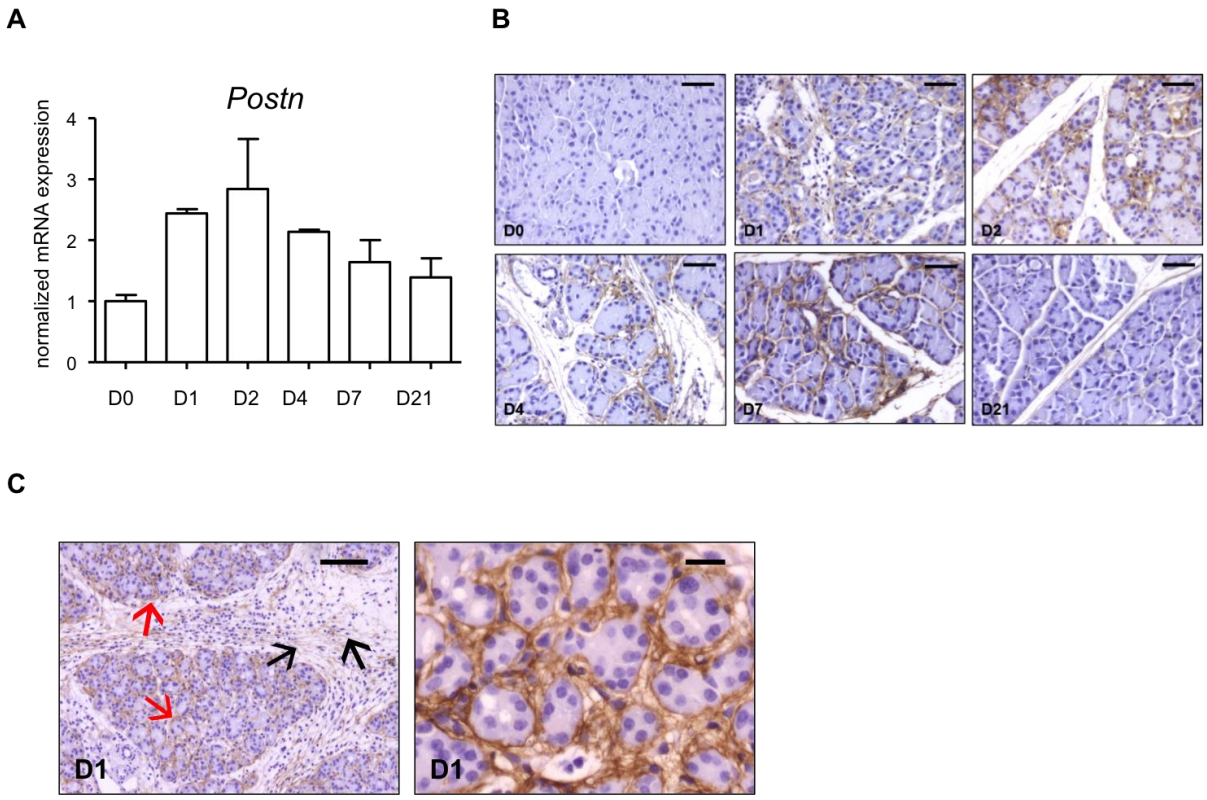

Figure 3.3: Postn expression in WT mice. A) RNA was isolated from untreated as well as caerulein treated WT mice, transcribed into cDNA and *Postn* expression levels were determined using qRT-PCR. *Ppib* was used as housekeeping gene. Data are expressed as means ± SEM (n≥3), unpaired two-tailed t-test. **B)** Formalin-fixed and paraffin embedded tissue from untreated and caerulein treated WT mice was stained for Periostin expression. Scale bars represent 50 µm. **C)** Immunohistochemistry showing Periostin localization during acute inflammation of the pancreas. Left picture: Black arrows indicate interlobular Periostin expression and red arrows display Periostin expression around acinar complexes. Right picture: High power field displaying Periostin expression around acinar complexes. Scale bars represent 100 µm (left picture) and 20 µm (right picture).

3.1.3 Periostin ablation does not influence pancreatitis severity

Analysis of blood serum obtained from WT and Postn$^{-/-}$ mice one day after the last caerulein injection as well as histological investigation of the pancreatic tissue showed that lack of Periostin did not affect severity of pancreatitis. No differences in serum amylase, calcium, lipase or lactate dehydrogenase (LDH) levels could be observed between the two genotypes at this time point (Figure 3.4 A). Furthermore, both genotypes displayed similar levels of immune cell infiltration in the acute inflammatory phase (D1 and D2) and also a detectable capability of ADM formation was observed in WT as well as in Postn$^{-/-}$ mice (Figure 3.4 B).

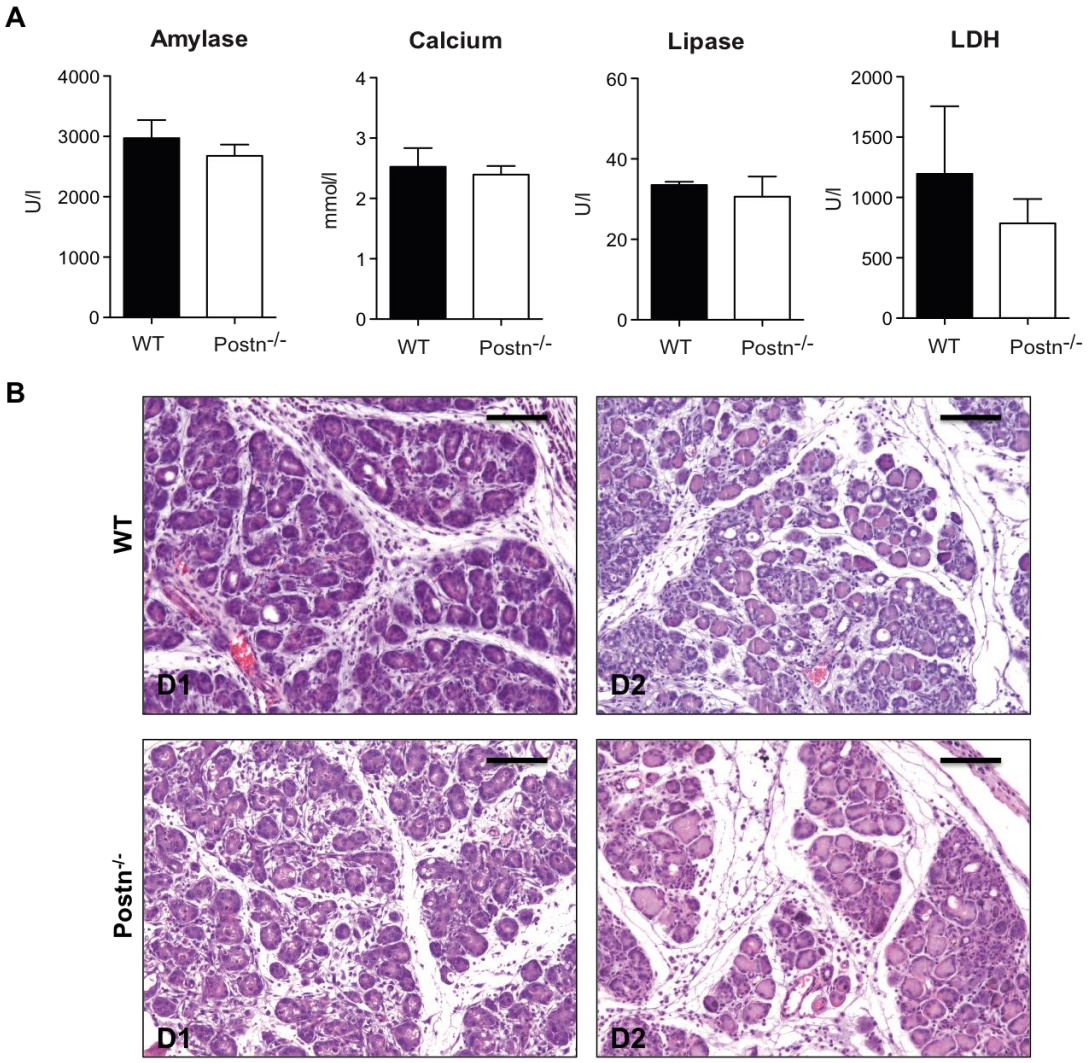

Figure 3.4 Severity of pancreatitis. A) Blood was taken from mice treated with caerulein one day after the last caerulein administration and centrifuged for 10 min at 2,000 g to obtain serum. Amylase, calcium, lipase and lactate dehydrogenase serum levels were determined at the clinical chemistry department at TU München. Data are expressed as means ± SEM (n≥3), unpaired two-tailed t-test. **B)** Representative HE staining one and two days after the last caerulein injection demonstrating that there is no difference in pancreatitis severity between WT and Postn$^{-/-}$ mice. Scale bars represent 100 µm.

3.1.4 Differences in stromal activation between WT and Postn$^{-/-}$ mice

Apart from immune cell infiltration and ADM formation, tissue damage of the pancreas provokes a stromal response. Fibroblasts and pancreatic stellate cells get temporarily activated, which is characterized by expression of α-Sma, and the production of extracellular matrix proteins. Periostin has been shown to keep pancreatic stellate cells in this activated state and to contribute to desmoplasia in this way (Erkan et al. 2007). Therefore, the activated stroma index was calculated to find out if the loss of Periostin influenced stromal activation.

At all time points Periostin deficient mice displayed a higher activated stroma index (Figure 3.5 B), since more α-Sma positive cells but less collagen deposition was found in these mice

compared to WT mice. Hence, these results indicate that Periostin ablation reduces the fibrotic response after acute pancreatitis.

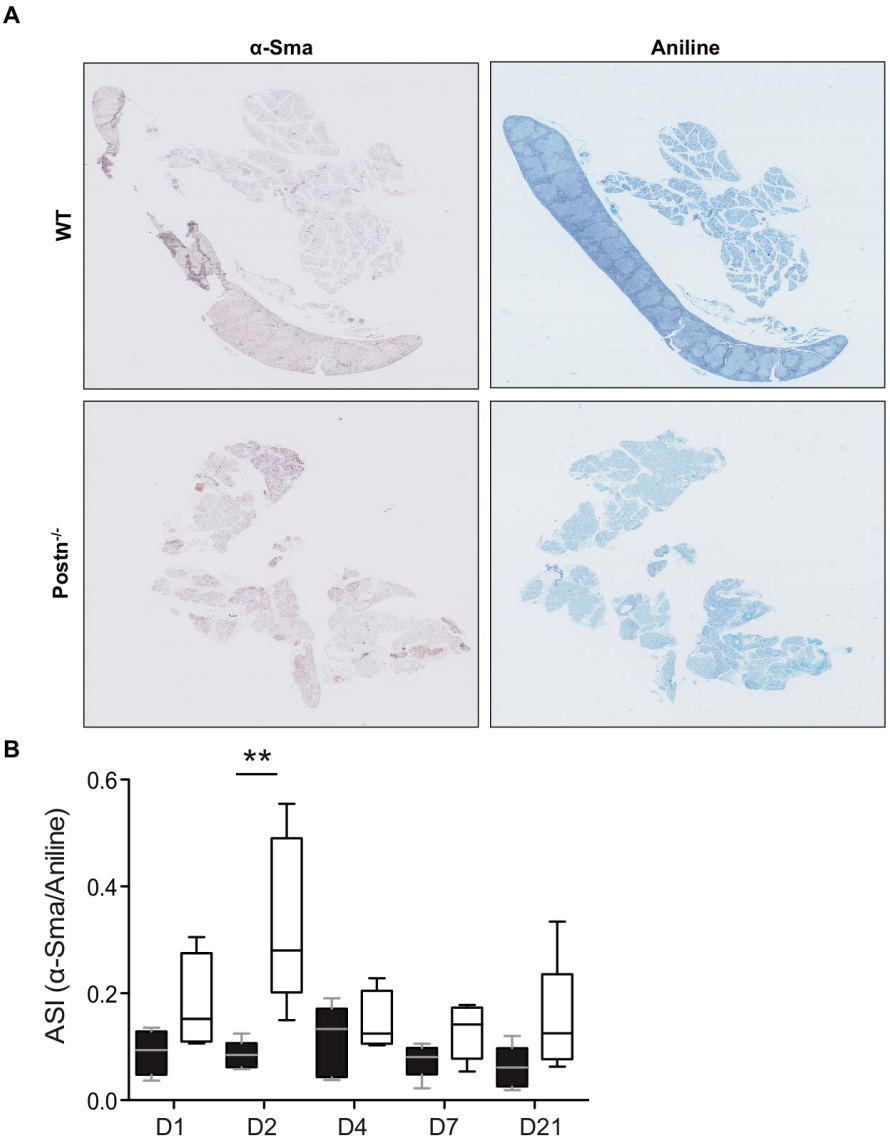

Figure 3.5 Activated stroma index. Consecutive sections of WT and Postn$^{-/-}$ pancreas tissue were stained for α -Sma and Aniline. **A)** Representative scanned pictures of a-Sma (left panel) and Aniline (right panel) from WT and Postn$^{-/-}$ mice after two days of the last caerulein injection. **B)** Calculated ASI for all time points showing that the activated stroma index is higher in Postn$^{-/-}$ mice. Data are expressed as means ± SEM (n≥3). ** P < 0.01, unpaired two-tailed t-test.

3.1.5 Impaired regeneration in Postn deficient mice

To further elucidate the influence of Periostin during pancreatic recovery, the course of pancreatitis in WT and Postn$^{-/-}$ mice was compared. After the acute inflammatory phase, WT mice showed a gradually regeneration indicated by an increased recovery of α-Amylase positive area as well as a stepwise decrease of infiltrating immune cells (Figure 3.6 A and B).

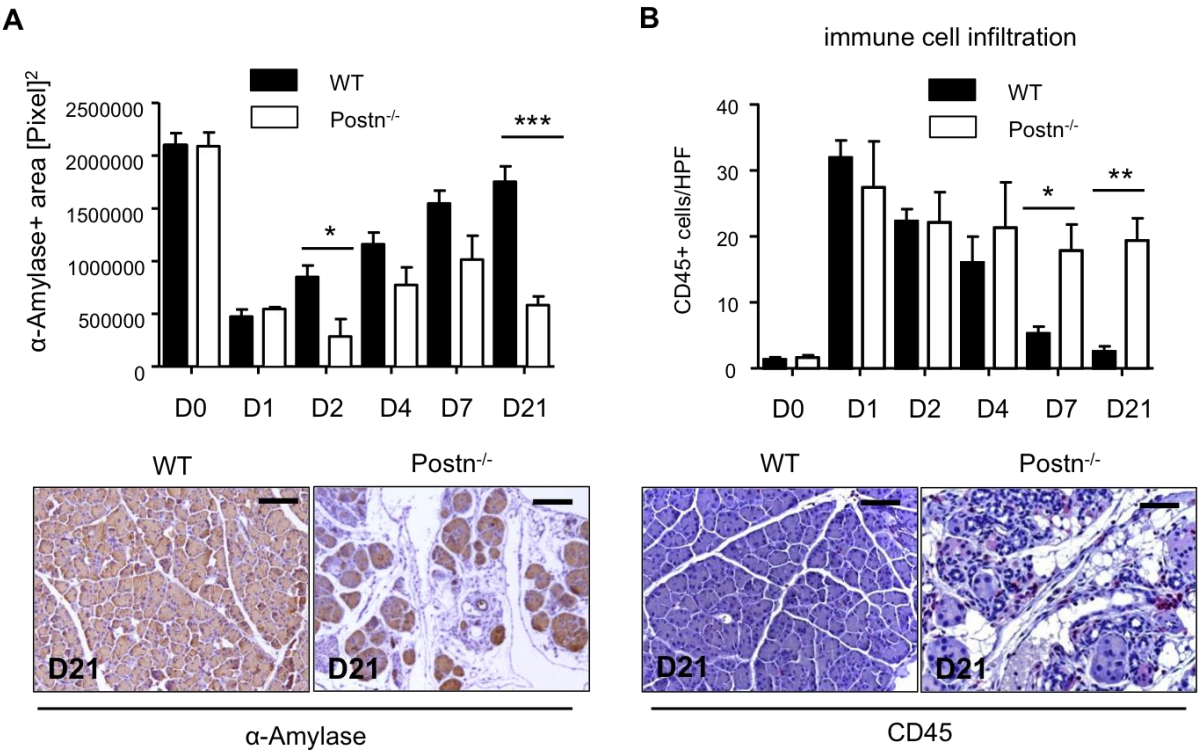

Figure 3.6 Exocrine recovery. Formalin-fixed and paraffin embedded tissue from caerulein-induced pancreatitis wild type and Periostin knock out mice obtained at different time points was stained for α-Amylase and the leukocyte marker CD45. 5 representative pictures of each genotype and time point were taken and **A)** α-Amylase positive area was calculated using the Axio Vision program. **B)** CD45+ cells were manually counted. Representative pictures for α-Amylase and CD45+ staining are shown. Data are expressed as means ± SEM (n≥3). Scale bars represent 100 µm. * P< 0.05; ** P < 0.01; *** P < 0.001, unpaired two-tailed t-test.

Additionally, the number of ADMs and the amount of proliferating cells declined step by step during recovery of the exocrine pancreas. At day seven almost no tubular complexes and BrdU positive cells were present (Figure 3.7 A and B). The pancreas of WT mice was nearly fully recovered by this time and at day twenty-one no difference to untreated WT mice (D0) could be observed. In contrast to WT mice, pancreatic regeneration was severely impaired in Postn$^{-/-}$ mice with differences being most distinctive at seven and twenty-one days after caerulein treatment. Contrary to WT mice, which showed a stepwise decrease in immune cell infiltration, Postn$^{-/-}$ mice exhibited persistent elevated levels of CD45 positive cells (Figure 3.6 B), which reached significance at day seven and twenty-one. Unsuccessful regeneration was further characterized by higher levels of ADMs in Postn$^{-/-}$ mice at all time points compared to WT mice (Figure 3.7 A). While in WT mice ADM formation was mainly observed in the acute phase of inflammation, which declined in the regenerative phase, in Postn$^{-/-}$ mice the presence of ADMs was strongly increased in the regenerative phase with significant differences to WT mice at D7. In parallel to persistent ADM formation, proliferation was also significantly elevated in Postn$^{-/-}$ mice at D7 (Figure 3.7 B).

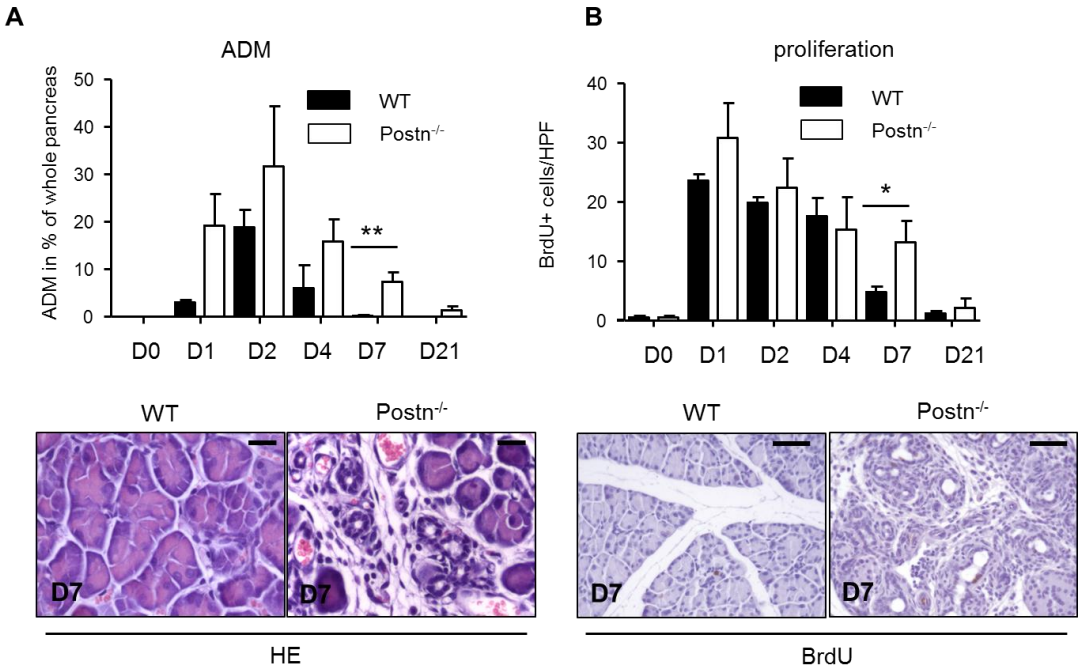

Figure 3.7 ADMs and proliferating cells in wild type and Postn$^{-/-}$ mice. Formalin-fixed and paraffin embedded tissue from caerulein-induced pancreatitis wild type and Periostin knock out mice obtained at different time points was HE stained or stained for the proliferation marker BrdU. **A)** Amount of ADMs is elevated at all time points in Postn$^{-/-}$ mice. **B)** Postn$^{-/-}$ mice exhibit more proliferating cells particularly at D7. Data are expressed as means ± SEM (n≥3). Scale bars represent 20 µm (ADM pictures) and 50 µm (BrdU stained pictures). * P<0.05; ** P<0.01, unpaired two-tailed t-test.

The most substantial difference between WT and Postn$^{-/-}$ mice was the development of pancreatic atrophy and lipomatosis in Postn deficient mice. Histopathological scoring revealed that Postn$^{-/-}$ mice developed pancreatic atrophy starting at D4 with reaching significant differences at D7 and D21 (Figure 3.8 A and B). These results were further confirmed by a significant decrease of pancreas mass seven and twenty-one days after caerulein administration in Postn$^{-/-}$ mice (Figure 3.8 C). In parallel to pancreatic atrophy, the pancreatic parenchyma was replaced by fat cells in Postn$^{-/-}$ mice beginning at D7. At D21 the majority of acini was replaced by adipocytes (Figure 3.8 D and E). Taking a closer look at the immunohistochemistry of α-Amylase staining at D21 α-Amylase positive fat cells were found indicating acinar-to-adipocyte transdifferentiation in Postn$^{-/-}$ mice after caerulein-induced pancreatitis (Figure 3.8 E).

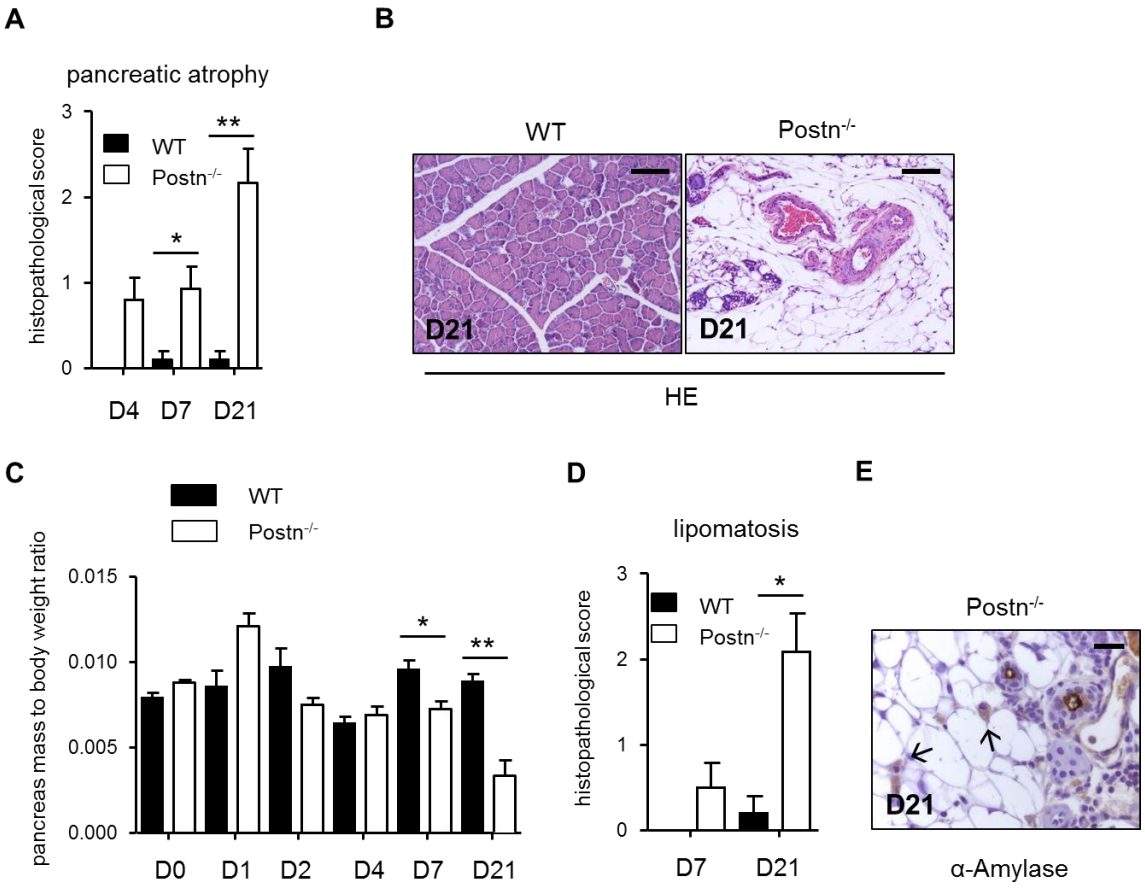

Figure 3.8: Pancreatic atrophy and lipomatosis in wild type and Postn$^{-/-}$ mice. Formalin-fixed and paraffin embedded pancreatic tissue from wild type and Postn$^{-/-}$ mice was HE stained and scored regarding to **A)** pancreatic atrophy. Scale bars represent 100 µm. **B)** Representative HE staining showing the loss of parenchyma in Postn$^{-/-}$ mice at D21. **C)** Pancreas mass and body weight was determined at all time points and the ratio was calculated. **D)** Scoring of HE stained tissue revealed that in Postn$^{-/-}$ mice lipomatosis emerged from D7 on. **E)** Representative α-Amylase stained picture from day 21 after the last caerulein administration showing fat cells and Amylase positive granules in the cytoplasm of adipocytes (arrows). Scale bar represents 20 µm. Data are expressed as means ± SEM (n≥3). * P<0.05; ** P>0.01, A and D Mann-Whitney U-test, C unpaired two-tailed t-test.

3.1.6 Dysregulated expression of progenitor, differentiation and adipogenesis marker in Postn$^{-/-}$ mice

To restore pancreatic architecture after tissue damage the initiation of a regenerative program is crucial. This requires transient acinar-to-ductal metaplasia where remaining acinar cells temporary re-express progenitor markers that induce cell proliferation, which is essential to replace the damaged tissue. Later during tissue regeneration the cells start to express acinar differentiation marker again in order to rebuild the exocrine compartment. Disturbances in expression of these progenitor- /differentiation gene pattern can lead to improper regeneration and even atrophy of the pancreas. Since the regeneration in Postn$^{-/-}$ mice was severely impaired, expression levels of progenitor markers known to be re-expressed during regeneration of the pancreatic compartment as well as expression of acinar differentiation genes were assessed.

qRT-PCR analysis revealed that mRNA expression levels of the progenitor markers *Hes1*, *Sox9* and *Pdx1* were significantly upregulated at day twenty-one in Postn$^{-/-}$ mice compared to WT mice (Figure 3.9 A). At the same time transcript levels of the differentiation marker basic helix-loop-helix (bHLH) transcription factor *Mist1* and recombination signal binding protein for immunoglobulin kappa J region-like *Rbpjl* were strongly reduced in Postn$^{-/-}$ mice twenty-one days after the last caerulein treatment (Figure 3.9 B). In addition to the pancreatic atrophy, the replacement of acinar cells by adipocytes at day twenty-one after caerulein administration was the most striking phenotype in Postn$^{-/-}$ mice. Thus, expression of the key regulator of adipogenesis, peroxisome proliferator-activated receptor-γ (Ppar-γ), was analyzed as well in Postn$^{-/-}$ and WT mice at D21. As anticipated, in WT mice hardly any *Ppar-γ* transcription levels were detectable whereas in Postn$^{-/-}$ mice *Ppar-γ* was significantly upregulated (Figure 3.9 C).

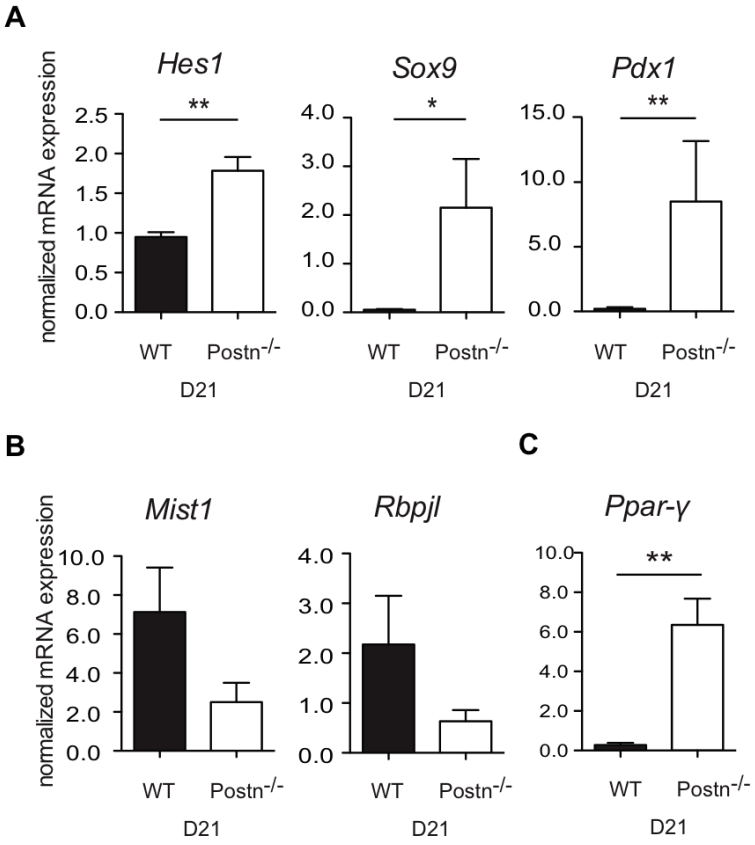

Figure 3.9: Expression levels of progenitor, differentiation and adipogenesis markers. RNA was isolated from WT and Postn$^{-/-}$ caerulein-induced pancreatitis mice at D21 and transcribed into cDNA. Subsequent analysis of **A)** progenitor markers *Hes1*, *Sox9* and *Pdx1*. **B)** Analysis of differentiation markers *Mist1* and *Rbpjl* as well as the **C)** adipogenesis marker *Ppar-γ* revealed that in Postn$^{-/-}$ mice progenitor markers were significantly upregulated, whereas differentiation markers were strongly downregulated. The transcript levels of *Ppar-γ* were significantly upregulated in Postn$^{-/-}$ mice at D21. Data are expressed as means ± SEM (n≥3). * P< 0.05; ** P< 0.01, Mann-Whitney U-test.

Taken together, these results show that the ECM protein Periostin is crucial for the efficient regeneration of the exocrine pancreatic compartment after caerulein-induced pancreatitis.

Ablation of this ECM molecule results in pancreatic atrophy and acinar-to-adipocyte differentiation most probably due to dysregulated expression of progenitor and differentiation markers. These findings highlight the importance of a proper mesenchymal-epithelial interaction in regeneration of the pancreas after tissue injury.

3.2 Periostin promotes pancreatic carcinogenesis

3.2.1 Characterization of $Kras^{G12D}$;$Postn^{-/-}$ mice

Immunohistochemical staining for Periostin in $Kras^{G12D}$ mice at eight, twelve and twenty-four weeks of age revealed that Periostin expression increased with age of mice. Localization of protein expression was mainly found around pre-neoplastic lesions such as ADMs and PanINs as well as inter- and intralobular (Figure 3.10).

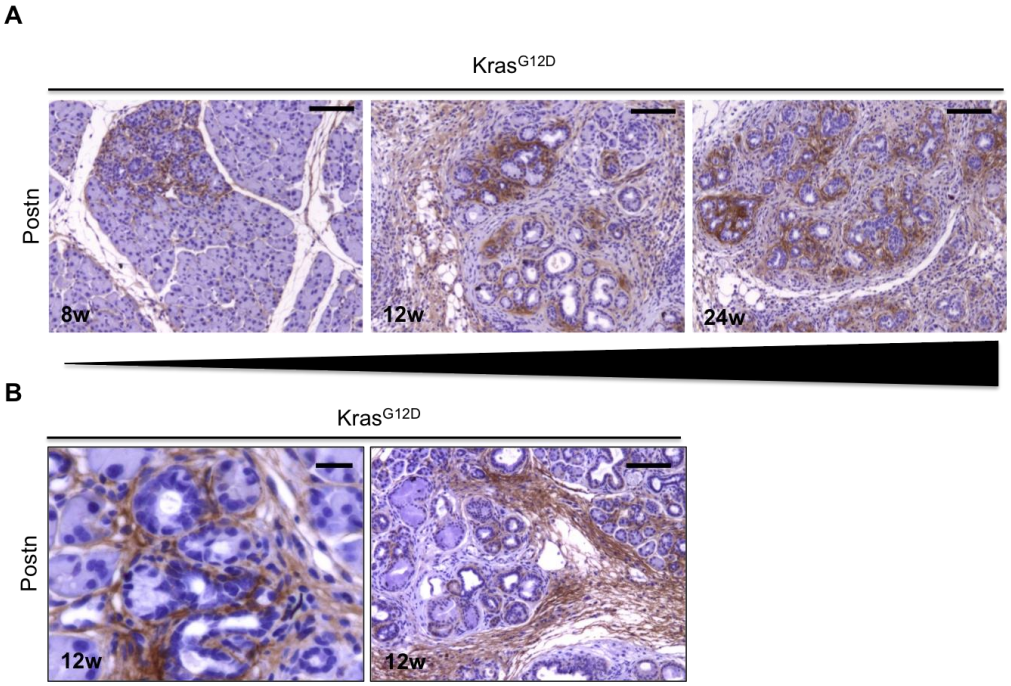

Figure 3.10 Periostin expression in $Kras^{G12D}$ mice. A) Representative immunohistochemistry staining for Periostin demonstrating that Periostin expression increased with age of mice. Scale bars represent 100 µm. **B)** Localization of Periostin expression is mainly found around precancerous lesions (left picture) or inter- and intralobular (right picture). Scale bars represent 20 µm (left picture) and 100 µm (right picture).

In order to analyze the influence of Postn on early pancreatic carcinogenesis, $Postn^{-/-}$ mice were crossed with $Kras^{G12D}$ mice to obtain $Kras^{G12D}$;$Postn^{-/-}$ mice. These mice were then examined at eight, twelve and twenty-four weeks of age to quantify PanIN lesions, proliferating cells, immune cell infiltration as well as metaplasia in comparison to corresponding $Kras^{G12D}$ mice. A morphological analysis of HE stained tissue sections of $Kras^{G12D}$;$Postn^{-/-}$ mice showed that $Kras^{G12D}$ mice exhibited a more malignant phenotype (Figure 3.11).

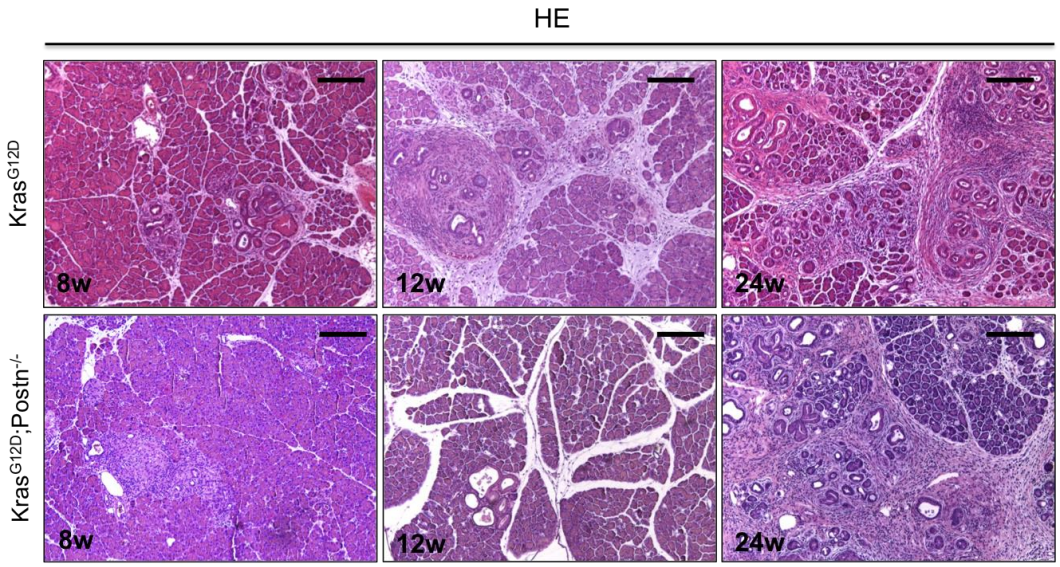

Figure 3.11 Pancreatic compartment of Kras^{G12D} and Kras^{G12D};Postn$^{-/-}$ mice. Representative HE staining of eight, twelve and twenty-four week old Kras^{G12D} and Kras^{G12D};Postn$^{-/-}$ mice. Scale bars represent 200 µm.

These observations were subsequently corroborated by analyzing alcian blue positive lesions. Quantification of lesions revealed that in both, Kras^{G12D} and Kras^{G12D};Postn$^{-/-}$ mice, the amount of PanIN lesions increased with age of mice. However, at all time points the number of lesions was reduced in Kras^{G12D};Postn$^{-/-}$ compared to Kras^{G12D} mice (Figure 3.12). The same results could be observed for proliferating cells, marked with BrdU, and CD45 positive infiltrating immune cells (Figure 3.12). At eight weeks of age a significant reduction of BrdU-positive cells could be detected. Also CD45 immune cells were less prominent in Kras^{G12D};Postn$^{-/-}$ mice, although the effect was not statistical significant.

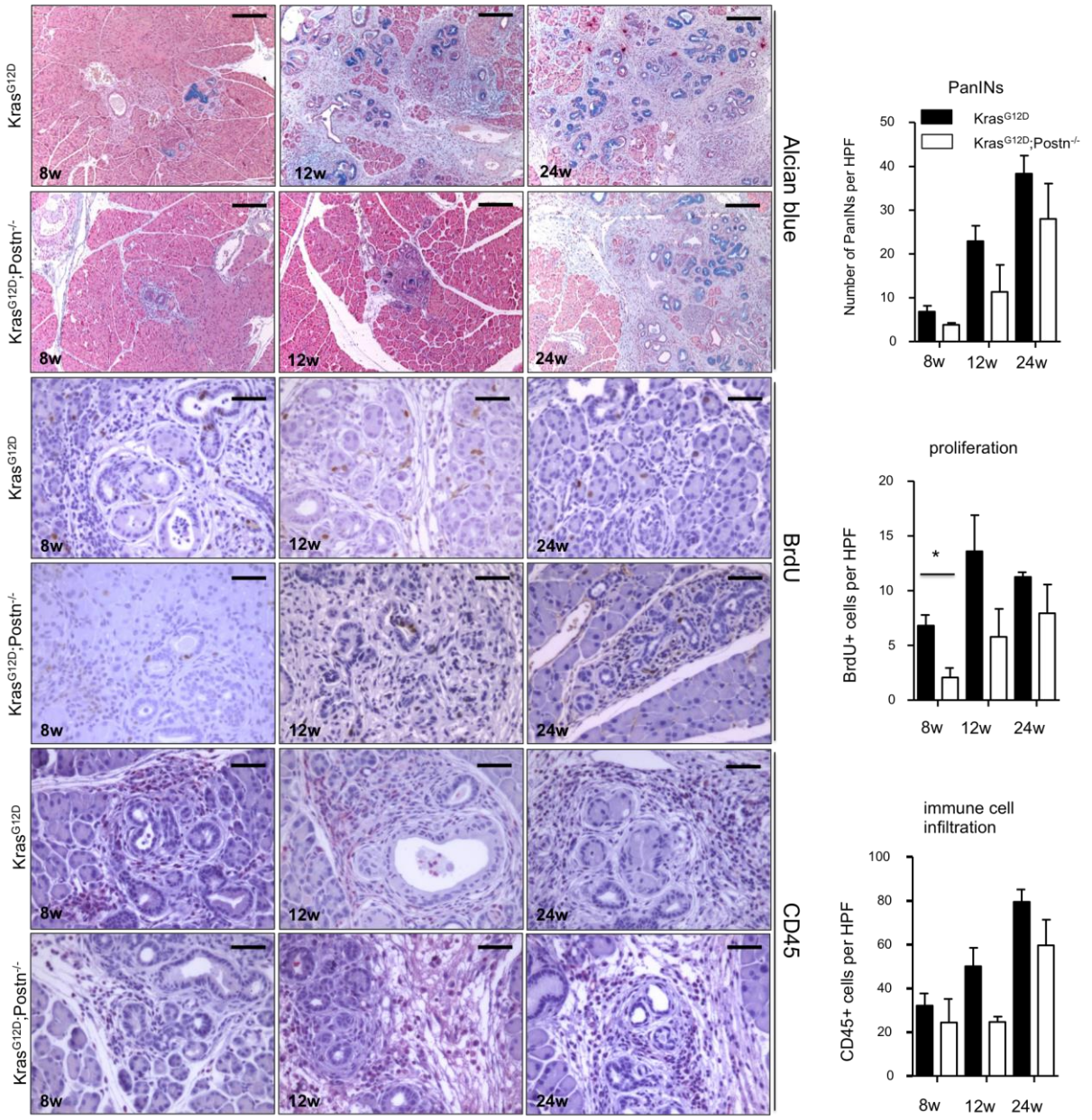

Figure 3.12 Characterization of Kras^{G12D} and Kras^{G12D};Postn$^{-/-}$ mice. Representative pictures of alcian blue staining (scale bars represent 200 µm), BrdU staining (scale bars represent 50 µm.) as well CD45+ staining (scale bars represent 50 µm) and corresponding quantifications. Data are expressed as means ± SEM (n≥3). * P<0.05, unpaired two-tailed t-test.

The trend to an overall more malignant phenotype of Kras^{G12D} mice at early time points was further confirmed by analyzing metaplasia. Therefore, the non-transformed parenchyma of mice was assessed by quantifying the α-Amylase stained area representing functional acinar cells. Kras^{G12D};Postn$^{-/-}$ mice displayed more intact pancreatic parenchyma especially at eight and twelve weeks of age in contrast to Kras^{G12D} mice, which showed a higher metaplastic pancreatic compartment at all time points (Figure 3.13).

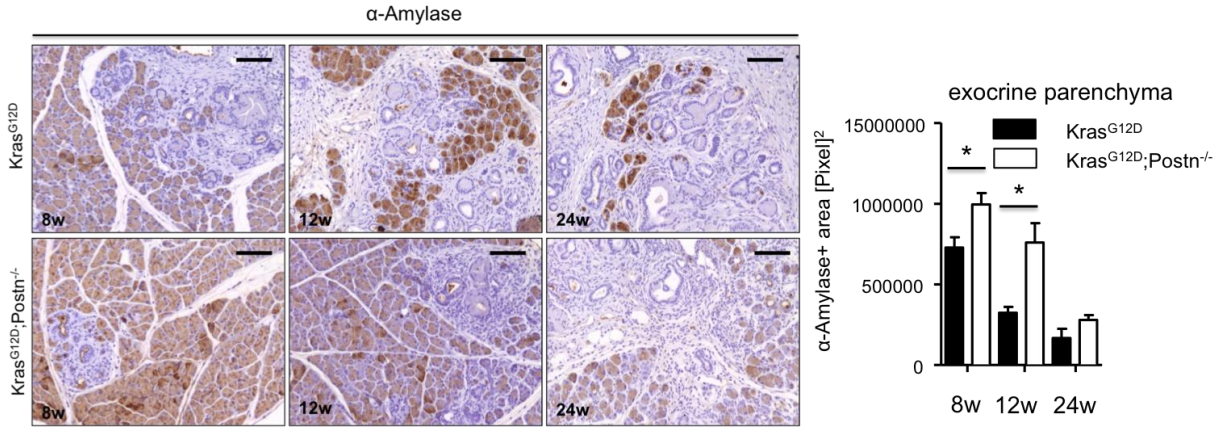

Figure 3.13 Assessment of non-transformed parenchyma. Representative immunohistochemistry staining for α-Amylase and quantification of exocrine parenchyma by calculating the α-Amylase positive area. Scale bars represent 100 µm. Data are expressed as means ± SEM (n≥3). * P<0.05, unpaired two-tailed t-test.

3.2.2 No difference in orthotopic tumor growth between WT and Postn$^{-/-}$ mice

To analyze the function of Periostin in pancreatic carcinogenesis into more detail, orthotopic tumor growth in WT and Postn$^{-/-}$ mice was analyzed. Therefore, one million murine pancreatic cancer cells harboring a heterozygous deletion of p53 and an activating Kras mutation were implanted into the head of the pancreas of mice. After three weeks the mice were sacrificed and the pancreatic tumors were analyzed. Assessment of tumor-to-body weight ratio revealed that there was no difference in tumor growth between the different genotypes (Figure 3.14 A). Further analysis of the tumors demonstrated similar amounts of proliferating cells (Figure 3.14 B and C). While Periostin seems to play a role in early pancreatic carcinogenesis, these results indicate that Periostin does not influence tumor development at late stages.

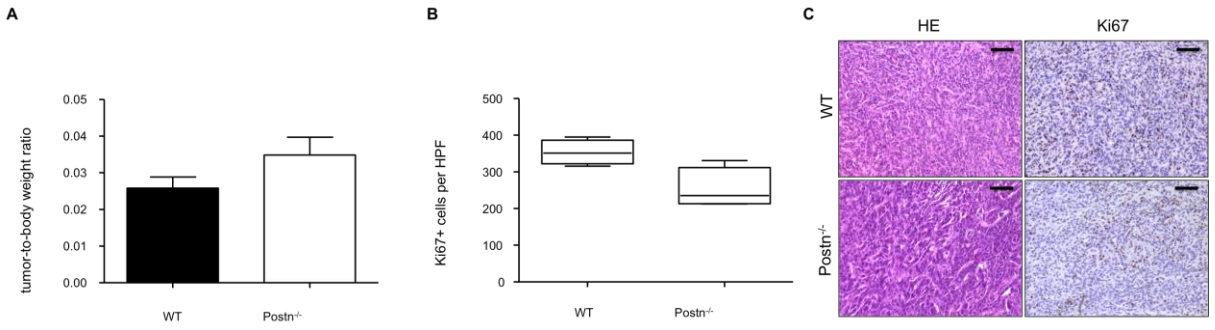

Figure 3.14 Orthotopic tumor growth in WT and Postn$^{-/-}$ mice. One million murine pancreatic cancer cells were implanted to the pancreas of WT and Postn$^{-/-}$ mice. After three weeks mice were sacrificed and orthotopic tumors were analyzed. **A)** Tumor-to-body weight ratio of WT and Postn$^{-/-}$ mice. **B)** Analysis of proliferating cells in orthotopic tumors of WT and Postn$^{-/-}$ mice. **C)** Representative pictures of HE and Ki67 staining of WT and Postn$^{-/-}$ tumors. Scale bars represent 100 µm. Data are expressed as means ± SEM (n≥4), unpaired two-tailed t-test.

3.2.3 Periostin promotes cellular transdifferentiation

To confirm the pro-tumorigenic role of Periostin, *in vitro* analyses were performed. Isolated acini from WT mice were cultured in a 3D collagen-gel system for three days. Upon stimulation with 500 ng/ml murine recombinant Periostin (mrPostn) acinar-to-ductal metaplasia (ADM) could be observed. Immunofluorescence staining of these 3D gels confirmed a transdifferentiation of acinar cells to tubular complexes since these ductal structures showed only a weak expression of the acinar marker α-Amylase and started to express the ductal marker CK19 (Figure 3.15).

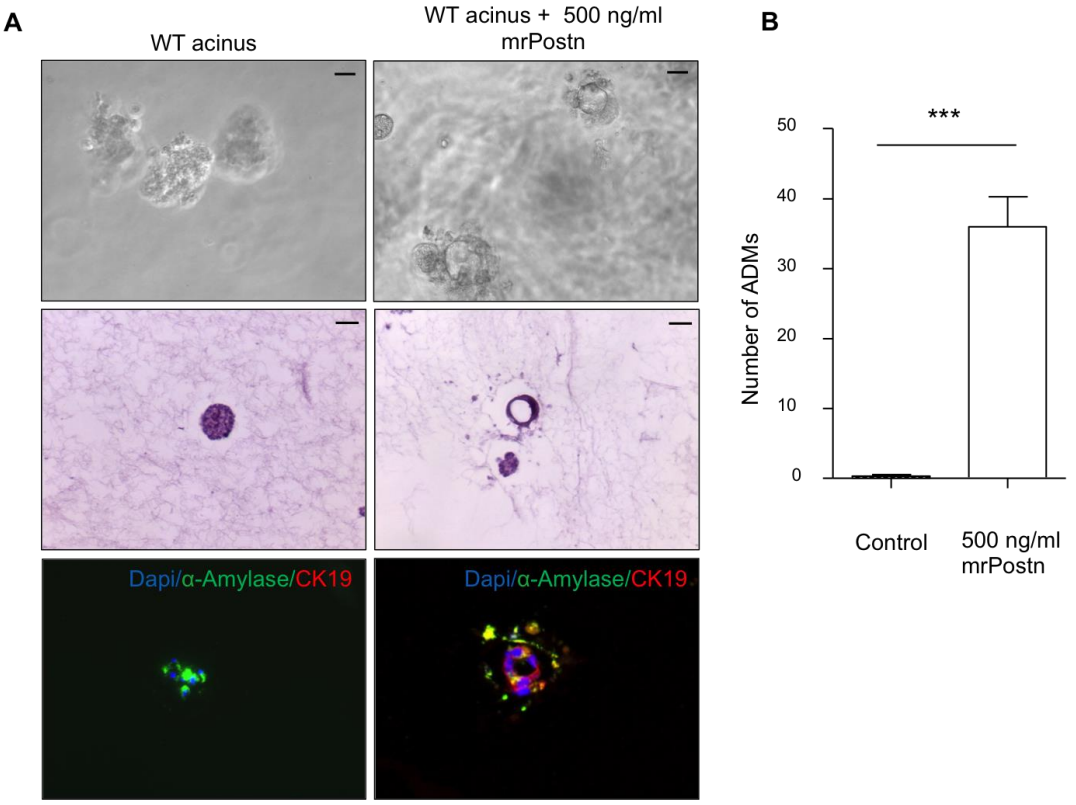

Figure 3.15 Periostin promotes acinar-to-ductal metaplasia. Acinar cells isolated from WT mice were cultured in a 3D culture system. Upon stimulation with 500 ng/ml mrPostn acinar cells underwent ADM formation. **A)** The left panel represents WT acini cells in the 3D cell culture system as well as representative HE staining of embedded 3D gels. Representative immunofluorescence staining demonstrates the expression of the acinar cell specific marker α-Amylase. The right panel shows ADM formation of WT acinar cells upon mrPostn stimulation. Immunofluorescence staining displays the expression of the ductal marker CK19. Scale bars represent 20 µm (microscopic picture) and 100 µm (HE staining). **B)** Quantification of ADMs demonstrating a significant enrichment of ADMs when WT acinar cells were stimulated with mrPostn. Data are expressed as means ± SEM (n≥3). *** P<0.001, unpaired two-tailed t-test.

The pro-tumorigenic function of Periostin was further verified by the soft agar colony formation assay. Here, murine pancreatic cancer cells (1050-KPC and 950-KPC) were cultured in soft agar over a period of 14 days and were stimulated with different concentrations of murine recombinant Periostin protein every second day. Untreated cells hardly exhibited any colony formation whereas upon stimulation with 1 µg/ml mrPostn tumor

colonies were clearly detectable in 1050-KPC cells and 950-KPC cells. However, in 950-KPC cells a significant increase in anchorage independent growth could be also detected at lower mrPostn concentration (Figure 3.16 A and B).

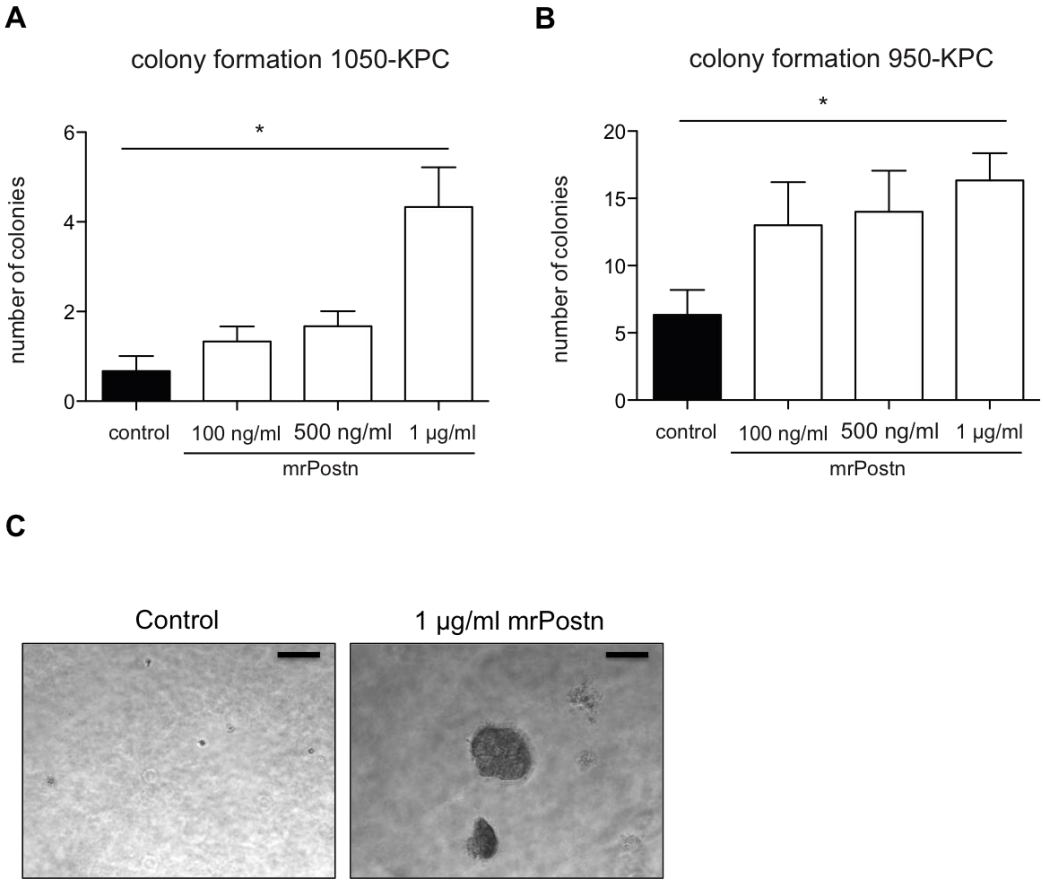

Figure 3.16 Soft agar assay. Murine pancreatic cancer cells were cultured in soft agar for 14 days and stimulated with different concentrations of mrPostn (100 ng/ml, 500 ng/ml, 1 µg/ml) every second day. After 14 days colonies were stained with 0.05% crystal violet and counted under the microscope**. A)** Upon stimulation with 1 µg/ml mrPostn colony formation was significantly increased in the cell line 1050-KPC. **B)** Colony formation was elevated upon 100 ng/ml, 500 ng/ml and 1 µg/ml mrPostn in cell line 950-KPC whereby the effect was significant when 1 µg/ml mrPostn was applied. **C)** Representative pictures of colony formation after 14 days of cell line 950-KPC. Data are expressed as means ± SEM (n≥3). * P<0.05, unpaired two-tailed t-test.

The in vitro findings indicate that in early stages of tumor development Periostin promotes ADM formation, whereas during cancer progression Periostin facilitates anchorage independent growth of tumor cells.

3.2.4 Inflammation-triggered carcinogenesis

To further analyze the effect of Periostin on cancer initiation, caerulein-mediated pancreatitis according to Figure 3.1 was performed in $Kras^{G12D}$;$Postn^{-/-}$ mice to trigger inflammation-induced pancreatic carcinogenesis. However, on the second day of caerulein injections the physical condition of $Kras^{G12D}$;$Postn^{-/-}$ mice worsened apparent from constrained movement and gasping and thus the mice had to be sacrificed after the fourth caerulein injection on the second day. HE staining of pancreatic tissue and analysis of leukocytes showed more

infiltrating immune cells in these mice (Figure 3.17 A and B). Staining for the macrophage specific marker F4/80 further revealed that Kras^{G12D};Postn$^{-/-}$ mice displayed a higher infiltration of macrophages after caerulein-induced pancreatitis (Figure 3.17 A and C).

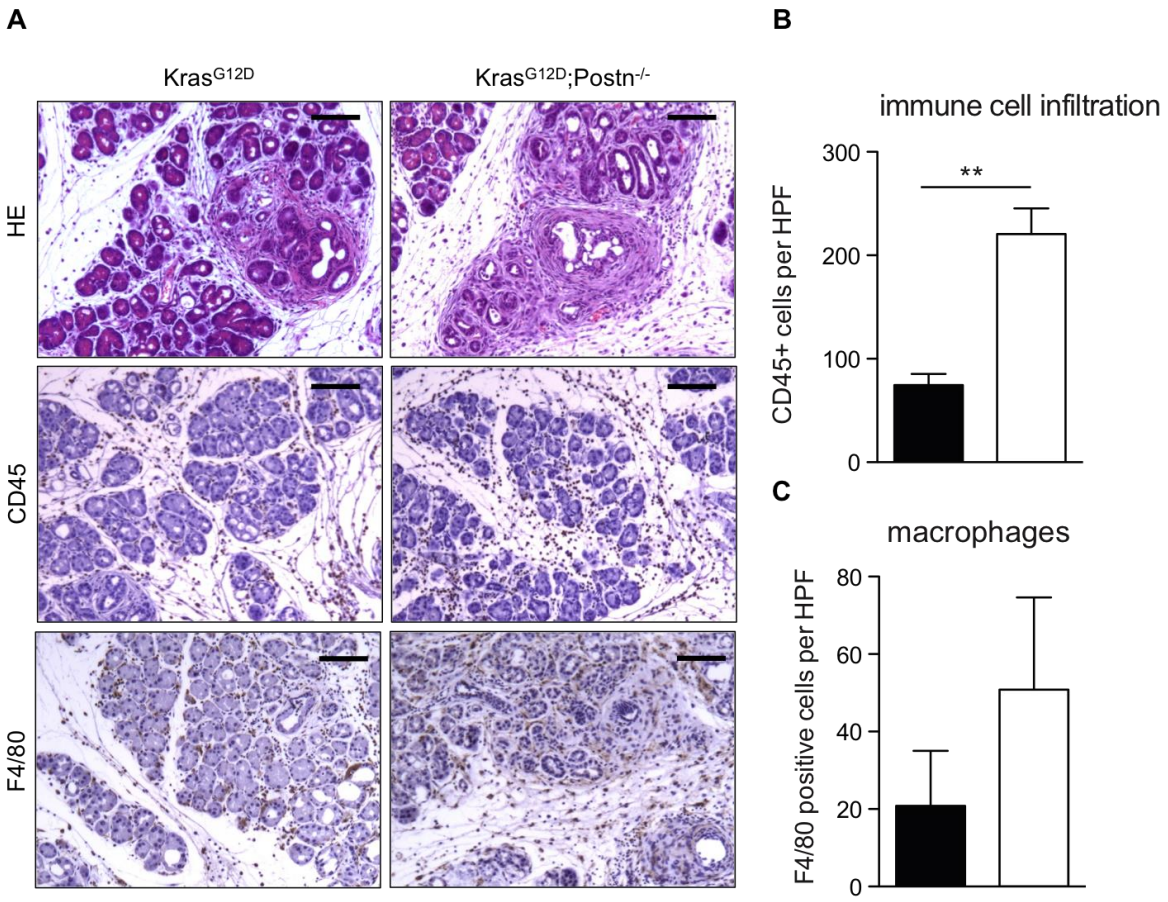

Figure 3.17 Pancreatitis in Kras^{G12D} and Kras^{G12D};Postn$^{-/-}$ mice. Immune cell infiltration was analyzed in paraffin embedded pancreatic tissue of caerulein-induced Kras^{G12D} and Kras^{G12D};Postn$^{-/-}$ mice**. A)** Representative pictures showing the higher amount of infiltrating CD45 and F4/80 cells in Kras^{G12D};Postn$^{-/-}$ mice after pancreatitis. Scale bars represent 100 µm. **B)** Quantification of CD45 and **C** F4/80 positive cells. Data are expressed as means ± SEM (n=3). ** P<0.01, unpaired two-tailed t-test.

Subsequent enzyme-linked immunosorbent assay with serum obtained from Kras^{G12D};Postn$^{-/-}$ mice showed significantly elevated serum IL-6 levels compared to caerulein-treated Kras^{G12D} control mice (Figure 3.18 A). The following histological analysis of lung tissue demonstrated thickened alveolar walls in Kras^{G12D};Postn$^{-/-}$ mice after caerulein-induced pancreatitis indicating severe lung damage in these mice (Figure 3.18 B).

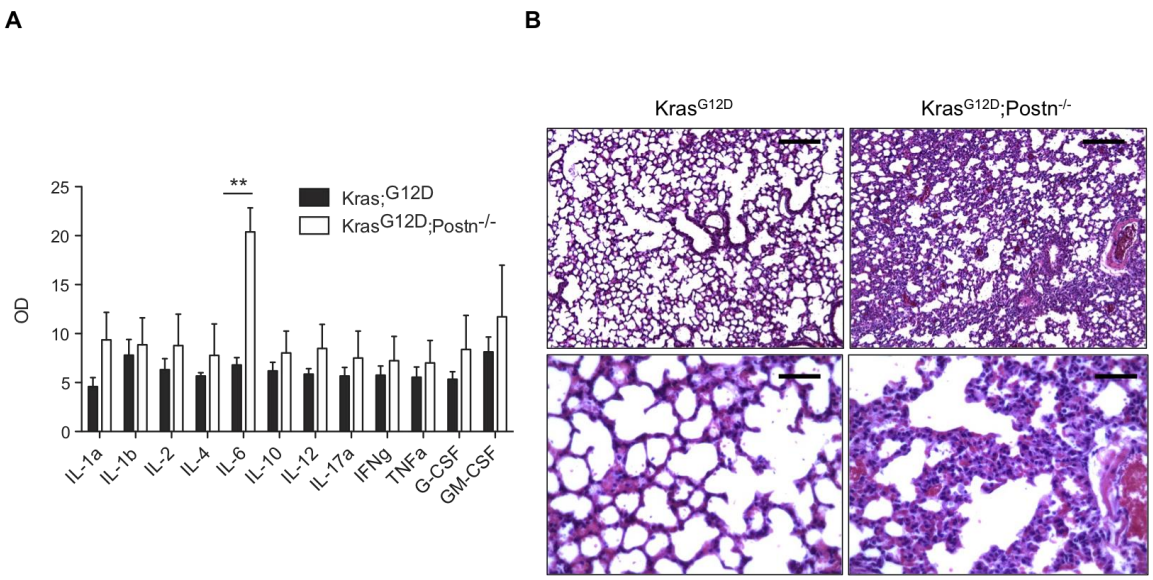

Figure 3.18 Pancreatitis-induced lung damage in Kras^{G12D};Postn$^{-/-}$ mice. Blood was taken from Kras^{G12D} and Kras^{G12D};Postn$^{-/-}$ mice and centrifuged for 10 min at 2,000g to obtain serum. **A)** Enzyme linked immunosorbent assay was performed with this serum to analyze different cytokine levels. Data are expressed as means ± SEM (n=3). **B)** Representative HE staining of pancreatic and lung tissue of Kras^{G12D} and Kras^{G12D};Postn$^{-/-}$ mice after pancreatitis. Scale bars represent 200 µm (upper panel) and 50 µm (lower panel), respectively. ** P<0.01, unpaired two-tailed t-test.

Since acute inflammation-induced carcinogenesis according to the above mentioned protocol was not feasible in Kras^{G12D};Postn$^{-/-}$ mice another approach was utilized to analyze pancreatic carcinogenesis. Chronic pancreatitis was induced by injecting a lower dose of caerulein (50 µg/kg bw) six times a day on three days a week over a period of six weeks. Two months after the last caerulein administration mice were sacrificed and the pancreatic compartment was analyzed. No significant differences in fibrosis, immune cell infiltration and activated stroma index could be observed (Figure 3.19 A-D). However, in Kras^{G12D};Postn$^{-/-}$ mice development of lipomatosis was observed, which to a lesser extent could also be detected in Kras^{G12D};Postn$^{+/-}$ mice but was absent in Kras^{G12D} mice. In parallel, a slightly lower pancreas mass-to-body weight ratio was found in Kras^{G12D};Postn$^{+/-}$ while a significant difference in pancreas mass-to-body weight ratio was detected in Kras^{G12D};Postn$^{-/-}$ mice compared to Kras^{G12D} control mice (Figure 3.19 E and F).

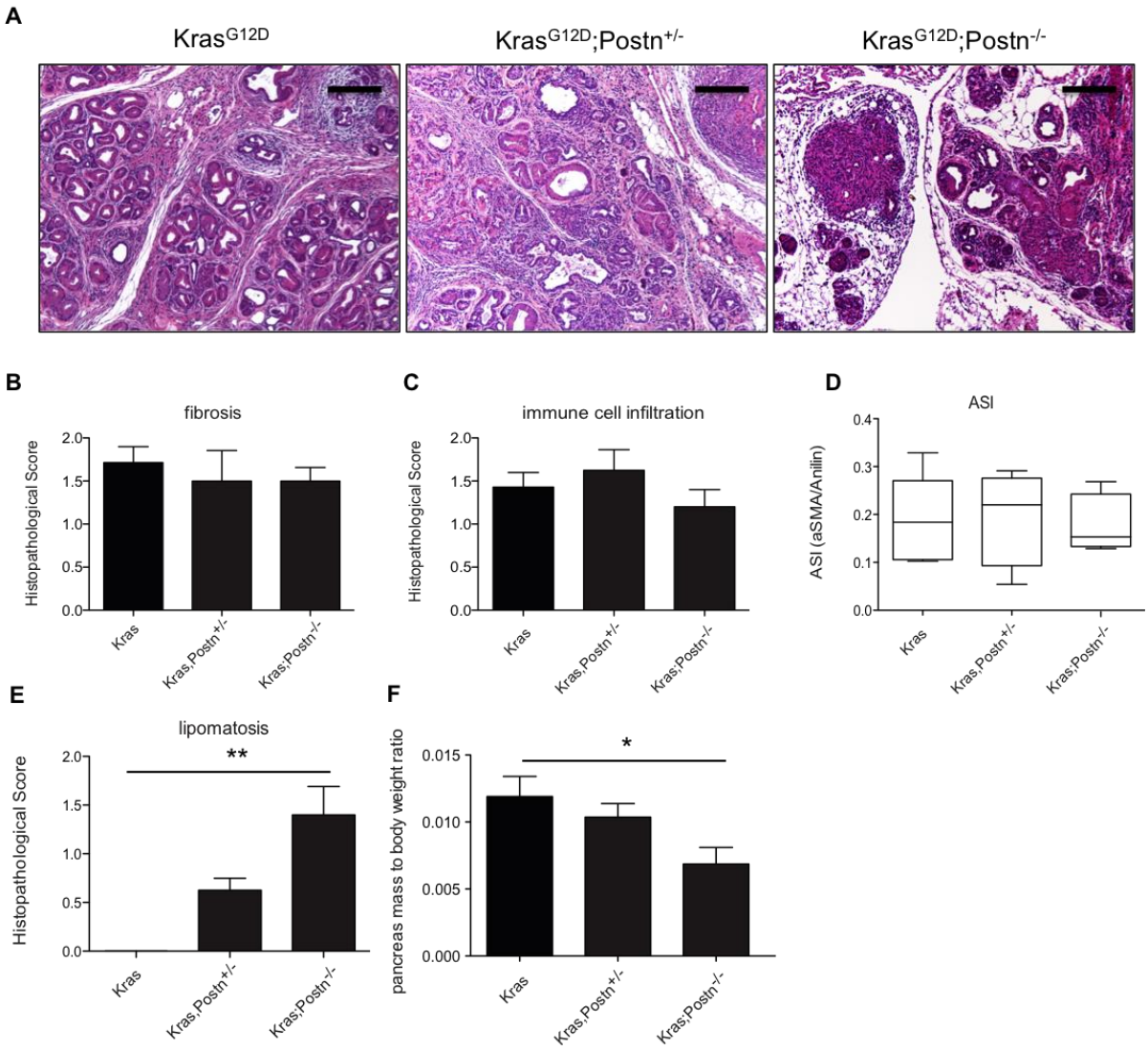

Figure 3.19 Characterization of chronic pancreatitis in Kras^{G12D}, Kras^{G12D};Postn$^{+/-}$ and Kras^{G12D};Postn$^{-/-}$ mice. Chronic pancreatitis was induced by six hourly caerulein injections per day (50 µg/kg bw) on three days a week over a period of six weeks. Two months after the last caerulein administration mice were sacrificed and tissue was formalin-fixed and paraffin embedded. **A)** Representative HE staining of pancreatic tissue of Kras^{G12D}, Kras^{G12D};Postn$^{+/-}$ and Kras^{G12D};Postn$^{-/-}$ mice. Scale bars represent 200 µm. **B)** Results of scoring the HE staining in regard to fibrosis and **C)** immune cell infiltration. **D)** Consecutive sections were stained for aniline and α-Sma and the activated stroma index was calculated. **E)** lipomatosis was analyzed together with a pathologist and **F)** pancreas to body weight ratio was determined. Data are expressed as means ± SEM (n≥4). * P<0.05; ** P<0.01, B and C as well as E Mann-Whitney U-test, D and F unpaired two-tailed t-test.

Inflammation-driven carcinogenesis is an important aspect in pancreatic cancer development. Since caerulein-induced pancreatitis could not be performed in Kras^{G12D};Postn$^{-/-}$ mice due to severe lung damage and although no substantial differences in inflammation-driven carcinogenesis could be observed when inducing chronic pancreatitis in Kras^{G12D} and Kras^{G12D};Postn$^{-/-}$ mice another strategy to analyze inflammation-triggered carcinogenesis was pursued. The aim was to analyze activation of Postn downstream signaling targets in order to identify candidates for an alternative pathway inhibition. Murine pancreatic cancer cells were stimulated with 500 ng/ml murine recombinant Periostin and protein was extracted after

different time points. Western blot analysis showed that Postn activated the mitogen-activated protein kinase ERK, the proto-oncogene tyrosine kinase SRC as well as the focal adhesion kinase (FAK). A strong activation was seen in phosphorylation of the tyrosine 397 of FAK (Figure 3.20). Therefore, to mimic ablation of Periostin signaling in further experiments $Kras^{G12D}$ mice were treated with an inhibitor (PF 573228) targeting the phosphorylation of the tyrosine 397 of FAK.

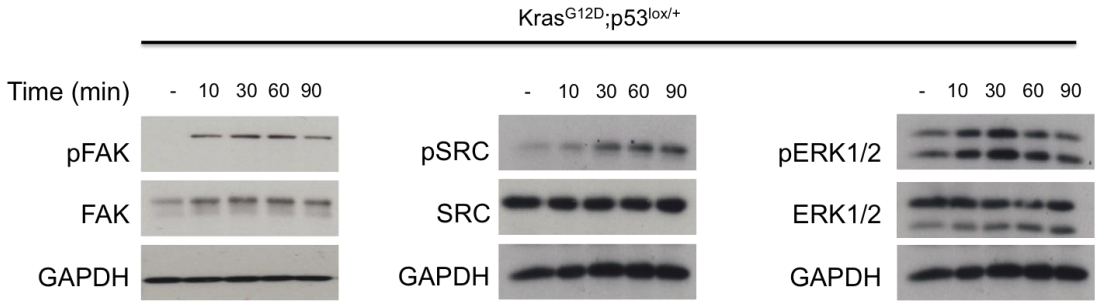

Figure 3.20 Signaling pathways activated by Periostin. Murine pancreatic cancer cell lines were stimulated with 500ng/ml mrPostn and protein was harvested after 0, 10, 30, 60 and 90 minutes. Representative western blots (n=3) demonstrated that the integrin and the MAPK signaling pathway got activated.

To analyze inflammation-triggered development of carcinogenesis, pancreatitis was induced in $Kras^{G12D}$ mice by administration of 100 µg/kg caerulein as depicted in Figure 3.1. Seven days after the last caerulein administration mice were sacrificed. One group of $Kras^{G12D}$ mice additionally received twice daily 30 mg/kg body weight of the FAK inhibitor starting on the day of the first caerulein injection. Morphologic assessment demonstrated that FAK inhibitor treated mice displayed a smaller pancreas compared to untreated mice but still bigger in size than the pancreas of wild type mice (Figure 3.21 A). Immunoblot analyses further showed a reduced pERK and pFAK activation (Figure 3.21 B). Inhibitor treated mice additionally had significantly fewer precancerous lesions as assessed by staining for Muc5 and accordingly to the smaller size of the pancreas also fewer proliferating cells as control animals (Figure 3.21 C and D).

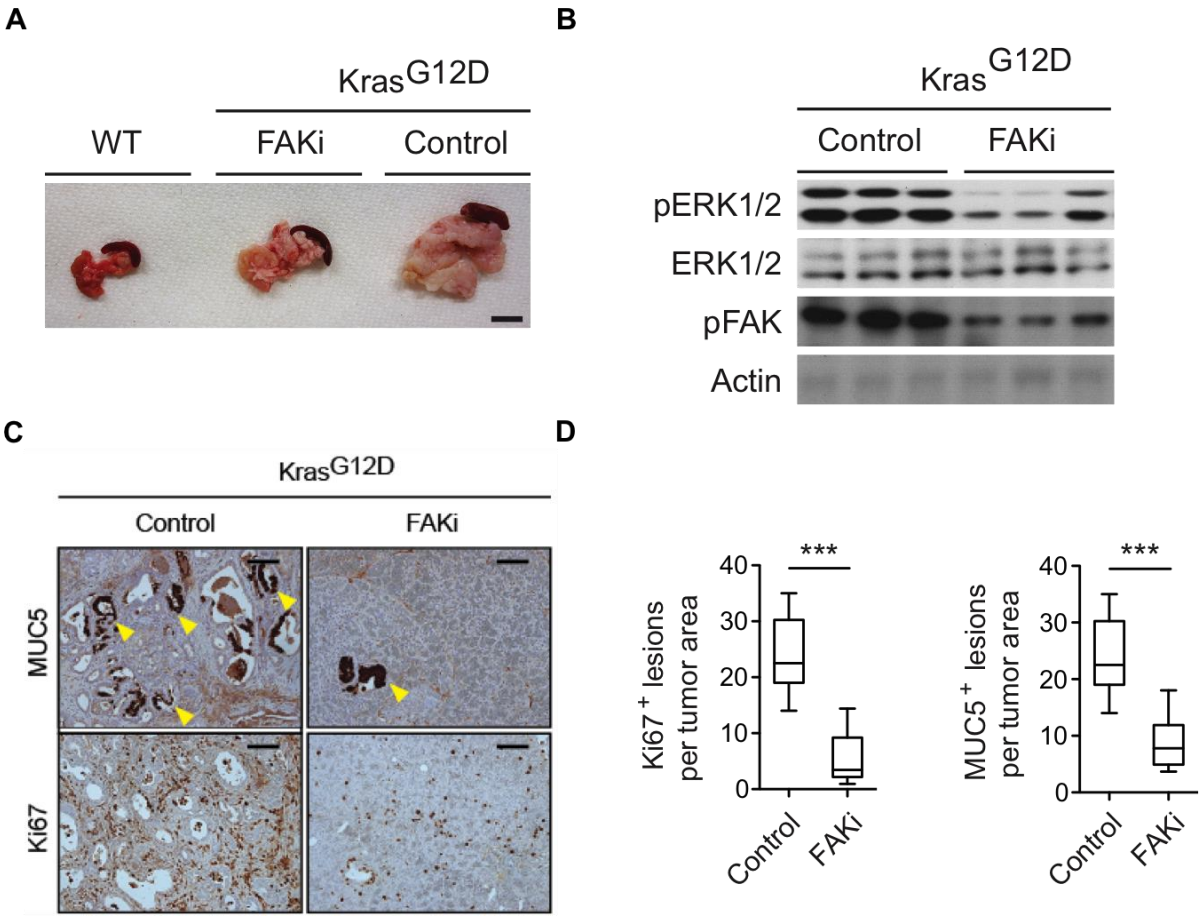

Figure 3.21 Treatment of Kras^{G12D} mice with FAKi. Kras^{G12D} mice were injected with 100 µg/kg bw caerulein for two consecutive days and additionally received twice daily i.p. injections of 30 mg/kg FAKi. After seven days mice were sacrificed and tissue was harvested. **A)** FAKi treated Kras^{G12D} mice exhibited a smaller pancreas than control mice. **B)** Immunoblot analysis demonstrated a reduced activation of ERK and FAK in FAKi treated mice. **C)** Representative immunohistochemistry for MUC5 and Ki67 displaying fewer lesions and proliferating cells in FAKi treated mice. Yellow arrows indicate MUC5 positive lesions. Scale bars represent 50 µm. **D)** Quantification of MUC5 positive lesions and proliferating cells revealed a significant reduction of PanIN lesions and proliferating cells in FAKi treated mice. Data are expressed as means ± SEM (n≥3). *** P<0.001, unpaired two-tailed t-test.

3.2.5 Prolonged survival of FAK inhibitor treated mice

To further scrutinize the effect of FAK inhibition on survival of mice, Kras^{G12D};p53$^{lox/lox}$ mice at the age of 30 days were treated twice daily with 30 mg/kg bw FAK inhibitor until the mice died or showed severe signs of morbidity. Moreover, a combination therapy consisting of FAK inhibitor and the chemotherapeutic drug gemcitabine was applied. Mice were given twice daily 30 mg/kg bw FAK inhibitor and three days a week for four cycles 100 mg/kg gemcitabine (Figure 3.22 A). As control survival of vehicle treated Kras^{G12D};p53$^{lox/lox}$ mice and survival of mice receiving gemcitabine monotherapy was assessed. As shown in Figure 3.22 B survival analysis displayed a significantly longer survival of mice treated with FAK inhibitor (median survival 65 days) compared to untreated (median survival 53 days) and gemcitabine treated mice (median survival 56 days). Furthermore, mice receiving a combination therapy consisting of gemcitabine and FAK inhibitor lived significantly longer (median survival 62

days) compared to vehicle treated mice. However, there was no additional survival benefit of the combination therapy to FAK inhibitor treatment only. Pictures taken of the tumors revealed that the pancreatic tumors of FAKi treated mice were smaller in size compared to untreated or gemcitabine only treated mice. Tumors of mice receiving combination therapy had a similar size as FAKi treated mice (Figure 3.22 C).

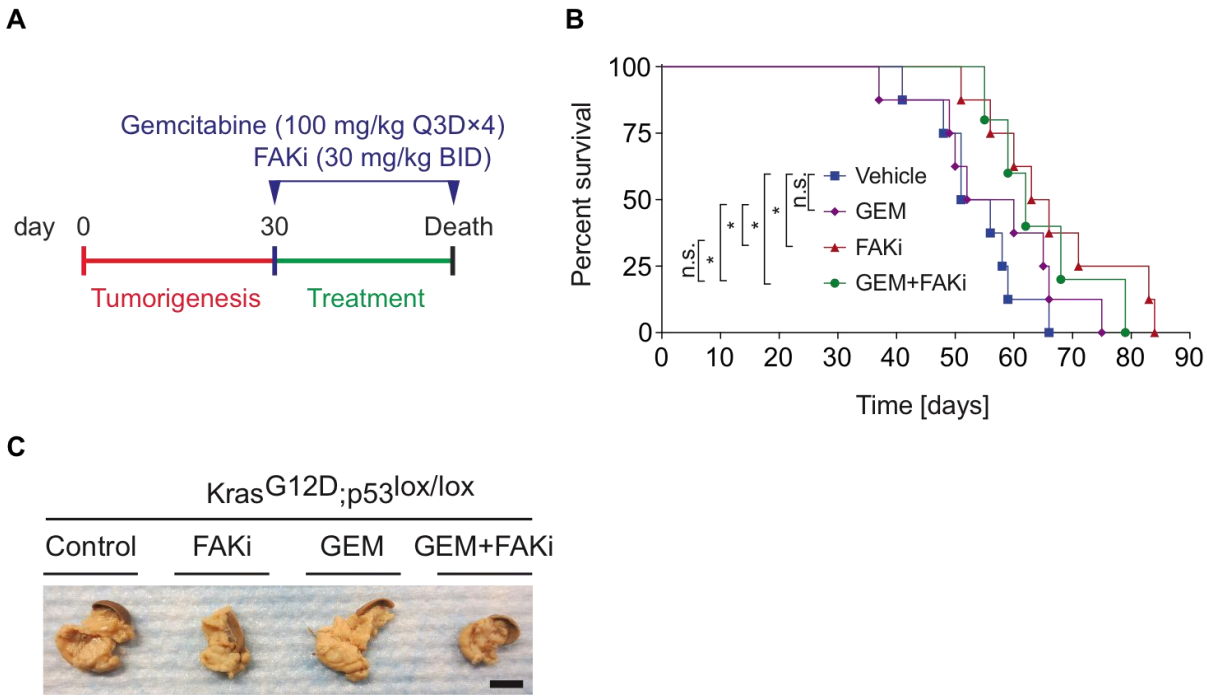

Figure 3.22: Survival analysis. A) Treatment protocol. **B)** Kaplan-Meier curves of gemcitabine, FAKi as well as gemcitabine plus FAKi treated $Kras^{G12D};p53^{lox/lox}$ mice and vehicle treated $Kras^{G12D};p53^{lox/lox}$ mice. **C)** Representative pictures taken from tumors of $Kras^{G12D};p53^{lox/lox}$ control mice, FAKi treated, GEM receiving and FAKi + GEM treated mice revealed smaller pancreatic tumors of FAKi treated and FAKi + GEM treated mice. n≥5; n.s.=not significant; * P<0.05, log-rank test.

Subsequent analysis of tumor tissue revealed significantly higher proliferating tumors of vehicle treated $Kras^{G12D};p53^{lox/lox}$ mice compared to FAKi treated mice. Also, the tumors of mice treated with gemcitabine had a significantly higher proliferation capacity compared to mice receiving FAKi treatment (Figure 3.23 A and B). No difference regarding proliferation could be observed between FAKi and FAKi + GEM treated mice (Figure 3.23 A and B). In line with these results is the observation that mice treated with FAKi and gemcitabine exhibited more apoptotic cells as shown by cleaved Caspase 3 positive cells (Figure 3.23 A and C). Immunohistochemical analysis further showed a higher pERK and pFAK activation in vehicle treated and gemcitabine treated $Kras^{G12D};p53^{lox/lox}$ mice compared to mice receiving FAK inhibitor monotherapy or combination therapy of FAKi and gemcitabine (Figure 3.23 D).

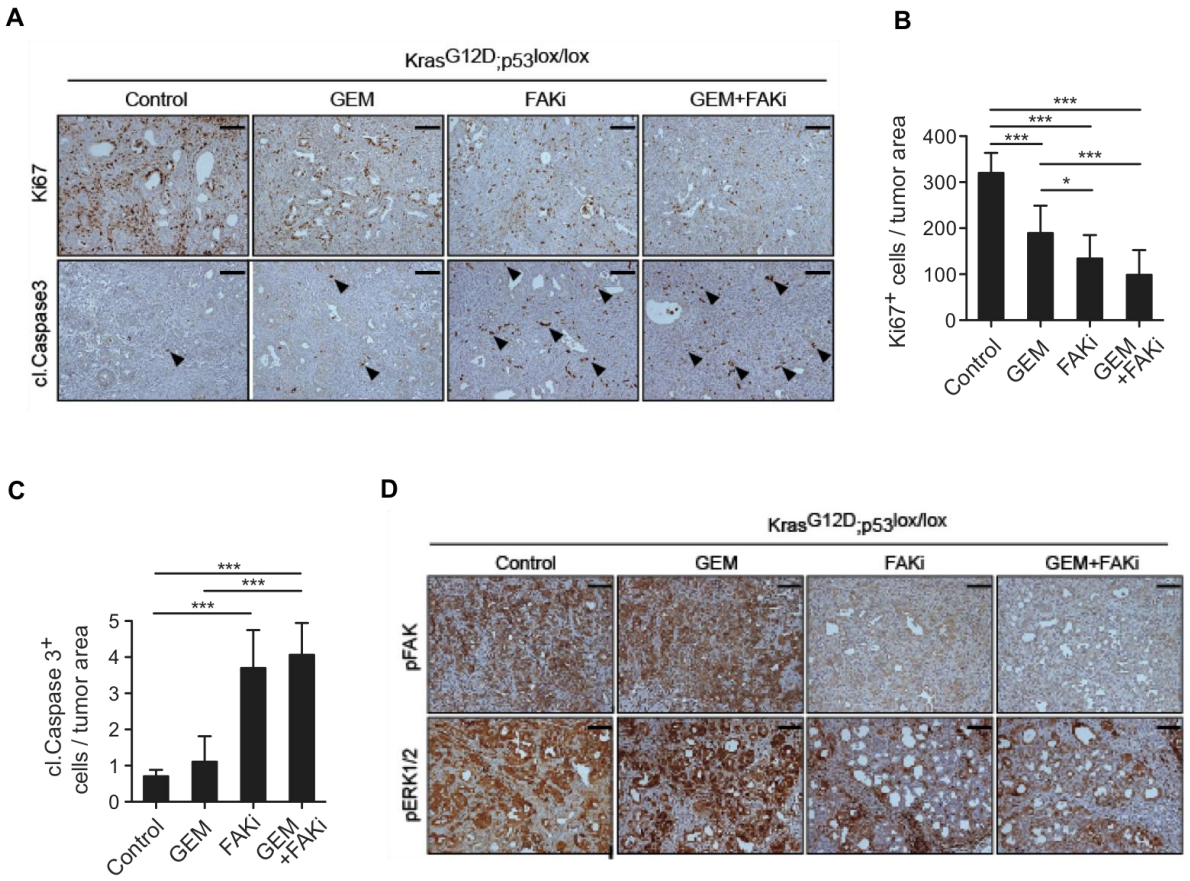

Figure 3.23 Immunohistochemical analysis of pancreatic tumors. A) Representative immunohistochemistry staining for Ki67 and cleaved Caspase 3 demonstrating that FAKi and FAKi + GEM treated tumors had fewer proliferating and at the same time more apoptotic cells compared to control and GEM treated mice. Black arrows indicate apoptotic cells. Scale bars represent 50 µm. **B)** Quantification of Ki67 positive cells. Data are expressed as means ± SEM (n≥3). **C)** Quantification of cleaved Caspase 3 positive cells. Data are expressed as means ± SEM (n≥3). **D)** Representative immunohistochemistry staining for pFAK and pERK showing reduced FAK and ERK activation in FAKi and FAKi + GEM treated mice. Scale bars represent 50 µm. * P<0.05; *** P<0.001, unpaired two-tailed t-test.

Taken together these findings indicate that Periostin promotes tumor initiation at very early stages since Periostin ablation in $Kras^{G12D}$ mice resulted in a less severe phenotype particularly at eight and twelve weeks of age. Moreover pancreatic cancer progression was significantly accelerated in caerulein treated $Kras^{G12D}$ mice as well as in the $Kras^{G12D};p53^{lox/lox}$ mouse model of pancreatic cancer. Inhibition of Periostin signaling by using an FAK inhibitor resulted in a blocked pancreatic carcinogenesis and longer survival of mice. Thus, Periostin and especially its downstream signaling pathways represent promising targets to inhibit pancreatic cancer initiation as well as progression.

3.3 Periostin supports metastatic spread

3.3.1 Periostin induces invasion and metastasis formation

Recent published literature has shown that in breast cancer Periostin has an important function in creating a metastatic niche at the secondary target organ (Malanchi et al. 2012). Moreover, Periostin expression was described to be present in liver and lymph node metastases of pancreatic cancer patients (Erkan et al. 2007). Thus, the influence of Periostin in supporting metastasis formation at distant organs in a mouse model was analyzed.

First the invasive potential of murine pancreatic cancer cells harboring a heterozygous deletion of p53 and an activating Kras mutation was investigated upon Periostin stimulation using the Boyden chamber invasion assay. Indeed, when stimulated with 500 ng/ml murine recombinant Periostin, pancreatic cancer cells showed a significantly higher invasive behavior compared to untreated cells. In contrast, treatment of cells with a lower dose of 100 ng/ml as well as with a higher dose of 1 µg/ml showed no effect indicating that tumor cell invasion depends on a restricted dose of Periostin in the tumor cell environment (Figure 3.24 A). Additional administration of either 10 µM FAK inhibitor or 10 µg/ml neutralizing Periostin antibody abolished the invasive potential as a significant decrease of invasion was detected (Figure 3.24 B).

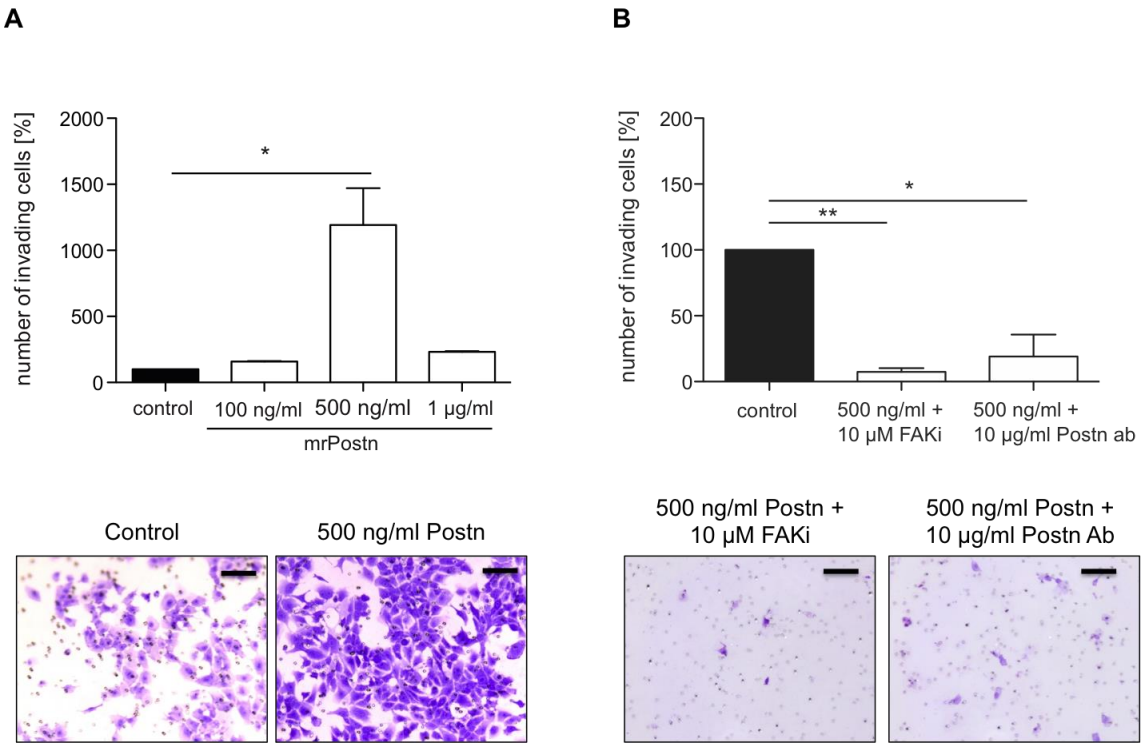

Figure 3.24 Periostin promotes invasion of pancreatic cancer cells. Murine pancreatic cancer cells were seeded on matrigel coated invasion chambers and invasive potential was assessed upon mrPostn treatment and simultaneous FAKi and neutralizing Postn antibody treatment. **A)** The number of invasive pancreatic cancer cells was significantly increased upon stimulation with 500 ng/ml mrPostn. Representative pictures are shown. Scale bars represent 100 µm. **B)** The treatment of

mrPostn (500 ng/ml) stimulated cells with either 10 µM FAKi or 10 µg/ml Postn antibody diminished the invasive behavior of pancreatic cancer cells significantly. Representative pictures are shown. Scale bars represent 100 µm. Data are expressed as means ± SEM (n=3). * P<0.05; ** P<0.01, unpaired two-tailed t-test.

To scrutinize if Periostin supports metastatic spread *in vivo* one million murine pancreatic cancer cells were injected into the tail vein of WT, Postn$^{+/-}$ and Postn$^{-/-}$ mice and tissue of these mice was analyzed for metastases formation after 5 weeks. When sacrificing the mice, macroscopic metastases in the lung of WT and Postn$^{+/-}$ mice could be observed whereas in Postn$^{-/-}$ mice no macroscopic metastases were visible (Figure 3.25 A). As illustrated in Figure 3.25 B and C the subsequent analysis of the HE stained lung tissue confirmed the absence of metastases in Posn$^{-/-}$ mice. Furthermore, the HE staining revealed that metastases in Postn$^{+/-}$ were smaller in size compared to the ones detected in WT mice. Staining of WT and Postn$^{+/-}$ lung metastases for Periostin (Figure 3.25 B) showed a strong expression of this ECM molecule in lung metastases whereas no Periostin expression could be detected in normal lung tissue indicating that cancer cells activate resident lung fibroblasts, which then express Periostin.

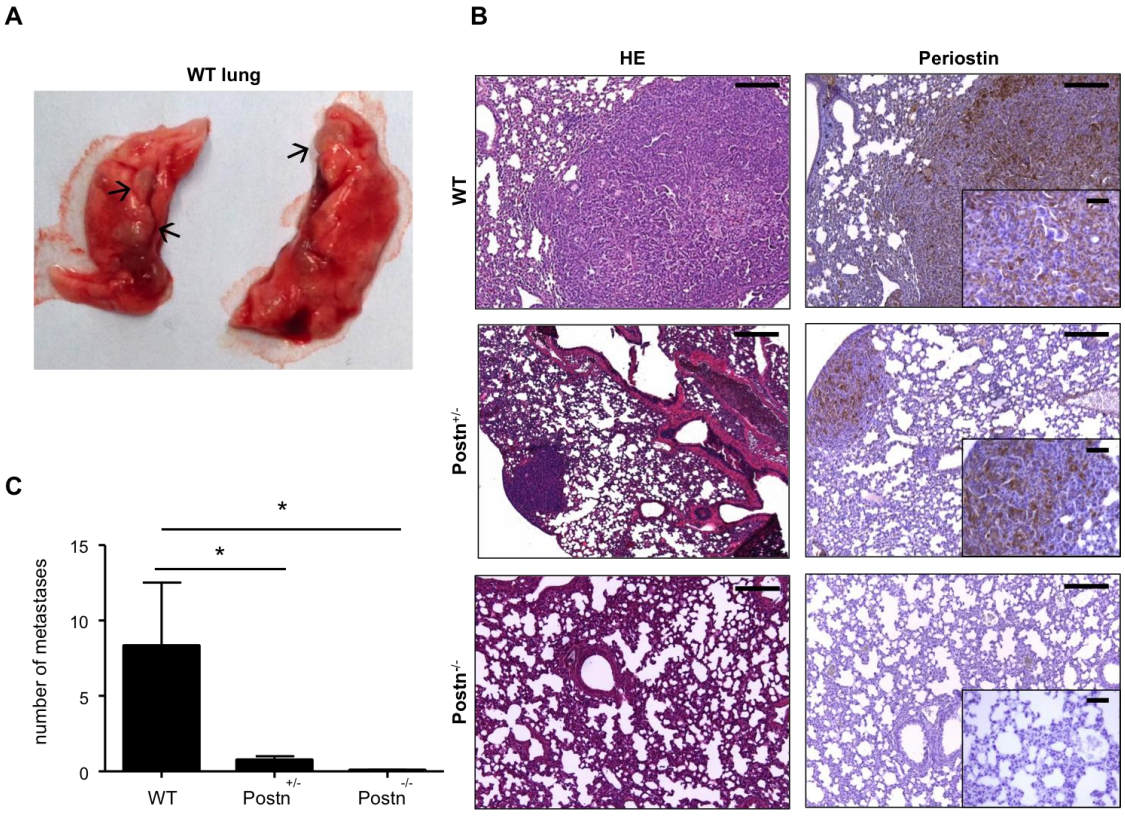

Figure 3.25: Metastasis formation *in vivo*. 1x10^6 murine pancreatic cancer cells in 150 µl PBS were injected to the tail vein of 8-week old WT, Postn$^{+/-}$ and Postn$^{-/-}$ mice and sacrificed after 5 weeks. **A)** Representative picture showing lung metastasis in a WT mouse five weeks after injection of pancreatic tumor cells to the tail vein. **B)** Representative HE staining (left panel) showing a big metastasis in the lung of a WT mouse, a smaller metastasis in a Postn$^{+/-}$ mouse and no metastasis in a Postn$^{-/-}$ mouse. Immunohistochemistry for Periostin showing that Periostin expression is induced in the lung metastasis of WT and Postn$^{+/-}$ mice (right panel). Scale bars represent 200 µm and 50 µm (inserts), respectively. **C)** Quantification of metastases in WT, Postn$^{+/-}$ and Postn$^{-/-}$ mice displaying significant

differences between WT and Postn$^{+/-}$ and WT and Postn$^{-/-}$ mice. Data are expressed as means ± SEM (n≥4). * P<0.05, Mann-Whitney U-test.

3.3.2 Inhibition of FAK results in reduction of metastasis formation

In a next step the ability of the FAK inhibitor in reducing metastasis formation was examined. Therefore, WT mice were injected with one million murine pancreatic cancer cells and additionally treated with a daily i.p. dose of 30 mg/kg bw FAK inhibitor for five weeks (Figure 3.26 A). When mice were sacrificed no macroscopic metastases were visible and further analysis of HE stained lung tissues demonstrated that FAK inhibitor treatment significantly reduced metastasis formation in WT mice since only one metastasis in one WT mouse was detected (Figure 3.26 B and C).

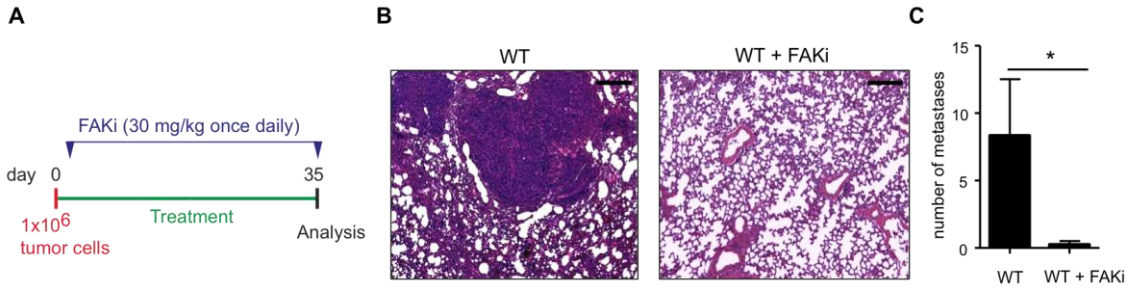

Figure 3.26: Treatment of tail vein injected WT mice with FAKi. After injection of 1x10^6 pancreatic cancer cells to the tail vein of WT mice, mice received a daily dose of 30 mg/kg bw for 5 weeks. **A)** Protocol of tail vein injected mice receiving FAKi treatment. **B)** Representative HE staining of WT and FAKi treated WT lung tissue. **C)** Quantitative analysis of metastases in WT and FAKi treated WT mice showing a significant reduction of metastases upon FAKi treatment. Data are expressed as means ± SEM (n≥4). * P<0.05, Mann-Whitney U-test.

3.2.6 Impaired survival of cancer cells in the secondary target organ of Postn$^{-/-}$ mice

After showing that ablation of Periostin inhibits metastasis formation in the secondary target organ an *in vivo* seeding assay was performed to find out if attachment of pancreatic cancer cells in Postn$^{-/-}$ mice is disturbed or if the cancer cells are able to attach but do not further proliferate or survive. WT, Postn$^{+/-}$ and Postn$^{-/-}$ mice were again injected with one million pancreatic cancer cells and sacrificed after 48 hours to check for attached cancer cells in the lung and sacrificed after 120 hours to analyze proliferation and survival of cancer cells in the lung tissue.

The results of the *in vivo* seeding assay revealed that in all genotypes pancreatic cancer cells have attached in the lung after 48 hours since in all lung tissues pERK positive cancer cells could be detected (Figure 3.27 A). While in WT mice even more pERK positive cells were identified after 120 hours in Postn$^{-/-}$ hardly any p-ERK positive cells were found (Figure 3.27 A and B). These results imply that Periostin promotes metastasis formation in WT mice by creating a niche in the lung tissue, which fosters proliferation and survival of cancer cells.

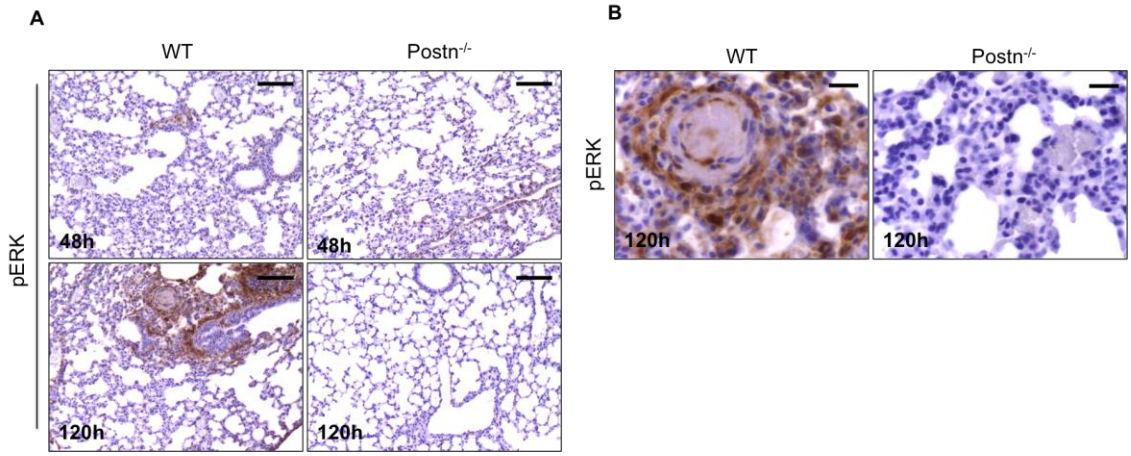

Figure 3.27 In vivo seeding assay. 1x10^6 murine pancreatic cancer cells were injected to the tail vein of WT and Postn$^{-/-}$ mice. After 48h and 120h mice were sacrificed and tissue was harvested. **A)** After 48 hours in WT as well as in Postn$^{-/-}$ mice pERK positive cells were detected whereas at 120 hours hardly and pERK positive cells were present in Postn$^{-/-}$ mice anymore. Scale bars represent 100 µm. **B)** Higher magnification showing the pERK positive cells in WT mice 120 hours after tail vein injection of mice. Scale bars represent 20 µm.

To check if Periostin influences proliferation of cancer cells in vitro, an MTT assay was performed. Pancreatic cancer cells were seeded in a 96-well plate and stimulated with different concentrations of recombinant Periostin. Untreated cancer cells were used as control. Over the course of five days proliferation of cancer cells was assessed. Surprisingly, no difference between untreated and Periostin stimulated cancer cells was detected in regard to proliferation (Figure 3.28). These findings might be due to the fact that the complete microenvironment is missing and that the cancer cells already show a high proliferative behavior.

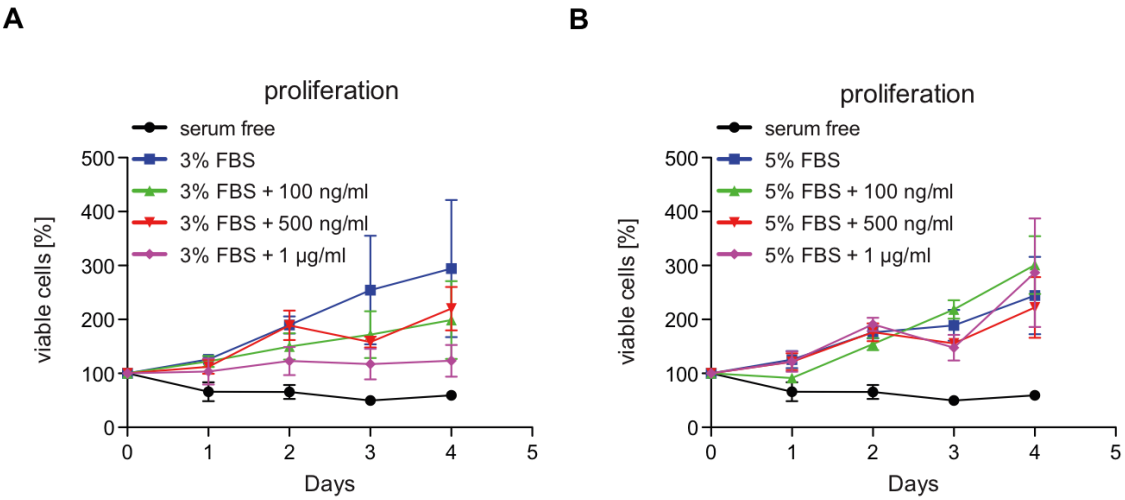

Figure 3.28 Proliferation of mrPostn treated pancreatic cancer cells. Murine pancreatic cancer cells cultured in DMEM supplemented with **A)** 3% FBS or **B)** 5% FBS were treated with 100 ng/ml, 500 ng/ml or 1 µg/ml mrPostn and proliferation was assessed. As control cells cultured in DMEM supplemented with either 3% FBS or 5% FBS as well as cells in serum free DMEM were used**.** No effect of mrPostn stimulation on proliferation could be observed. Data are expressed as means ± SEM (n=3), unpaired two-paired t-test.

3.3.3 No difference in tumor cell release

In order to analyze if there is not only a difference in tumor cell proliferation and survival in the secondary target organ upon Periostin ablation but also in cell release from the primary tumor the amount of circulating tumor cells in $Kras^{G12D};p53^{lox/+}$ and FAKi treated $Kras^{G12D};p53^{lox/+}$ mice was assessed. Blood of 11-week old mice treated either with a daily dose of 30 mg/kg bw FAK inhibitor or vehicle control for seven days was cultured in DMEM supplemented with 10% FBS for 10 days. Attached epithelial cells were stained with crystal violet, counted and compared between the two groups.

As shown in Figure 3.29 no difference in tumor cell release was found in FAKi treated and untreated $Kras^{G12D};p53^{lox/lox}$ mice. After 10 days in culture, similar amounts of epithelial cells normalized to the blood volume taken were detected.

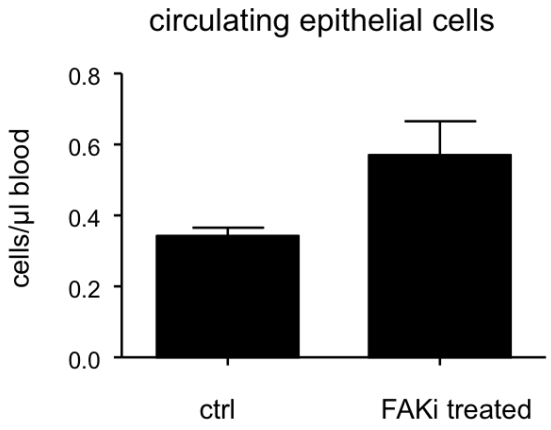

Figure 3.29 Analysis of circulating epithelial cells. $Kras^{G12D};p53^{lox/+}$ mice at the age of 10 weeks were treated with a daily dose of FAK inhibitor (30 mg/kg bw) or with vehicle control. After seven days blood was taken and cultured in DMEM supplemented with 10% FBS for 10 days. Attached epithelial cells were stained with 0.05% crystal violet and counted under the microscope and correlated to the blood volume taken. Data are expressed as means ± SEM (n≥4), unpaired two-tailed t-test.

3.3.4 Analysis of transcriptional regulation of Periostin expression

To analyze how cancer cells activate fibroblasts or pancreatic stellate cells, which then express Periostin, the human Periostin promoter sequence was analyzed for potential transcription factor binding sites. Among others, the in silico analysis revealed binding sites for c-MYC and NFTAc2 in the Periostin promoter. In subsequent experiments the Periostin promoter sequence was cloned into a luciferase reporter vector and transfection experiments in the HeLa cell line were performed to find out if expression of c-MYC and NFATc2 are able to activate the Periostin promoter.

Transfection experiments demonstrated that c-MYC expression is able to induce transcriptional activity of the Periostin promoter (Figure 3.30 A) whereas no increase of transcriptional activity was observed when NFATc2 was expressed (Figure 3.30 B).

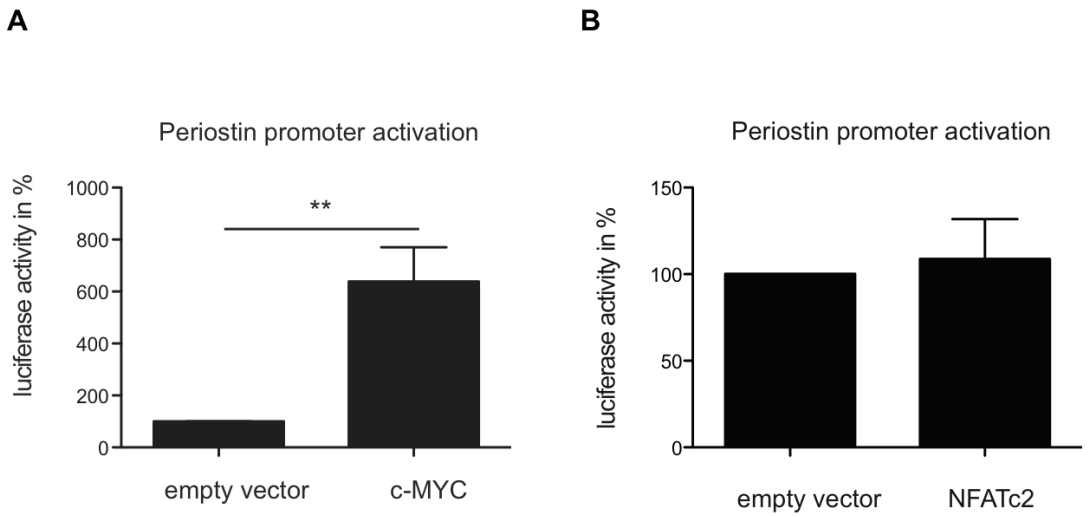

Figure 3.30 Transcriptional activation of the Periostin promoter. A 2.276 kb sequence of the Periostin promoter was cloned into a pGL3 luciferase reporter vector and activation of the Periostin promoter was analyzed upon expression of c-MYC or NFATc2. **A)** Upon expression of c-MYC a significant activation of luciferase activity was detected. **B)** No activation of luciferase activity could be found after expression of NFATc2. Data are expressed as means ± SEM (n=3). ** P<0.01, unpaired two-tailed t-test.

4 Discussion

Pancreatic cancer is the seventh leading cause of cancer deaths in men and women worldwide (Torre et al. 2015) and with 85% pancreatic ductal adenocarcinoma represents the most common pancreatic neoplasm (Hezel et al. 2006). Despite intensive research the 5-year survival rate of pancreatic cancer patients has not fundamentally improved over the last three decades. It stays persistently low at 7% (Siegel, Miller, and Jemal 2015). This is primarily due to the absence of suitable biomarkers and a late detection of this deadly disease when metastases are already present and a resection of the tumor is not an option any more. One of the established risk factors contributing to PDAC development is chronic pancreatitis (Lowenfels et al. 1993). Steady inflammatory processes stimulate continuous acinar cell metaplasia and a strong tissue fibrosis, which is thought to be a prerequisite for oncogene-mediated transformation and tumor development.

Under physiological conditions the exocrine compartment of the pancreas has a high regeneration capacity and acinar-to-ductal metaplasia (ADM) is only transiently induced for tissue recovery. In detail, upon inflammation the pancreatic acinar cells transiently lose their characteristic phenotype and trans/dedifferentiate into duct-like structures. Hereby, the cells temporarily re-express pancreatic progenitor genes and exhibit a proliferative phenotype in order to replace the damaged tissue. When the pancreas fully recovers the inflammation subsides and the acinar cells regain their morphologic structure and express differentiation genes again (Jensen et al. 2005). However, when the inflammation persists and oncogenic stimuli are present, the acinar cells keep their proliferative features and preinvasive tumor lesions can arise. Understanding the molecular mechanism and role of proteins involved in tissue repair of the pancreas is of upmost importance since sustained tissue damage can result in development of precancerous lesions (Coussens and Werb 2002).

One of the main characteristics of acute and chronic pancreatitis as well as PDAC is the fibrotic response, which is particularly abundant in chronic pancreatitis and PDAC. In fact, tumor desmoplasia can constitute up to 80 percent of the tumor mass (Erkan et al. 2008, Mollenhauer, Roether, and Kern 1987). The stromal compartment consists of different cell types such as pancreatic stellate cells, fibroblasts, endothelial and nerve cells as well as extracellular matrix proteins. Activated pancreatic stellate cells have been identified to contribute substantially to the huge deposition of ECM and thus to the vast fibrotic reaction in PDAC (Bachem et al. 2005). However, for a long time the desmoplastic reaction has been considered as a passive entity but it becomes clearer now that it plays an active role in pancreatic carcinogenesis and metastatic spread. However, so far its functional relevance is still controversial. One of the highly upregulated ECM proteins in pancreatic cancer is Periostin (Erkan et al. 2007, Friess et al. 2003). In vitro studies have demonstrated a pro-tumorigenic role of Periostin in pancreatic cancer (Erkan et al. 2007, Baril et al. 2007).

Though, the function of Periostin *in vivo* has not been analyzed so far neither in pancreatitis nor in pancreatic neoplasms. Thus, the aim of this study was on the one hand to characterize the role of Periostin in acute pancreatitis and following tissue recovery. On the other hand the influence of the ECM protein Periostin in pancreatic tumorigenesis and metastatic spread was analyzed. Additionally, the inhibition of Periostin signaling as a potential new therapeutic option in treatment of pancreatic cancer was assessed.

4.1 The role of Periostin in acute pancreatitis and regeneration

The mechanisms contributing to successful regeneration of the exocrine compartment after caerulein-induced tissue damage are still not fully resolved. While it is known that morphological changes of acinar cells (ADM) and changes of the gene expression profile, which includes the re-expression of pancreatic progenitor genes such as Hes1 and Pdx1, are required, the role of the mesenchymal compartment and expression of Periostin in pancreatic regeneration has not been addressed so far (Jensen et al. 2005). Since no data from pancreatitis mouse models exist as of yet, this study focuses on analyzing the function of the ECM protein Periostin in inflammation and exocrine recovery using Periostin global knock out mice.

4.1.1 Periostin in the acute phase of pancreatitis

First, the endocrine and exocrine pancreatic compartment in healthy 8-week old mice was analyzed. Histological examination revealed no differences in Periostin deficient mice compared to corresponding wild type mice. This finding is in line with a recent study analyzing endocrine compartment regeneration after partial pancreatectomy, where the authors also did not observe any abnormalities in healthy Periostin deficient pancreata (Smid, Faulkes, and Rudnicki 2015). Also in other organs such as heart, no differences in the cardiac parenchyma were found in healthy Periostin deficient mice (Shimazaki et al. 2008). Moreover, in the present study no variation in the pancreas mass-to-body weight ratio in healthy 8-week old Periostin deficient and wild type mice was measurable. Hence, the lack of Periostin expression during embryogenesis seems not to overtly affect the development of the pancreatic compartment.

During severe acute pancreatitis an upregulation of Periostin mRNA and protein expression was detected in wild type mice, which reached its peak two days after the last caerulein injection and then declined step by step until it returned to almost basal levels after twenty-one days. Similar observations have been made in other inflammatory diseases. In a mouse model of abdominal aortic aneurysms Periostin expression is also temporarily induced in the aortic wall upon inflammation of the tissue and afterwards gradually decreases until it reaches basal expression levels. However, in the abdominal aortic aneurysms model a re-

expression of Periostin can be observed at later time points during the progression phase of abdominal aortic aneurysms (Yamashita et al. 2013).

In the acute phase of pancreatitis deposition of Periostin was mostly found around acinar complexes and to a lesser extend interlobular. In the regenerative phase Periostin was primarily localized in regenerative areas. So far, nobody else has analyzed Periostin expression in severe acute pancreatitis. However, a study performed with human chronic pancreatic tissue found similar results regarding the Periostin localization. Erkan and colleagues detected elevated Periostin expression in pancreatic tissue of chronic pancreatitis patients whereby the localization of this ECM molecule was mainly found in periacinar spaces (Erkan et al. 2009), which indicates that a direct contact of Periostin and epithelial cells exists.

To further characterize the role of Periostin in acute pancreatitis, caerulein-induced tissue injury was analyzed in Periostin deficient mice and compared to wild type mice. In the acute phase of pancreatic inflammation no difference was found between mice lacking Periostin expression and wild type mice. Both genotypes displayed a comparable high infiltration of immune cells and transdifferentiation of acinar to duct-like cells. Additionally, amylase, lipase, lactate dehydrogenase and calcium serum levels were alike in both mice one day after the last injection with caerulein confirming a similar severity of pancreatitis. During acute pancreatitis as well as in the regenerative phase a higher proportion of α-Sma positive cells was detected in Periostin deficient mice and at the same time collagen deposition was reduced. Since earlier reports have demonstrated that Periostin has an important function in activating PSCs and keeping them in an activated state, these results might occur controversial at first glance (Erkan et al. 2007). However, despite the higher amount of a-Sma positive cells collagen deposition was decreased indicating that loss of Periostin results in less fibrosis, which is characterized by deposition of huge amounts of ECM proteins such as collagen. Hence, these findings are in line with reports showing that Periostin contributes to the fibrogenic activity of PSCs (Erkan et al. 2007). Furthermore, these results are in accordance with other studies, which also showed that loss of Periostin results in reduced collagen deposition in acute myocardial infarction and inflammation of the liver (Shimazaki et al. 2008, Huang et al. 2015).

4.1.2 Periostin in pancreatic regeneration

Surprisingly, significant differences during the course of pancreatic regeneration were observed. While wild type mice stepwise recovered, regeneration of the exocrine compartment in Periostin deficient mice was severely impaired. It is known that Periostin expression is induced after different tissue injuries and that it plays an important role in regeneration in various pathological conditions. After myocardial infarction for instance, Periostin expression is highly upregulated and can be found in the infarct border of hearts.

By recruiting activated fibroblasts through the integrin signaling pathway, Periostin supports healing of the injured organ. As in this study, in Periostin deficient mice an impaired cardiac regeneration can be observed, which results in rupture of the heart (Shimazaki et al. 2008). However, no evidence for such a role of Periostin in pancreatitis has been reported so far. The most significant features of the impaired regeneration were a persistent high immune cell infiltration as well as higher levels of ADMs and severe pancreatic atrophy characterized by a decrease in pancreas mass and loss of pancreatic parenchyma. Additionally, α-Amylase expressing acinar cells were replaced by adipocytes indicating acinar-to-adipocyte differentiation. These results are very interesting since so far impaired pancreatic regeneration with coincident pancreatic atrophy was only described in mice lacking intrinsic factors such as the transcription factors Gata6, c-Myc or Prox1 (Martinelli et al. 2013, Bonal et al. 2009, Westmoreland et al. 2012). Extracellular matrix molecules have not been described to possess a major function in acinar differentiation commitment as of yet. The prerequisite for successful regeneration of the pancreatic compartment after tissue damage is the proper performance of a regenerative program. This includes the temporary re-expression of pancreatic progenitor markers and a transiently alteration of acinar cell morphology (Jensen et al. 2005). During pancreatic recovery the expression of acinar differentiation genes and the acinar cell phenotype is restored. In Periostin deficient mice the process of dedifferentiation was seriously disturbed. A lasting significant upregulation of progenitor markers and a strongly decreased expression of differentiation markers twenty-one days after the last caerulein injection was detected in Postn deficient mice compared to wild type mice. Furthermore, sustained ADM formation and increased cell proliferation was detected in Periostin deficient mice, which is in line with the persistent dedifferentiated state of acinar cells in these mice.

4.1.3 Periostin deficiency promotes acinar-to-adipocyte differentiation

The most striking finding in this study was the acinar-to-adipocyte differentiation in Periostin deficient mice starting seven days after the last caerulein injection and reaching most significant differences at day twenty-one when nearly the whole exocrine compartment was replaced by fat cells. This trans-differentiation of acinar cells to adipocytes was accompanied by a significant upregulation of the key regulator of adipogenesis Ppar-γ in mice lacking Periostin expression twenty-one days after the last caerulein injection. Similar effects were described in c-Myc and Gata6 deficient mice. Both genotypes developed pancreatic atrophy with simultaneous emergence of lipomatosis. While lineage-tracing studies confirmed the acinar origin of the adipocytes in c-Myc deficient mice, in Gata6 deficient mice only a subset of adipocytes derived from epithelial cells (Bonal et al. 2009, Martinelli et al. 2013). In this study α-Amylase containing granules in the cytoplasm of adipocytes were observed indicating acinar cells as the source of adipocytes. However, an additional mesenchymal

origin of adipocytes cannot be excluded and further studies using lineage tracing are crucial to elucidate this issue. In conclusion, this is the first study showing that loss of one ECM protein can affect differentiation commitment of acinar cells and that proper epithelial-mesenchymal crosstalk is crucial for regeneration of the exocrine compartment. However, further experiments are needed to identify the underlying molecular mechanisms since it still has to be elucidated how Periostin influences expression of progenitor, differentiation and adipogenesis markers.

4.2 Periostin in pancreatic tumorigenesis and metastatic spread

Despite intensive research in the last 30 years no effective treatment options for PDAC have been found so far. One of the main reasons for failed chemotherapy is the poor perfusion in PDAC. Due to the fact that around 80% of the pancreatic tumor mass consists of tumor stroma, therapy approaches for PDAC now focus on the mesenchymal compartment rather than on epithelial cells. While depleting the tumor stroma and thereby increasing delivery and distribution of chemotherapeutic drugs to the cancer has shown promising results in a mouse model of pancreatic cancer, this therapeutic approach has failed in a phase II clinical trial (Olive et al. 2009). Furthermore, more recent studies in different mouse models of pancreatic cancer additionally demonstrated that depleting the tumor stroma resulted in more aggressive tumors and a shorter survival of mice (Ozdemir et al. 2014, Rhim et al. 2014). Thus, new therapy approaches aim at remodeling the tumor stroma rather than to deplete it. Treatment of ptf1aCre$^{+/-}$;LSL-Kras$^{G12D/+}$;p53$^{lox/+}$ (KPC) mice with a vitamin D receptor ligand for instance has shown promising effects in remodeling the stroma in these mice. Activated pancreatic stellate cells were forced back into their quiescent state by vitamin D receptor ligand treatment indicated by a change in gene expression of stellate cells, which resulted in a less tumor-supportive microenvironment. Moreover, combination therapy consisting of the vitamin D receptor ligand calcipotriol and the chemotherapeutic drug gemcitabine was successful in reducing tumor volume of KPC mice as well as decreasing stromal activation and fibrosis (Sherman et al. 2014). In this thesis the influence of the stroma protein Periostin in pancreatic cancer initiation and progression as well as metastatic spread was investigated. It is well established that Periostin is upregulated in a variety of epithelial cancers such as non-small cell lung cancer, prostate, breast, colorectal and pancreatic cancer and promotes tumor progression and metastatic spread (Hong et al. 2013, Tian et al. 2015, Zhang et al. 2010, Bao et al. 2004, Erkan et al. 2007). In pancreatic cancer however, only data from *in vitro* studies or xenograft mouse models exist so far. Thus, in the present study conditional pancreatic cancer mouse models with an additional deletion of the *Postn* gene were generated and characterized.

4.2.1 Periostin in cancer initiation and progression

In the $Kras^{G12D}$ mouse model pre-neoplastic lesions develop at a very young age of mice and all steps of PDAC development according to the human disease are recapitulated (Hingorani et al. 2003). Therefore, this mouse model is often used to analyze early steps of pancreatic carcinogenesis. Here, in eight-week old $Kras^{G12D}$ mice already a strong stromal reaction with a high expression of the ECM molecule Periostin around precancerous lesions and damaged acini was detected. With increased age of mice the expression of Periostin increased as well and was not only found around pre-neoplastic lesions and damaged acini cells, but also an interlobular localization was detectable. These results are in accordance with previous studies showing a high Periostin expression in human pancreatic cancer tissue whereas in normal pancreatic tissue no Periostin expression was found. Additionally, the localization of Periostin expression was described to be present in the ECM surrounding damaged acinar cells, which coincides with the data in this study (Erkan et al. 2007). The role of Periostin in cancer initiation has been studied in a variety of cancers. The majority of *in vitro* and *in vivo* studies show that Periostin has a pro-tumorigenic function for instance by promoting cancer cell proliferation of pancreatic, gastric and colorectal cancer cells (Ben et al. 2011, Kikuchi et al. 2014, Tai, Dai, and Chen 2005). Also in cancer progression Periostin plays a major role as it promotes tumor lymphangiogenesis in head and neck cancer or angiogenesis in oral and breast cancer (Kudo et al. 2012, Siriwardena et al. 2006, Shao et al. 2004). However, there are also a few studies, which did not find a major effect of Periostin in cancer initiation and progression or even showed that Periostin can suppress cancer formation (Lv et al. 2014, Kim et al. 2005). A study performed with human pancreatic cancer cells overexpressing Periostin for instance found a reduced tumor volume in nude mice while cancer cells stimulated with high concentrations of recombinant Periostin (1 µg/ml) exhibited a high migratory behavior (Kanno et al. 2008). A recent study, which analyzed the function of Periostin in breast cancer *in vivo*, did not observe any changes in tumor initiation. The amount of hyperplastic lesions as well as tumor growth was not altered in Periostin deficient mice (Sriram et al. 2015). However, another study utilizing an aptamer (PNDA-3) directed against Periostin could show that orthotopic breast tumor growth was significantly reduced compared to control mice (Lee et al. 2013). In ovarian cancer overexpression of Periostin resulted in increased tumor growth and by using a neutralizing monoclonal Periostin antibody subcutaneous and intraperitoneal ovarian tumor growth in severe combined immunodeficiency (SCID) mice was significantly reduced (Sriram et al. 2015, Zhu et al. 2011, Zhu et al. 2010). Though, it is difficult to compare the different obtained results since the experiments in ovarian cancer were performed in immunocompromised mice whereas in the setting of breast cancer the experiments were performed in FVB/N and MMTV-PyMT mice, which have an intact immune system. It is well known that the interaction of tumor cells with

the tumor microenvironment plays an important role in cancer development. Due to the lack of an intact immune system in immunocompromised mice an altered tumor microenvironment develops and impairs cancer development. Moreover, the studies performed in ovarian cancer and pancreatic cancer described above overexpressed Periostin in an ovarian and pancreatic cancer cell line, respectively; albeit in pancreatic cancer mesenchymal cells only express Periostin. In the current study, $Kras^{G12D}$ mice lacking Periostin expression showed a delayed initiation of PDAC. Postn depleted $Kras^{G12D}$ mice presented a lower amount of PanIN lesions, reduced proliferating cells and infiltrating leukocytes as well as a significant higher percentage of functional exocrine parenchyma at early ages (eight and twelve weeks). However, at later stages the differences were less distinctive indicating that Periostin influences cancer initiation. These results were further confirmed by the data obtained from the orthotopic injection of murine pancreatic tumor cells to the pancreas of wild type or Periostin deficient mice. No difference in tumor growth or tumor volume could be observed indicating that Periostin does not have a major impact in late stage tumors. These results are in line with the study performed in the breast cancer model in which no differences in development and progression of orthotopic tumors were detected (Sriram et al. 2015).

Cellular transformation is an important step in cancer initiation. The formation of acinar-to-ductal metaplasia for instance has been implicated to be an initial step of PDAC development (Zhu et al. 2007). In the process of ADM formation acinar cells change their morphology and gene expression profile and upon oncogenic stimuli such as mutant Kras expression these lesions remain in their dedifferentiated state and can progress to PanIN lesions and PDAC (Morris et al. 2010, Habbe et al. 2008, De La et al. 2008). In this thesis, it could be shown that the stimulation of wild type acinar cells with murine recombinant Periostin resulted in acinar-to-ductal metaplasia in a 3D culture system. Thus, the ability of Periostin to induce cellular transformation of acinar cells confirms the pro-tumorigenic role of Periostin at early steps of pancreatic carcinogenesis. Another hallmark of cancer is the capability of tumor cells to overcome anoikis and grow anchorage-independently. Here, the treatment of murine pancreatic cancer cell lines with murine recombinant Periostin facilitated anchorage-independent growth of cancer cells in soft agar. These results are in agreement with other studies demonstrating that Periostin fosters anchorage-independent growth of pancreatic and head and neck cancer cells in soft agar colony formation assays (Kudo et al. 2006, Ben et al. 2011). These findings confirm the tumor-promoting role of Periostin since it not only promotes cellular transformation of acinar cells but also enhances malignant transformation of tumor cells.

Usually, PDAC development in $Kras^{G12D}$ mice does not occur until the mice are 12-15 months of age. Additionally, only a small proportion of $Kras^{G12D}$ mice develops full-blown PDAC (Hingorani et al. 2003, Guerra et al. 2007). Apart from introducing other mutations in $Kras^{G12D}$ mice the low frequency of PDAC development can be increased by caerulein-induced acute pancreatitis (Carriere et al. 2009). Therefore, inflammation-triggered carcinogenesis in $Kras^{G12D}$ and $Kras^{G12D}$;$Postn^{-/-}$ mice was performed by injecting mice with 100 µg/kg bw i.p. caerulein. Surprisingly, caerulein treatment in $Kras^{G12D}$;$Postn^{-/-}$ mice resulted in a strong inflammatory response and severe lung damage indicated by a significant high amount of CD45+ leukocytes in the pancreas and thickened alveolar walls, respectively. In the clinic acute lung injury as consequence of severe acute pancreatitis is a known complication and often involves mortality of patients (Pastor, Matthay, and Frossard 2003). However, most of acute pancreatitis patients suffer from a mild form of this disease. Only a small subset of patients develop multiple organ failure due to systemic activation of the immune system and accompanied acute lung damage (Frossard, Steer, and Pastor 2008). Currently, the mechanisms leading to acute lung damage after severe acute pancreatitis are under investigation and Zhang and colleagues could demonstrate that severe acute pancreatitis induced by caerulein injections in wild type mice over a period of five days resulted in multiple organ damage of mice. Especially the lungs were injured and showed alveolar thickness as observed in $Kras^{G12D}$;$Postn^{-/-}$ mice. The underlying mechanism of acute pancreatitis induced lung injury was linked to IL-6 trans-signaling (Zhang et al. 2013). In the present study also high serum IL-6 levels were detected after inducing acute pancreatitis in $Kras^{G21D}$;$Postn^{-/-}$ mice and it is very likely that the acute lung injury is also driven by IL-6 trans-signaling. Thus, the lack of Periostin in the setting of oncogenic Kras seems to facilitate the systemic inflammatory response syndrome, which results in acute lung damage of mice most probably through IL-6 trans-signaling. The systemic inflammatory response syndrome is characterized by a higher permeability of endothelial barriers and a strongly elevated release of pro-inflammatory cytokines such as IL-6. It is well known that endothelial permeability is regulated by cell-matrix adhesion molecules and that upon inflammation changes in endothelial permeability can occur (del Zoppo and Milner 2006). Activation of integrin signaling which occurs upon ligand binding to the different integrin receptors for instance has been shown to maintain endothelial barrier function whereas integrin blocking resulted in increased permeability (Wu, Ustinova, and Granger 2001). One study could show that a reduction of the ECM protein Fibronectin in sheep resulted in increased pulmonary permeability (Cohler, Saba, and Lewis 1985). Further studies implicate an important role for the focal adhesion kinase in maintaining endothelial permeability. Experiments in endothelial cell specific FAK knock out mice revealed that lack of FAK in endothelial cells resulted in lung hemorrhage, increased albumin influx, edema and neutrophil infiltration in the lung

(Schmidt et al. 2013). Therefore, it is tempting to speculate that the loss of Periostin results in an impaired integrin signaling and consequently in increased endothelial permeability, which facilitates the systemic inflammatory response syndrome and lung damage.

In addition to acute pancreatitis-induced carcinogenesis, the induction of chronic pancreatitis has also been reported to accelerate PDAC development (Guerra et al. 2007). Hence, chronic pancreatitis was induced in $Kras^{G12D}$, $Kras^{G12D}$;$Postn^{+/-}$ and $Kras^{G12D}$;$Postn^{-/-}$ mice by administration of 50 µg/kg bw i.p. caerulein. The mice received six hourly caerulein injections on three days a week for a period of six weeks. Two months after the last caerulein injection the mice were sacrificed and the pancreatic compartment was analyzed. Interestingly, despite the inflammatory insult over six weeks none of the mice had developed pancreatic cancer. Furthermore, no difference in immune cell infiltration or activated stroma index could be observed. The only difference was found in the development of lipomatosis which was detected in $Kras^{G12D}$;$Postn^{+/-}$ mice and which was even more distinctive in $Kras^{G12D}$;$Postn^{-/-}$ mice. In parallel, mice developing lipomatosis also showed a decline in the pancreas-to-body mass ratio. Possible reasons for the unsuccessful development of pancreatic cancer might be that the mice have been sacrificed at a too early time point. Close examination of the HE stained pancreatic tissue of all chronic pancreatitis mice together with a pathologist revealed that all mice had developed ADMs as well as PanIN lesions which started to progress to PDAC. Therefore, differences in PDAC development might be present when the mice are sacrificed at a later time point.

Despite the failure to induce chronic pancreatitis-triggered PDAC development in this experimental setting, inflammation-induced carcinogenesis is an important step in pancreatic cancer development. To further investigate the role of Periostin in inflammation-initiated pancreatic carcinogenesis, downstream targets of Periostin signaling were assessed in order to find treatment targets. Upon stimulation of cancer cells with recombinant Periostin the activation of focal adhesion kinase, the proto-oncogene non-tyrosine receptor kinase SRC and extracellular signal related kinase was found being the most activated downstream proteins. The activation of the integrin signaling pathway, in particular the autophosphorylation of the focal adhesion kinase upon Periostin stimulation has been reported in various other physiological and pathophysiological conditions (Li et al. 2010, Zhang et al. 2015, Baril et al. 2007). Thus in further experiments the FAK inhibitor PF 573228 was used, which prevents the phosphorylation of tyrosine 397 of the focal adhesion kinase. The results of inflammation-triggered carcinogenesis in $Kras^{G12D}$ and FAK inhibitor treated $Kras^{G12D}$ mice revealed a blocked pancreatic carcinogenesis evident by a much smaller pancreas, a significant reduction of preinvasive lesions and less proliferating cells upon treatment with the inhibitor. Apart from inhibited FAK phosphorylation also the

phosphorylation of ERK was strongly reduced. Even more impressive was the effect of FAK inhibitor treatment in $Kras^{G12D}$,$p53^{lox/lox}$ mice. Assessment of survival revealed that mice receiving FAK inhibitor treatment twice daily displayed a significant longer survival compared to both, vehicle and gemcitabine treated mice. However, no survival benefit was achieved using a combination therapy consisting of FAK inhibitor and gemcitabine compared to the FAK inhibitor treatment only. Histological analysis of the pancreatic compartment furthermore revealed that FAK inhibitor treated mice exhibited a significant reduction of proliferating cells as well as a significant increase of apoptotic cells. As observed in the $Kras^{G12D}$ model treated with the FAK inhibitor, a strong reduction of ERK phosphorylation could be detected in $Kras^{G12D}$;$p53^{lox/lox}$ mice as well. These results indicate that FAK inhibition simultaneously results in a reduced activation of ERK and thereby delays progression of PDAC. The potential of FAK inhibitors as anti-cancer therapy are more and more evolving during the last few years. Early studies silencing FAK in breast cancer cells showed a decrease in adhesion, colony formation and reduced tumor growth in nude mice (Golubovskaya et al. 2009). The use of an FAK inhibitor (TAE226) targeting the phosphorylation sites of tyrosine 397 and 861 has recently been shown to inhibit angiogenesis in colon cancer (Schultze et al. 2010). Another FAK inhibitor (PF-562271) targeting not only FAK but also the non-receptor tyrosine kinase Pyk2 showed promising effects in inhibiting growth and metastasis of breast cancer cells in an in vivo mouse model as well as tumor growth of orthotopic implanted pancreatic cancer cells in athymic mice (Roberts et al. 2008, Stokes et al. 2011). Stokes et al. could further show that FAK inhibition resulted in an altered microenvironment since the recruitment of mesenchymal cells to the tumor microenvironment was impaired (Stokes et al. 2011). The FAK inhibitor (PF 573228) used in the present study has also been shown to decrease breast cancer cell migration (Wendt and Schiemann 2009). Since in most pancreatic cancer patients FAK is upregulated, the inhibition of this kinase represents a promising target in pancreatic cancer therapy. A study performed by Hochwald et al showed that subcutaneously transplanted human pancreatic cancer cells into nude mice exhibited a reduced tumor growth upon treatment with the FAK inhibitor 1,2,4,5-Benzenetetraamine tetrahydrochloride. Additionally, a reduction of ERK phosphorylation was found when the group treated human pancreatic cancer cell lines with the FAK inhibitor. Furthermore, another study of this group demonstrated that FAK inhibitor treatment of pancreatic cancer cell lines resulted in decreased cell survival and reduced cell proliferation (Liu et al. 2008, Hochwald et al. 2009). The results obtained in the current thesis are in agreement with the above-described findings in the literature. Moreover, the experiments in this study are performed in syngenic mouse models, which is an advantage compared to the so far performed studies analyzing the effects of FAK inhibition in xenograft or cell culture models only.

4.2.2 Periostin and metastatic spread

Pancreatic cancer is a highly metastatic disease. At the time of diagnosis the majority of pancreatic cancer patients already display metastases at secondary sites such as lung or liver. Therefore, analyzing the mechanism contributing to metastatic spread is of upmost importance in order to inhibit tumor cell release and metastasis formation at early time points. Periostin expression has been shown to increase the invasive behavior of various cancer cell lines (Kudo et al. 2006, Michaylira et al. 2010, Liu and Liu 2011). Also, pancreatic cancer cell lines exhibit an increased invasive behavior upon Periostin stimulation, which was shown by different independent studies using human pancreatic cancer cell lines (Ben et al. 2011, Erkan et al. 2007, Baril et al. 2007). While in the study performed by Ben et al. human cancer cell lines were infected with a Periostin recombinant adenovirus plasmid, Erkan et al and Baril et al. stimulated human pancreatic cancer cell lines with different concentrations of recombinant Periostin. In the present study treatment of murine cancer cells with recombinant Periostin was performed as well. Similar to the results described by Erkan et al, a dose-dependent effect regarding invasion was observed. While the concentration of 100 ng/ml and 1 µg/ml of Periostin hardly affected invasion of murine pancreatic cancer cells, a significant increase of invasive behavior was found when 500 ng/ml recombinant Periostin was used. In contrast to the results described by Erkan et al and the results obtained in this thesis, the study performed by Baril et al. found an increased invasive behavior of cancer cells with increasing Periostin concentrations. However, concentration-dependent effects of Periostin have already been described in a previous study on tumor cell migration. While a low concentration of 150 ng/ml Periostin inhibited migration of pancreatic cancer cells, a higher concentration of 1 µg/ml has been shown to promote cancer cell migration (Kanno et al. 2008). To validate that pancreatic cancer cell invasion is directly influenced by Periostin signaling, not only an FAK inhibitor but also a neutralizing Periostin antibody was used in the invasion assay. FAK inhibition as well as Periostin antibody treatment of murine pancreatic cancer cells resulted in a significant reduction of cancer cell invasion showing that invasion of cancer cells is in fact dependent on Periostin. Comparable results have been shown in a human osteosarcoma cell line in which the invasive behavior of cancer cells was also reduced upon downregulation of Periostin gene expression via shRNA (Liu, Huang, and Qin 2010).

To further prove the important function of Periostin in metastasis formation at secondary target organs murine pancreatic cancer cells were injected to the tail vein of wild type, Periostin heterozygous and homozygous knock out mice. While in all wild type mice huge metastases were found, heterozygous Periostin knock out mice exhibited fewer and much smaller metastases. Homozygous Periostin knock out mice however, displayed no metastasis formation at all. Subsequent analysis of the lung tissue from wild type and $Postn^{+/-}$

mice demonstrated Periostin expression in lung metastases whereas in the surrounding healthy lung tissue no Periostin expression could be detected. These results indicate that infiltrating cancer cells activate resident lung fibroblasts, which then express Periostin. Similar results have been described in a breast cancer mouse model that spontaneously metastasizes to the lung. Only in the lung stroma induced by infiltrating breast cancer cells Periostin expression was found whereas metastasis free animals did not exhibit Periostin expression in the alveolar lung tissue. Furthermore, the study showed that the breast cancer mouse model lacking Periostin expression had a significantly reduction of metastasis formation which is in line with the results of the tail vein injection experiments in $Postn^{-/-}$ mice described in this thesis (Malanchi et al. 2012). Further experiments analyzing the underlying mechanism of metastasis formation revealed that FAK signaling plays an important role in metastatic spread since upon FAK inhibitor treatment the colonization of secondary target organs with cancer cells was significantly reduced in tail vein injected wild type mice. The ability of FAK inhibition (achieved either by inhibitors or gene silencing) to reduce metastasis formation has also been reported in a nude mouse orthotopic xenograft model of pancreatic cancer as well as in a preclinical model of breast cancer metastasis (Stokes et al. 2011, Duxbury et al. 2004, Walsh et al. 2010). To detect whether already the attachment of tumor cells in the secondary organ is influenced, an in vivo seeding assay was performed. Thereby, cancer cells were injected again into the blood stream and the lung tissue was isolated shortly afterwards. The generated data demonstrated that in both wild type and Periostin knock out mice tumor cells attached in the lung tissue but that only in wild type mice the tumor cells were able to survive and proliferate. However, Periostin does not seem to induce proliferation of murine pancreatic tumor cells directly as *in vitro* proliferation assays did not show an increased survival of pancreatic cancer cells upon Periostin stimulation. In contrast to these results Periostin was reported to induce proliferation of different cancer cell lines *in vitro* including gastric, human pancreatic as well as colorectal cancer cell lines (Kikuchi et al. 2014, Ben et al. 2011, Tai, Dai, and Chen 2005, Erkan et al. 2007). A possible reason for the incapability of inducing proliferation of cancer cells might be the already high proliferative phenotype of the used murine pancreatic cancer cell line. Also, the missing microenvironment might be a limiting factor. It is quite reasonable that Periostin does not induce proliferation of tumor cells directly but by stimulating fibroblasts, which in turn influence proliferation of cancer cells. Indeed, one study analyzing the influence of Periostin on keratinocyte proliferation revealed that Periostin is required for IL-6 production of fibroblasts, which then results in proliferation of keratinocytes (Taniguchi et al. 2014).

In a recent publication it has been reported that circulating tumor cells can already be detected in the blood before pancreatic cancer development occurs (Rhim et al. 2012). Due

to the fact that FAK inhibitor treated mice demonstrated less metastases and that FAK inhibition resulted in reduced cancer cell invasion *in vitro*, it was of interest whether FAK inhibition also alters the release of primary tumor cells into the blood stream. Therefore, tumor cell release of $Kras^{G12D};p53^{lox/+}$ mice into the blood was analyzed and compared to FAK inhibitor treated $Kras^{G12D};p53^{lox/+}$ mice. Surprisingly, no difference in the amount of circulating tumor cells between untreated and FAK inhibitor treated mice could be observed. These results are very interesting since *in vitro* assays clearly showed that upon FAK inhibitor treatment invasion of murine pancreatic cancer cells, which were initially isolated from $Kras^{G12D};p53^{lox/+}$ mice, displayed a significant reduction of invasive behavior. One possible explanation for this contradictory finding might be the late treatment of $Kras^{G12D};p53^{lox/+}$ mice. At the age of 10 weeks already a high amount of circulating tumor cells might be present in the blood and the effects of FAK inhibition to prevent primary tumor cell release might not be noticeable. It would be very interesting to analyze if there are any differences in circulating tumor cells when younger mice are treated with the FAK inhibitor. Another reason why no difference in tumor cell release was found could be due to the heterogeneity of mice. While some of the $Kras^{G12D};p53^{lox/+}$ mice at the age of 11 weeks already showed tumor development other mice only displayed few precancerous lesions. Thus in further experiments the number of mice in this setting has to be increased and only mice with similar phenotype should be included.

The metastatic experiments clearly demonstrate that invasive cancer cells activate resident fibroblasts in the secondary organ, which start to express and secrete Periostin to form a tumor friendly microenvironmental niche. As of yet it is known that Periostin is secreted by pancreatic stellate cells and fibroblasts, which have been activated by cancer cells (Erkan et al. 2007). Also mechanical stress as it occurs in bone fractures has been shown to induce Periostin expression (Wilde et al. 2003). Further studies demonstrated that Periostin expression is induced in response to TGF-β2 and TGF-β3 (Malanchi et al. 2012). On the transcriptional level however, still little is known about the regulation of Periostin gene expression. So far only a few transcription factors have been identified to regulate expression of Periostin. The basic helix-loop-helix transcription factor Twist1 for instance was shown to upregulate Periostin expression in malignant pleural mesothelioma cells (Komiya et al. 2014) whereas the zinc finger transcription factor YingYang-1 was reported to negatively regulate Periostin gene expression (Romeo et al. 2011). In order to analyze how Periostin expression is initiated and regulated on a transcriptional level, an in silico analysis was performed to discover transcription factor binding sites in the Periostin promoter. Afterwards, luciferase reporter assays revealed that the Periostin promoter is activated upon c-MYC expression whereas NFATc2 did not show any effect. The findings of this study indicate that fibroblasts

and pancreatic stellate cells once activated by cancer cells express c-MYC, which translocates to the nucleus and induces Periostin expression.

4.4 Conclusions and outlook

The data of this study elucidated various functions of the extracellular matrix protein Periostin in different pancreatic pathophysiological conditions.

The results of the first part of this thesis highlight the importance of mesenchymal-epithelial crosstalk in regeneration of the exocrine pancreatic compartment after caerulein-induced tissue damage. However, further studies have to be performed to clarify the molecular mechanism how Periostin influences gene expression of acinar cells. Furthermore, acinar cells as the major source of adipocytes need to be confirmed by conducting lineage tracing experiments.

In the second part of the study Periostin was found to promote early tumorigenesis in pancreatic cancer and metastatic spread while inhibition of Periostin signaling via the application of an FAK inhibitor impressively delayed cancer progression as well as metastasis formation. To further affirm that lack of Periostin results in delayed carcinogenesis $Kras^{G12D}$;$p53^{lox/+}$;$Postn^{-/-}$ mice are currently generated and will be analyzed in regard to tumor formation. To investigate whether metastasis formation in the secondary target organ is specific to Periostin or if the ablation of other ECM molecules also results in reduced or abolished colonization at distant organs, experiments with Tenascin-C knock out mice are performed at the moment. Nevertheless, in this study the importance of Periostin and its downstream target FAK in pancreatic carcinogenesis and metastatic spread was demonstrated and the use of FAK inhibitors as therapeutic drugs was shown to be a promising approach to inhibit pancreatic carcinogenesis and metastatic spread. Indeed, phase I clinical trials have already been performed showing that FAK inhibitors are well-tolerated and safe. Currently, different FAK inhibitors are undergoing further clinical testing in patients with various solid cancers such as ovarian or non small cell lung cancer.

5 Summary

In this thesis the function of the extracellular matrix protein Periostin in pancreatitis and following recovery as well as in pancreatic tumorigenesis and metastatic spread was investigated. After acute pancreatitis the exocrine pancreatic compartment, which mainly consists of α-Amylase producing acinar cells, has shown to exhibit an extraordinary ability to recover. Therefore, the acinar cells transiently transdifferentiate into duct-like cells and additionally express pancreatic progenitor markers to induce cell proliferation. This way, the damaged tissue can be replaced and organ integrity is restored. While intrinsic factors have been shown to play an important role in the proper execution of this regeneration program, the influence of extracellular matrix proteins has not been investigated so far. Data of this study have demonstrated that Periostin ablation does not influence pancreatitis severity but strongly affects recovery of the exocrine compartment. Loss of Periostin resulted in an impaired regeneration, which was characterized by persistent inflammation of the tissue as well as pancreatic atrophy and acinar-to-adipocyte differentiation. Furthermore, analysis of pancreatic progenitor and differentiation markers displayed significantly elevated levels of progenitor markers and accordingly reduced transcript levels of differentiation markers indicating that loss of Periostin keeps the acinar cells in an undifferentiated state. Taken together, the results of the first part of this study have shown that epithelial-mesenchymal crosstalk is indispensable for the proper regeneration of the exocrine pancreatic compartment after acute pancreatitis.

In the second part of this thesis Periostin and its downstream signaling pathway was identified to promote pancreatic carcinogenesis and metastatic spread. In vitro experiments showed that Periostin fosters cellular transformation of cells and increases the invasive behavior of pancreatic cancer cells. A mouse model of pancreatic cancer lacking the expression of Periostin was generated and confirmed the tumor-promoting role of Periostin. At early ages, mice deficient of Periostin exhibited less precancerous lesions, proliferating cells and a fewer degree of metaplasia. Experiments analyzing metastatic colonization displayed that Periostin is necessary for successful survival and proliferation of cells in the secondary target organ. Additionally, inhibition of Periostin signaling by the use of an FAK inhibitor has effectively prolonged survival of pancreatic cancer mice and significantly reduced metastasis formation in the lung. Thus, the data of the second part of this study have demonstrated that Periostin plays a tumor-promoting role in PDAC development and progression, which is mediated by the activation of the integrin signaling pathway. Moreover, Periostin contributes to metastasis formation by creating a tumor-friendly microenvironment in the secondary target organ, which favors survival and growth of pancreatic cancer cells. The use of FAK inhibitors might be a promising approach to inhibit pancreatic carcinogenesis and metastatic spread.

6 References

Ahmed, S. A., C. Wray, H. L. Rilo, K. A. Choe, A. Gelrud, J. A. Howington, A. M. Lowy, and J. B. Matthews. 2006. "Chronic pancreatitis: recent advances and ongoing challenges." *Curr Probl Surg* 43 (3):127-238. doi: 10.1067/j.cpsurg.2005.12.005.

Aichler, M., C. Seiler, M. Tost, J. Siveke, P. K. Mazur, P. Da Silva-Buttkus, D. K. Bartsch, P. Langer, S. Chiblak, A. Durr, H. Hofler, G. Kloppel, K. Muller-Decker, M. Brielmeier, and I. Esposito. 2012. "Origin of pancreatic ductal adenocarcinoma from atypical flat lesions: a comparative study in transgenic mice and human tissues." *J Pathol* 226 (5):723-34. doi: 10.1002/path.3017.

Al-Aynati, M. M., N. Radulovich, R. H. Riddell, and M. S. Tsao. 2004. "Epithelial-cadherin and beta-catenin expression changes in pancreatic intraepithelial neoplasia." *Clin Cancer Res* 10 (4):1235-40.

Amato, E., M. D. Molin, A. Mafficini, J. Yu, G. Malleo, B. Rusev, M. Fassan, D. Antonello, Y. Sadakari, P. Castelli, G. Zamboni, A. Maitra, R. Salvia, R. H. Hruban, C. Bassi, P. Capelli, R. T. Lawlor, M. Goggins, and A. Scarpa. 2014. "Targeted next-generation sequencing of cancer genes dissects the molecular profiles of intraductal papillary neoplasms of the pancreas." *J Pathol* 233 (3):217-27. doi: 10.1002/path.4344.

Amundadottir, L. T., S. Thorvaldsson, D. F. Gudbjartsson, P. Sulem, K. Kristjansson, S. Arnason, J. R. Gulcher, J. Bjornsson, A. Kong, U. Thorsteinsdottir, and K. Stefansson. 2004. "Cancer as a complex phenotype: pattern of cancer distribution within and beyond the nuclear family." *PLoS Med* 1 (3):e65. doi: 10.1371/journal.pmed.0010065.

Apte, M. V., P. S. Haber, T. L. Applegate, I. D. Norton, G. W. McCaughan, M. A. Korsten, R. C. Pirola, and J. S. Wilson. 1998. "Periacinar stellate shaped cells in rat pancreas: identification, isolation, and culture." *Gut* 43 (1):128-33.

Apte, M. V., P. S. Haber, S. J. Darby, S. C. Rodgers, G. W. McCaughan, M. A. Korsten, R. C. Pirola, and J. S. Wilson. 1999. "Pancreatic stellate cells are activated by proinflammatory cytokines: implications for pancreatic fibrogenesis." *Gut* 44 (4):534-41.

Apte, M. V., and J. S. Wilson. 2012. "Dangerous liaisons: pancreatic stellate cells and pancreatic cancer cells." *J Gastroenterol Hepatol* 27 Suppl 2:69-74. doi: 10.1111/j.1440-1746.2011.07000.x.

Arslan, A. A., K. J. Helzlsouer, C. Kooperberg, X. O. Shu, E. Steplowski, H. B. Bueno-de-Mesquita, C. S. Fuchs, M. D. Gross, E. J. Jacobs, A. Z. Lacroix, G. M. Petersen, R. Z. Stolzenberg-Solomon, W. Zheng, D. Albanes, L. Amundadottir, W. R. Bamlet, A. Barricarte, S. A. Bingham, H. Boeing, M. C. Boutron-Ruault, J. E. Buring, S. J. Chanock, S. Clipp, J. M. Gaziano, E. L. Giovannucci, S. E. Hankinson, P. Hartge, R. N. Hoover, D. J. Hunter, A. Hutchinson, K. B. Jacobs, P. Kraft, S. M. Lynch, J. Manjer, J. E. Manson, A. McTiernan, R. R. McWilliams, J. B. Mendelsohn, D. S. Michaud, D. Palli, T. E. Rohan, N. Slimani, G. Thomas, A. Tjonneland, G. S. Tobias, D. Trichopoulos, J. Virtamo, B. M. Wolpin, K. Yu, A. Zeleniuch-Jacquotte, A. V. Patel, and Consortium Pancreatic Cancer Cohort. 2010. "Anthropometric measures, body mass index, and pancreatic cancer: a pooled analysis from the Pancreatic Cancer Cohort Consortium (PanScan)." *Arch Intern Med* 170 (9):791-802. doi: 10.1001/archinternmed.2010.63.

Bachem, M. G., E. Schneider, H. Gross, H. Weidenbach, R. M. Schmid, A. Menke, M. Siech, H. Beger, A. Grunert, and G. Adler. 1998. "Identification, culture, and characterization of pancreatic stellate cells in rats and humans." *Gastroenterology* 115 (2):421-32.

Bachem, M. G., M. Schunemann, M. Ramadani, M. Siech, H. Beger, A. Buck, S. Zhou, A. Schmid-Kotsas, and G. Adler. 2005. "Pancreatic carcinoma cells induce fibrosis by

stimulating proliferation and matrix synthesis of stellate cells." *Gastroenterology* 128 (4):907-21.
Bailey, J. M., B. J. Swanson, T. Hamada, J. P. Eggers, P. K. Singh, T. Caffery, M. M. Ouellette, and M. A. Hollingsworth. 2008. "Sonic hedgehog promotes desmoplasia in pancreatic cancer." *Clin Cancer Res* 14 (19):5995-6004. doi: 10.1158/1078-0432.CCR-08-0291.
Bao, S., G. Ouyang, X. Bai, Z. Huang, C. Ma, M. Liu, R. Shao, R. M. Anderson, J. N. Rich, and X. F. Wang. 2004. "Periostin potently promotes metastatic growth of colon cancer by augmenting cell survival via the Akt/PKB pathway." *Cancer Cell* 5 (4):329-39.
Bardeesy, N., and R. A. DePinho. 2002. "Pancreatic cancer biology and genetics." *Nat Rev Cancer* 2 (12):897-909. doi: 10.1038/nrc949.
Baril, P., R. Gangeswaran, P. C. Mahon, K. Caulee, H. M. Kocher, T. Harada, M. Zhu, H. Kalthoff, T. Crnogorac-Jurcevic, and N. R. Lemoine. 2007. "Periostin promotes invasiveness and resistance of pancreatic cancer cells to hypoxia-induced cell death: role of the beta4 integrin and the PI3k pathway." *Oncogene* 26 (14):2082-94. doi: 10.1038/sj.onc.1210009.
Ben, Q. W., X. L. Jin, J. Liu, X. Cai, F. Yuan, and Y. Z. Yuan. 2011. "Periostin, a matrix specific protein, is associated with proliferation and invasion of pancreatic cancer." *Oncol Rep* 25 (3):709-16. doi: 10.3892/or.2011.1140.
Bonal, C., F. Thorel, A. Ait-Lounis, W. Reith, A. Trumpp, and P. L. Herrera. 2009. "Pancreatic inactivation of c-Myc decreases acinar mass and transdifferentiates acinar cells into adipocytes in mice." *Gastroenterology* 136 (1):309-319 e9. doi: 10.1053/j.gastro.2008.10.015.
Burris, H. A., 3rd, M. J. Moore, J. Andersen, M. R. Green, M. L. Rothenberg, M. R. Modiano, M. C. Cripps, R. K. Portenoy, A. M. Storniolo, P. Tarassoff, R. Nelson, F. A. Dorr, C. D. Stephens, and D. D. Von Hoff. 1997. "Improvements in survival and clinical benefit with gemcitabine as first-line therapy for patients with advanced pancreas cancer: a randomized trial." *J Clin Oncol* 15 (6):2403-13.
Caldas, C., S. A. Hahn, L. T. da Costa, M. S. Redston, M. Schutte, A. B. Seymour, C. L. Weinstein, R. H. Hruban, C. J. Yeo, and S. E. Kern. 1994. "Frequent somatic mutations and homozygous deletions of the p16 (MTS1) gene in pancreatic adenocarcinoma." *Nat Genet* 8 (1):27-32. doi: 10.1038/ng0994-27.
Campbell, S. L., R. Khosravi-Far, K. L. Rossman, G. J. Clark, and C. J. Der. 1998. "Increasing complexity of Ras signaling." *Oncogene* 17 (11 Reviews):1395-413. doi: 10.1038/sj.onc.1202174.
Cano, D. A., M. Hebrok, and M. Zenker. 2007. "Pancreatic development and disease." *Gastroenterology* 132 (2):745-62. doi: 10.1053/j.gastro.2006.12.054.
Canto, M. I., M. Goggins, R. H. Hruban, G. M. Petersen, F. M. Giardiello, C. Yeo, E. K. Fishman, K. Brune, J. Axilbund, C. Griffin, S. Ali, J. Richman, S. Jagannath, S. V. Kantsevoy, and A. N. Kalloo. 2006. "Screening for early pancreatic neoplasia in high-risk individuals: a prospective controlled study." *Clin Gastroenterol Hepatol* 4 (6):766-81; quiz 665. doi: 10.1016/j.cgh.2006.02.005.
Carriere, C., A. L. Young, J. R. Gunn, D. S. Longnecker, and M. Korc. 2009. "Acute pancreatitis markedly accelerates pancreatic cancer progression in mice expressing oncogenic Kras." *Biochem Biophys Res Commun* 382 (3):561-5. doi: 10.1016/j.bbrc.2009.03.068.
Cohler, L. F., T. M. Saba, and E. P. Lewis. 1985. "Lung vascular injury with protease infusion. Relationship to plasma fibronectin." *Ann Surg* 202 (2):240-7.
Colucci, G., F. Giuliani, V. Gebbia, M. Biglietto, P. Rabitti, G. Uomo, S. Cigolari, A. Testa, E. Maiello, and M. Lopez. 2002. "Gemcitabine alone or with cisplatin for the treatment of patients with locally advanced and/or metastatic pancreatic carcinoma: a

prospective, randomized phase III study of the Gruppo Oncologia dell'Italia Meridionale." *Cancer* 94 (4):902-10.
Comoglio, P. M., and L. Trusolino. 2005. "Cancer: the matrix is now in control." *Nat Med* 11 (11):1156-9. doi: 10.1038/nm1105-1156.
Conroy, T., F. Desseigne, M. Ychou, O. Bouche, R. Guimbaud, Y. Becouarn, A. Adenis, J. L. Raoul, S. Gourgou-Bourgade, C. de la Fouchardiere, J. Bennouna, J. B. Bachet, F. Khemissa-Akouz, D. Pere-Verge, C. Delbaldo, E. Assenat, B. Chauffert, P. Michel, C. Montoto-Grillot, M. Ducreux, Unicancer Groupe Tumeurs Digestives of, and Prodige Intergroup. 2011. "FOLFIRINOX versus gemcitabine for metastatic pancreatic cancer." *N Engl J Med* 364 (19):1817-25. doi: 10.1056/NEJMoa1011923.
Coussens, L. M., and Z. Werb. 2002. "Inflammation and cancer." *Nature* 420 (6917):860-7. doi: 10.1038/nature01322.
Cullinan, S. A., C. G. Moertel, T. R. Fleming, J. R. Rubin, J. E. Krook, L. K. Everson, H. E. Windschitl, D. I. Twito, R. F. Marschke, J. F. Foley, and et al. 1985. "A comparison of three chemotherapeutic regimens in the treatment of advanced pancreatic and gastric carcinoma. Fluorouracil vs fluorouracil and doxorubicin vs fluorouracil, doxorubicin, and mitomycin." *JAMA* 253 (14):2061-7.
Dahinden, C., B. Ingold, P. Wild, G. Boysen, V. D. Luu, M. Montani, G. Kristiansen, T. Sulser, P. Buhlmann, H. Moch, and P. Schraml. 2010. "Mining tissue microarray data to uncover combinations of biomarker expression patterns that improve intermediate staging and grading of clear cell renal cell cancer." *Clin Cancer Res* 16 (1):88-98. doi: 10.1158/1078-0432.CCR-09-0260.
Daniel, V. C., L. Marchionni, J. S. Hierman, J. T. Rhodes, W. L. Devereux, C. M. Rudin, R. Yung, G. Parmigiani, M. Dorsch, C. D. Peacock, and D. N. Watkins. 2009. "A primary xenograft model of small-cell lung cancer reveals irreversible changes in gene expression imposed by culture in vitro." *Cancer Res* 69 (8):3364-73. doi: 10.1158/0008-5472.CAN-08-4210.
Datto, M. B., Y. Li, J. F. Panus, D. J. Howe, Y. Xiong, and X. F. Wang. 1995. "Transforming growth factor beta induces the cyclin-dependent kinase inhibitor p21 through a p53-independent mechanism." *Proc Natl Acad Sci U S A* 92 (12):5545-9.
De Jesus-Acosta, A., O'Dwyer P.J.,Ramanathan, R.K.,Von Hoff, D.D., Maitra, A., Rasheed, Z., Zheng, L., Rajeshkumar, N.V., Le, D.T., Hoering, A., Bolejack, V., Yabuuchi, S., Laheru, D.A., . 2014. "A phase II study of vismodegib, a hedgehog (Hh) pathway inhibitor, combined with gemcitabine and nab-paclitaxel (nab-P) in patients (pts) with untreated metastatic pancreatic ductal adenocarcinoma (PDA)." 2014 Gastrointestinal Cancers Symposium.
De La, O. Jp, L. L. Emerson, J. L. Goodman, S. C. Froebe, B. E. Illum, A. B. Curtis, and L. C. Murtaugh. 2008. "Notch and Kras reprogram pancreatic acinar cells to ductal intraepithelial neoplasia." *Proc Natl Acad Sci U S A* 105 (48):18907-12. doi: 10.1073/pnas.0810111105.
Deer, E. L., J. Gonzalez-Hernandez, J. D. Coursen, J. E. Shea, J. Ngatia, C. L. Scaife, M. A. Firpo, and S. J. Mulvihill. 2010. "Phenotype and genotype of pancreatic cancer cell lines." *Pancreas* 39 (4):425-35. doi: 10.1097/MPA.0b013e3181c15963.
del Zoppo, G. J., and R. Milner. 2006. "Integrin-matrix interactions in the cerebral microvasculature." *Arterioscler Thromb Vasc Biol* 26 (9):1966-75. doi: 10.1161/01.ATV.0000232525.65682.a2.
Duxbury, M. S., H. Ito, M. J. Zinner, S. W. Ashley, and E. E. Whang. 2004. "Focal adhesion kinase gene silencing promotes anoikis and suppresses metastasis of human pancreatic adenocarcinoma cells." *Surgery* 135 (5):555-62. doi: 10.1016/j.surg.2003.10.017.
Edlund, H. 2002. "Pancreatic organogenesis--developmental mechanisms and implications for therapy." *Nat Rev Genet* 3 (7):524-32. doi: 10.1038/nrg841.

Ellis, L. M., and I. J. Fidler. 2010. "Finding the tumor copycat. Therapy fails, patients don't." *Nat Med* 16 (9):974-5. doi: 10.1038/nm0910-974.

Erkan, M., J. Kleeff, A. Gorbachevski, C. Reiser, T. Mitkus, I. Esposito, T. Giese, M. W. Buchler, N. A. Giese, and H. Friess. 2007. "Periostin creates a tumor-supportive microenvironment in the pancreas by sustaining fibrogenic stellate cell activity." *Gastroenterology* 132 (4):1447-64. doi: 10.1053/j.gastro.2007.01.031.

Erkan, M., C. W. Michalski, S. Rieder, C. Reiser-Erkan, I. Abiatari, A. Kolb, N. A. Giese, I. Esposito, H. Friess, and J. Kleeff. 2008. "The activated stroma index is a novel and independent prognostic marker in pancreatic ductal adenocarcinoma." *Clin Gastroenterol Hepatol* 6 (10):1155-61. doi: 10.1016/j.cgh.2008.05.006.

Erkan, M., C. Reiser-Erkan, C. W. Michalski, S. Deucker, D. Sauliunaite, S. Streit, I. Esposito, H. Friess, and J. Kleeff. 2009. "Cancer-stellate cell interactions perpetuate the hypoxia-fibrosis cycle in pancreatic ductal adenocarcinoma." *Neoplasia* 11 (5):497-508.

Etemad, B., and D. C. Whitcomb. 2001. "Chronic pancreatitis: diagnosis, classification, and new genetic developments." *Gastroenterology* 120 (3):682-707.

Evans, D. B., G. R. Varadhachary, C. H. Crane, C. C. Sun, J. E. Lee, P. W. Pisters, J. N. Vauthey, H. Wang, K. R. Cleary, G. A. Staerkel, C. Charnsangavej, E. A. Lano, L. Ho, R. Lenzi, J. L. Abbruzzese, and R. A. Wolff. 2008. "Preoperative gemcitabine-based chemoradiation for patients with resectable adenocarcinoma of the pancreatic head." *J Clin Oncol* 26 (21):3496-502. doi: 10.1200/JCO.2007.15.8634.

Everhart, J., and D. Wright. 1995. "Diabetes mellitus as a risk factor for pancreatic cancer. A meta-analysis." *JAMA* 273 (20):1605-9.

Frantz, C., K. M. Stewart, and V. M. Weaver. 2010. "The extracellular matrix at a glance." *J Cell Sci* 123 (Pt 24):4195-200. doi: 10.1242/jcs.023820.

Friess, H., J. Ding, J. Kleeff, L. Fenkell, J. A. Rosinski, A. Guweidhi, J. F. Reidhaar-Olson, M. Korc, J. Hammer, and M. W. Buchler. 2003. "Microarray-based identification of differentially expressed growth- and metastasis-associated genes in pancreatic cancer." *Cell Mol Life Sci* 60 (6):1180-99. doi: 10.1007/s00018-003-3036-5.

Frossard, J. L., M. L. Steer, and C. M. Pastor. 2008. "Acute pancreatitis." *Lancet* 371 (9607):143-52. doi: 10.1016/S0140-6736(08)60107-5.

Fukushima, N., Y. Kikuchi, T. Nishiyama, A. Kudo, and M. Fukayama. 2008. "Periostin deposition in the stroma of invasive and intraductal neoplasms of the pancreas." *Mod Pathol* 21 (8):1044-53. doi: 10.1038/modpathol.2008.77.

Gidekel Friedlander, S. Y., G. C. Chu, E. L. Snyder, N. Girnius, G. Dibelius, D. Crowley, E. Vasile, R. A. DePinho, and T. Jacks. 2009. "Context-dependent transformation of adult pancreatic cells by oncogenic K-Ras." *Cancer Cell* 16 (5):379-89. doi: 10.1016/j.ccr.2009.09.027.

Gillan, L., D. Matei, D. A. Fishman, C. S. Gerbin, B. Y. Karlan, and D. D. Chang. 2002. "Periostin secreted by epithelial ovarian carcinoma is a ligand for alpha(V)beta(3) and alpha(V)beta(5) integrins and promotes cell motility." *Cancer Res* 62 (18):5358-64.

Goldstein, D., R. H. El-Maraghi, P. Hammel, V. Heinemann, V. Kunzmann, J. Sastre, W. Scheithauer, S. Siena, J. Tabernero, L. Teixeira, G. Tortora, J. L. Van Laethem, R. Young, D. N. Penenberg, B. Lu, A. Romano, and D. D. Von Hoff. 2015. "nab-Paclitaxel plus gemcitabine for metastatic pancreatic cancer: long-term survival from a phase III trial." *J Natl Cancer Inst* 107 (2). doi: 10.1093/jnci/dju413.

Golubovskaya, V. M., M. Zheng, L. Zhang, J. L. Li, and W. G. Cance. 2009. "The direct effect of focal adhesion kinase (FAK), dominant-negative FAK, FAK-CD and FAK siRNA on gene expression and human MCF-7 breast cancer cell tumorigenesis." *BMC Cancer* 9:280. doi: 10.1186/1471-2407-9-280.

Guerra, C., and M. Barbacid. 2013. "Genetically engineered mouse models of pancreatic adenocarcinoma." *Mol Oncol* 7 (2):232-47. doi: 10.1016/j.molonc.2013.02.002.

Guerra, C., A. J. Schuhmacher, M. Canamero, P. J. Grippo, L. Verdaguer, L. Perez-Gallego, P. Dubus, E. P. Sandgren, and M. Barbacid. 2007. "Chronic pancreatitis is essential for induction of pancreatic ductal adenocarcinoma by K-Ras oncogenes in adult mice." *Cancer Cell* 11 (3):291-302. doi: 10.1016/j.ccr.2007.01.012.

Gukovsky, I., A. Lugea, M. Shahsahebi, J. H. Cheng, P. P. Hong, Y. J. Jung, Q. G. Deng, B. A. French, W. Lungo, S. W. French, H. Tsukamoto, and S. J. Pandol. 2008. "A rat model reproducing key pathological responses of alcoholic chronic pancreatitis." *Am J Physiol Gastrointest Liver Physiol* 294 (1):G68-79. doi: 10.1152/ajpgi.00006.2007.

Habbe, N., G. Shi, R. A. Meguid, V. Fendrich, F. Esni, H. Chen, G. Feldmann, D. A. Stoffers, S. F. Konieczny, S. D. Leach, and A. Maitra. 2008. "Spontaneous induction of murine pancreatic intraepithelial neoplasia (mPanIN) by acinar cell targeting of oncogenic Kras in adult mice." *Proc Natl Acad Sci U S A* 105 (48):18913-8. doi: 10.1073/pnas.0810097105.

Hahn, S. A., M. Schutte, A. T. Hoque, C. A. Moskaluk, L. T. da Costa, E. Rozenblum, C. L. Weinstein, A. Fischer, C. J. Yeo, R. H. Hruban, and S. E. Kern. 1996. "DPC4, a candidate tumor suppressor gene at human chromosome 18q21.1." *Science* 271 (5247):350-3.

Hassan, M. M., M. L. Bondy, R. A. Wolff, J. L. Abbruzzese, J. N. Vauthey, P. W. Pisters, D. B. Evans, R. Khan, T. H. Chou, R. Lenzi, L. Jiao, and D. Li. 2007. "Risk factors for pancreatic cancer: case-control study." *Am J Gastroenterol* 102 (12):2696-707. doi: 10.1111/j.1572-0241.2007.01510.x.

Heinemann, V., D. Quietzsch, F. Gieseler, M. Gonnermann, H. Schonekas, A. Rost, H. Neuhaus, C. Haag, M. Clemens, B. Heinrich, U. Vehling-Kaiser, M. Fuchs, D. Fleckenstein, W. Gesierich, D. Uthgenannt, H. Einsele, A. Holstege, A. Hinke, A. Schalhorn, and R. Wilkowski. 2006. "Randomized phase III trial of gemcitabine plus cisplatin compared with gemcitabine alone in advanced pancreatic cancer." *J Clin Oncol* 24 (24):3946-52. doi: 10.1200/JCO.2005.05.1490.

Hezel, A. F., A. C. Kimmelman, B. Z. Stanger, N. Bardeesy, and R. A. Depinho. 2006. "Genetics and biology of pancreatic ductal adenocarcinoma." *Genes Dev* 20 (10):1218-49. doi: 10.1101/gad.1415606.

Hingorani, S. R., E. F. Petricoin, A. Maitra, V. Rajapakse, C. King, M. A. Jacobetz, S. Ross, T. P. Conrads, T. D. Veenstra, B. A. Hitt, Y. Kawaguchi, D. Johann, L. A. Liotta, H. C. Crawford, M. E. Putt, T. Jacks, C. V. Wright, R. H. Hruban, A. M. Lowy, and D. A. Tuveson. 2003. "Preinvasive and invasive ductal pancreatic cancer and its early detection in the mouse." *Cancer Cell* 4 (6):437-50.

Hingorani, S. R., L. Wang, A. S. Multani, C. Combs, T. B. Deramaudt, R. H. Hruban, A. K. Rustgi, S. Chang, and D. A. Tuveson. 2005. "Trp53R172H and KrasG12D cooperate to promote chromosomal instability and widely metastatic pancreatic ductal adenocarcinoma in mice." *Cancer Cell* 7 (5):469-83. doi: 10.1016/j.ccr.2005.04.023.

Hochwald, S. N., C. Nyberg, M. Zheng, D. Zheng, C. Wood, N. A. Massoll, A. Magis, D. Ostrov, W. G. Cance, and V. M. Golubovskaya. 2009. "A novel small molecule inhibitor of FAK decreases growth of human pancreatic cancer." *Cell Cycle* 8 (15):2435-43.

Hong, L. Z., X. W. Wei, J. F. Chen, and Y. Shi. 2013. "Overexpression of periostin predicts poor prognosis in non-small cell lung cancer." *Oncol Lett* 6 (6):1595-1603. doi: 10.3892/ol.2013.1590.

Horiuchi, K., N. Amizuka, S. Takeshita, H. Takamatsu, M. Katsuura, H. Ozawa, Y. Toyama, L. F. Bonewald, and A. Kudo. 1999. "Identification and characterization of a novel protein, periostin, with restricted expression to periosteum and periodontal ligament

and increased expression by transforming growth factor beta." *J Bone Miner Res* 14 (7):1239-49. doi: 10.1359/jbmr.1999.14.7.1239.
Hruban, R. H., N. V. Adsay, J. Albores-Saavedra, C. Compton, E. S. Garrett, S. N. Goodman, S. E. Kern, D. S. Klimstra, G. Kloppel, D. S. Longnecker, J. Luttges, and G. J. Offerhaus. 2001. "Pancreatic intraepithelial neoplasia: a new nomenclature and classification system for pancreatic duct lesions." *Am J Surg Pathol* 25 (5):579-86.
Hruban, R. H., M. Goggins, J. Parsons, and S. E. Kern. 2000. "Progression model for pancreatic cancer." *Clin Cancer Res* 6 (8):2969-72.
Hruban, R. H., A. D. van Mansfeld, G. J. Offerhaus, D. H. van Weering, D. C. Allison, S. N. Goodman, T. W. Kensler, K. K. Bose, J. L. Cameron, and J. L. Bos. 1993. "K-ras oncogene activation in adenocarcinoma of the human pancreas. A study of 82 carcinomas using a combination of mutant-enriched polymerase chain reaction analysis and allele-specific oligonucleotide hybridization." *Am J Pathol* 143 (2):545-54.
Hruban, R. H., R. E. Wilentz, and A. Maitra. 2005. "Identification and analysis of precursors to invasive pancreatic cancer." *Methods Mol Med* 103:1-13.
Huang, Y., W. Liu, H. Xiao, A. Maitikabili, Q. Lin, T. Wu, Z. Huang, F. Liu, Q. Luo, and G. Ouyang. 2015. "Matricellular protein periostin contributes to hepatic inflammation and fibrosis." *Am J Pathol* 185 (3):786-97. doi: 10.1016/j.ajpath.2014.11.002.
Hwang, R. F., T. Moore, T. Arumugam, V. Ramachandran, K. D. Amos, A. Rivera, B. Ji, D. B. Evans, and C. D. Logsdon. 2008. "Cancer-associated stromal fibroblasts promote pancreatic tumor progression." *Cancer Res* 68 (3):918-26. doi: 10.1158/0008-5472.CAN-07-5714.
Hynes, R. O. 2009. "The extracellular matrix: not just pretty fibrils." *Science* 326 (5957):1216-9. doi: 10.1126/science.1176009.
Hyun, J. J., and H. S. Lee. 2014. "Experimental models of pancreatitis." *Clin Endosc* 47 (3):212-6. doi: 10.5946/ce.2014.47.3.212.
Jensen, J. N., E. Cameron, M. V. Garay, T. W. Starkey, R. Gianani, and J. Jensen. 2005. "Recapitulation of elements of embryonic development in adult mouse pancreatic regeneration." *Gastroenterology* 128 (3):728-41.
Jimenez, R. E., A. L. Warshaw, K. Z'Graggen, W. Hartwig, D. Z. Taylor, C. C. Compton, and C. Fernandez-del Castillo. 1999. "Sequential accumulation of K-ras mutations and p53 overexpression in the progression of pancreatic mucinous cystic neoplasms to malignancy." *Ann Surg* 230 (4):501-9; discussion 509-11.
Kanda, M., H. Matthaei, J. Wu, S. M. Hong, J. Yu, M. Borges, R. H. Hruban, A. Maitra, K. Kinzler, B. Vogelstein, and M. Goggins. 2012. "Presence of somatic mutations in most early-stage pancreatic intraepithelial neoplasia." *Gastroenterology* 142 (4):730-733 e9. doi: 10.1053/j.gastro.2011.12.042.
Kanno, A., K. Satoh, A. Masamune, M. Hirota, K. Kimura, J. Umino, S. Hamada, A. Satoh, S. Egawa, F. Motoi, M. Unno, and T. Shimosegawa. 2008. "Periostin, secreted from stromal cells, has biphasic effect on cell migration and correlates with the epithelial to mesenchymal transition of human pancreatic cancer cells." *Int J Cancer* 122 (12):2707-18. doi: 10.1002/ijc.23332.
Kii, I., T. Nishiyama, M. Li, K. Matsumoto, M. Saito, N. Amizuka, and A. Kudo. 2010. "Incorporation of tenascin-C into the extracellular matrix by periostin underlies an extracellular meshwork architecture." *J Biol Chem* 285 (3):2028-39. doi: 10.1074/jbc.M109.051961.
Kikuchi, Y., A. Kunita, C. Iwata, D. Komura, T. Nishiyama, K. Shimazu, K. Takeshita, J. Shibahara, I. Kii, Y. Morishita, M. Yashiro, K. Hirakawa, K. Miyazono, A. Kudo, M. Fukayama, and T. G. Kashima. 2014. "The niche component periostin is produced by

cancer-associated fibroblasts, supporting growth of gastric cancer through ERK activation." *Am J Pathol* 184 (3):859-70. doi: 10.1016/j.ajpath.2013.11.012.
Kim, C. J., N. Yoshioka, Y. Tambe, R. Kushima, Y. Okada, and H. Inoue. 2005. "Periostin is down-regulated in high grade human bladder cancers and suppresses in vitro cell invasiveness and in vivo metastasis of cancer cells." *Int J Cancer* 117 (1):51-8. doi: 10.1002/ijc.21120.
Klein, W. M., R. H. Hruban, A. J. Klein-Szanto, and R. E. Wilentz. 2002. "Direct correlation between proliferative activity and dysplasia in pancreatic intraepithelial neoplasia (PanIN): additional evidence for a recently proposed model of progression." *Mod Pathol* 15 (4):441-7. doi: 10.1038/modpathol.3880544.
Komiya, E., K. Ohnuma, H. Yamazaki, R. Hatano, S. Iwata, T. Okamoto, N. H. Dang, T. Yamada, and C. Morimoto. 2014. "CD26-mediated regulation of periostin expression contributes to migration and invasion of malignant pleural mesothelioma cells." *Biochem Biophys Res Commun* 447 (4):609-15. doi: 10.1016/j.bbrc.2014.04.037.
Kudo, Y., S. Iizuka, M. Yoshida, P. T. Nguyen, S. B. Siriwardena, T. Tsunematsu, M. Ohbayashi, T. Ando, D. Hatakeyama, T. Shibata, K. Koizumi, M. Maeda, N. Ishimaru, I. Ogawa, and T. Takata. 2012. "Periostin directly and indirectly promotes tumor lymphangiogenesis of head and neck cancer." *PLoS One* 7 (8):e44488. doi: 10.1371/journal.pone.0044488.
Kudo, Y., I. Ogawa, S. Kitajima, M. Kitagawa, H. Kawai, P. M. Gaffney, M. Miyauchi, and T. Takata. 2006. "Periostin promotes invasion and anchorage-independent growth in the metastatic process of head and neck cancer." *Cancer Res* 66 (14):6928-35. doi: 10.1158/0008-5472.CAN-05-4540.
Kuhlmann, K. F., S. M. de Castro, J. G. Wesseling, F. J. ten Kate, G. J. Offerhaus, O. R. Busch, T. M. van Gulik, H. Obertop, and D. J. Gouma. 2004. "Surgical treatment of pancreatic adenocarcinoma; actual survival and prognostic factors in 343 patients." *Eur J Cancer* 40 (4):549-58. doi: 10.1016/j.ejca.2003.10.026.
Lee, Y. J., I. S. Kim, S. A. Park, Y. Kim, J. E. Lee, D. Y. Noh, K. T. Kim, S. H. Ryu, and P. G. Suh. 2013. "Periostin-binding DNA aptamer inhibits breast cancer growth and metastasis." *Mol Ther* 21 (5):1004-13. doi: 10.1038/mt.2013.30.
Levy, L., and C. S. Hill. 2005. "Smad4 dependency defines two classes of transforming growth factor {beta} (TGF-{beta}) target genes and distinguishes TGF-{beta}-induced epithelial-mesenchymal transition from its antiproliferative and migratory responses." *Mol Cell Biol* 25 (18):8108-25. doi: 10.1128/MCB.25.18.8108-8125.2005.
Li, D., K. Xie, R. Wolff, and J. L. Abbruzzese. 2004. "Pancreatic cancer." *Lancet* 363 (9414):1049-57. doi: 10.1016/S0140-6736(04)15841-8.
Li, G., R. Jin, R. A. Norris, L. Zhang, S. Yu, F. Wu, R. R. Markwald, A. Nanda, S. J. Conway, S. S. Smyth, and D. N. Granger. 2010. "Periostin mediates vascular smooth muscle cell migration through the integrins alphavbeta3 and alphavbeta5 and focal adhesion kinase (FAK) pathway." *Atherosclerosis* 208 (2):358-65. doi: 10.1016/j.atherosclerosis.2009.07.046.
Li, W., P. Gao, Y. Zhi, W. Xu, Y. Wu, J. Yin, and J. Zhang. 2015. "Periostin: its role in asthma and its potential as a diagnostic or therapeutic target." *Respir Res* 16:57. doi: 10.1186/s12931-015-0218-2.
Liu, C., S. J. Huang, and Z. L. Qin. 2010. "Inhibition of periostin gene expression via RNA interference suppressed the proliferation, apoptosis and invasion in U2OS cells." *Chin Med J (Engl)* 123 (24):3677-83.
Liu, W., D. A. Bloom, W. G. Cance, E. V. Kurenova, V. M. Golubovskaya, and S. N. Hochwald. 2008. "FAK and IGF-IR interact to provide survival signals in human

pancreatic adenocarcinoma cells." *Carcinogenesis* 29 (6):1096-107. doi: 10.1093/carcin/bgn026.
Liu, Y., and B. A. Liu. 2011. "Enhanced proliferation, invasion, and epithelial-mesenchymal transition of nicotine-promoted gastric cancer by periostin." *World J Gastroenterol* 17 (21):2674-80. doi: 10.3748/wjg.v17.i21.2674.
Louvet, C., R. Labianca, P. Hammel, G. Lledo, M. G. Zampino, T. Andre, A. Zaniboni, M. Ducreux, E. Aitini, J. Taieb, R. Faroux, C. Lepere, A. de Gramont, Gercor, and Giscad. 2005. "Gemcitabine in combination with oxaliplatin compared with gemcitabine alone in locally advanced or metastatic pancreatic cancer: results of a GERCOR and GISCAD phase III trial." *J Clin Oncol* 23 (15):3509-16. doi: 10.1200/JCO.2005.06.023.
Lowenfels, A. B., P. Maisonneuve, G. Cavallini, R. W. Ammann, P. G. Lankisch, J. R. Andersen, E. P. Dimagno, A. Andren-Sandberg, and L. Domellof. 1993. "Pancreatitis and the risk of pancreatic cancer. International Pancreatitis Study Group." *N Engl J Med* 328 (20):1433-7. doi: 10.1056/NEJM199305203282001.
Lund, H., H. Tonnesen, M. H. Tonnesen, and O. Olsen. 2006. "Long-term recurrence and death rates after acute pancreatitis." *Scand J Gastroenterol* 41 (2):234-8. doi: 10.1080/00365520510024133.
Lv, H., R. Liu, J. Fu, Q. Yang, J. Shi, P. Chen, M. Ji, B. Shi, and P. Hou. 2014. "Epithelial cell-derived periostin functions as a tumor suppressor in gastric cancer through stabilizing p53 and E-cadherin proteins via the Rb/E2F1/p14ARF/Mdm2 signaling pathway." *Cell Cycle* 13 (18):2962-74. doi: 10.4161/15384101.2014.947203.
Maitra, A., N. V. Adsay, P. Argani, C. Iacobuzio-Donahue, A. De Marzo, J. L. Cameron, C. J. Yeo, and R. H. Hruban. 2003. "Multicomponent analysis of the pancreatic adenocarcinoma progression model using a pancreatic intraepithelial neoplasia tissue microarray." *Mod Pathol* 16 (9):902-12. doi: 10.1097/01.MP.0000086072.56290.FB.
Maitra, A., N. Fukushima, K. Takaori, and R. H. Hruban. 2005. "Precursors to invasive pancreatic cancer." *Adv Anat Pathol* 12 (2):81-91.
Maitra, A., and R. H. Hruban. 2008. "Pancreatic cancer." *Annu Rev Pathol* 3:157-88. doi: 10.1146/annurev.pathmechdis.3.121806.154305.
Malanchi, I., A. Santamaria-Martinez, E. Susanto, H. Peng, H. A. Lehr, J. F. Delaloye, and J. Huelsken. 2012. "Interactions between cancer stem cells and their niche govern metastatic colonization." *Nature* 481 (7379):85-9. doi: 10.1038/nature10694.
Malumbres, M., and M. Barbacid. 2003. "RAS oncogenes: the first 30 years." *Nat Rev Cancer* 3 (6):459-65. doi: 10.1038/nrc1097.
Martinelli, P., M. Canamero, N. del Pozo, F. Madriles, A. Zapata, and F. X. Real. 2013. "Gata6 is required for complete acinar differentiation and maintenance of the exocrine pancreas in adult mice." *Gut* 62 (10):1481-8. doi: 10.1136/gutjnl-2012-303328.
Maruhashi, T., I. Kii, M. Saito, and A. Kudo. 2010. "Interaction between periostin and BMP-1 promotes proteolytic activation of lysyl oxidase." *J Biol Chem* 285 (17):13294-303. doi: 10.1074/jbc.M109.088864.
Masamune, A., K. Kikuta, T. Watanabe, K. Satoh, M. Hirota, and T. Shimosegawa. 2008. "Hypoxia stimulates pancreatic stellate cells to induce fibrosis and angiogenesis in pancreatic cancer." *Am J Physiol Gastrointest Liver Physiol* 295 (4):G709-17. doi: 10.1152/ajpgi.90356.2008.
Masia, R., M. Mino-Kenudson, A. L. Warshaw, M. B. Pitman, and J. Misdraji. 2011. "Pancreatic mucinous cystic neoplasm of the main pancreatic duct." *Arch Pathol Lab Med* 135 (2):264-7. doi: 10.1043/1543-2165-135.2.264.
Masuoka, M., H. Shiraishi, S. Ohta, S. Suzuki, K. Arima, S. Aoki, S. Toda, N. Inagaki, Y. Kurihara, S. Hayashida, S. Takeuchi, K. Koike, J. Ono, H. Noshiro, M. Furue, S. J. Conway, Y. Narisawa, and K. Izuhara. 2012. "Periostin promotes chronic allergic

inflammation in response to Th2 cytokines." *J Clin Invest* 122 (7):2590-600. doi: 10.1172/JCI58978.
Matthaei, H., A. Semaan, and R. H. Hruban. 2015. "The genetic classification of pancreatic neoplasia." *J Gastroenterol*. doi: 10.1007/s00535-015-1037-4.
Mazur, P. K., H. Einwachter, M. Lee, B. Sipos, H. Nakhai, R. Rad, U. Zimber-Strobl, L. J. Strobl, F. Radtke, G. Kloppel, R. M. Schmid, and J. T. Siveke. 2010. "Notch2 is required for progression of pancreatic intraepithelial neoplasia and development of pancreatic ductal adenocarcinoma." *Proc Natl Acad Sci U S A* 107 (30):13438-43. doi: 10.1073/pnas.1002423107.
Mazur, P. K., B. M. Gruner, H. Nakhai, B. Sipos, U. Zimber-Strobl, L. J. Strobl, F. Radtke, R. M. Schmid, and J. T. Siveke. 2010. "Identification of epidermal Pdx1 expression discloses different roles of Notch1 and Notch2 in murine Kras(G12D)-induced skin carcinogenesis in vivo." *PLoS One* 5 (10):e13578. doi: 10.1371/journal.pone.0013578.
Michalski, C. W., A. Gorbachevski, M. Erkan, C. Reiser, S. Deucker, F. Bergmann, T. Giese, M. Weigand, N. A. Giese, H. Friess, and J. Kleeff. 2007. "Mononuclear cells modulate the activity of pancreatic stellate cells which in turn promote fibrosis and inflammation in chronic pancreatitis." *J Transl Med* 5:63. doi: 10.1186/1479-5876-5-63.
Michaylira, C. Z., G. S. Wong, C. G. Miller, C. M. Gutierrez, H. Nakagawa, R. Hammond, A. J. Klein-Szanto, J. S. Lee, S. B. Kim, M. Herlyn, J. A. Diehl, P. Gimotty, and A. K. Rustgi. 2010. "Periostin, a cell adhesion molecule, facilitates invasion in the tumor microenvironment and annotates a novel tumor-invasive signature in esophageal cancer." *Cancer Res* 70 (13):5281-92. doi: 10.1158/0008-5472.CAN-10-0704.
Miyamoto, Y., A. Maitra, B. Ghosh, U. Zechner, P. Argani, C. A. Iacobuzio-Donahue, V. Sriuranpong, T. Iso, I. M. Meszoely, M. S. Wolfe, R. H. Hruban, D. W. Ball, R. M. Schmid, and S. D. Leach. 2003. "Notch mediates TGF alpha-induced changes in epithelial differentiation during pancreatic tumorigenesis." *Cancer Cell* 3 (6):565-76.
Moertel, C. G. 1978. "Chemotherapy of gastrointestinal cancer." *N Engl J Med* 299 (19):1049-52. doi: 10.1056/NEJM197811092991906.
Mollenhauer, J., I. Roether, and H. F. Kern. 1987. "Distribution of extracellular matrix proteins in pancreatic ductal adenocarcinoma and its influence on tumor cell proliferation in vitro." *Pancreas* 2 (1):14-24.
Moore, M. J., D. Goldstein, J. Hamm, A. Figer, J. R. Hecht, S. Gallinger, H. J. Au, P. Murawa, D. Walde, R. A. Wolff, D. Campos, R. Lim, K. Ding, G. Clark, T. Voskoglou-Nomikos, M. Ptasynski, W. Parulekar, and Group National Cancer Institute of Canada Clinical Trials. 2007. "Erlotinib plus gemcitabine compared with gemcitabine alone in patients with advanced pancreatic cancer: a phase III trial of the National Cancer Institute of Canada Clinical Trials Group." *J Clin Oncol* 25 (15):1960-6. doi: 10.1200/JCO.2006.07.9525.
Morris, J. P. th, D. A. Cano, S. Sekine, S. C. Wang, and M. Hebrok. 2010. "Beta-catenin blocks Kras-dependent reprogramming of acini into pancreatic cancer precursor lesions in mice." *J Clin Invest* 120 (2):508-20. doi: 10.1172/JCI40045.
Moskaluk, C. A., R. H. Hruban, and S. E. Kern. 1997. "p16 and K-ras gene mutations in the intraductal precursors of human pancreatic adenocarcinoma." *Cancer Res* 57 (11):2140-3.
Mulkeen, A. L., P. S. Yoo, and C. Cha. 2006. "Less common neoplasms of the pancreas." *World J Gastroenterol* 12 (20):3180-5.
Neoptolemos, J. P., D. D. Stocken, H. Friess, C. Bassi, J. A. Dunn, H. Hickey, H. Beger, L. Fernandez-Cruz, C. Dervenis, F. Lacaine, M. Falconi, P. Pederzoli, A. Pap, D. Spooner, D. J. Kerr, M. W. Buchler, and Cancer European Study Group for

Pancreatic. 2004. "A randomized trial of chemoradiotherapy and chemotherapy after resection of pancreatic cancer." *N Engl J Med* 350 (12):1200-10. doi: 10.1056/NEJMoa032295.

Neuschwander-Tetri, B. A., K. R. Bridle, L. D. Wells, M. Marcu, and G. A. Ramm. 2000. "Repetitive acute pancreatic injury in the mouse induces procollagen alpha1(I) expression colocalized to pancreatic stellate cells." *Lab Invest* 80 (2):143-50.

Norris, R. A., B. Damon, V. Mironov, V. Kasyanov, A. Ramamurthi, R. Moreno-Rodriguez, T. Trusk, J. D. Potts, R. L. Goodwin, J. Davis, S. Hoffman, X. Wen, Y. Sugi, C. B. Kern, C. H. Mjaatvedt, D. K. Turner, T. Oka, S. J. Conway, J. D. Molkentin, G. Forgacs, and R. R. Markwald. 2007. "Periostin regulates collagen fibrillogenesis and the biomechanical properties of connective tissues." *J Cell Biochem* 101 (3):695-711. doi: 10.1002/jcb.21224.

Obata, J., M. Yano, H. Mimura, T. Goto, R. Nakayama, Y. Mibu, C. Oka, and M. Kawaichi. 2001. "p48 subunit of mouse PTF1 binds to RBP-Jkappa/CBF-1, the intracellular mediator of Notch signalling, and is expressed in the neural tube of early stage embryos." *Genes Cells* 6 (4):345-60.

Oettle, H., D. Richards, R. K. Ramanathan, J. L. van Laethem, M. Peeters, M. Fuchs, A. Zimmermann, W. John, D. Von Hoff, M. Arning, and H. L. Kindler. 2005. "A phase III trial of pemetrexed plus gemcitabine versus gemcitabine in patients with unresectable or metastatic pancreatic cancer." *Ann Oncol* 16 (10):1639-45. doi: 10.1093/annonc/mdi309.

Ohmuraya, M., M. Hirota, K. Araki, H. Baba, and K. Yamamura. 2006. "Enhanced trypsin activity in pancreatic acinar cells deficient for serine protease inhibitor kazal type 3." *Pancreas* 33 (1):104-6. doi: 10.1097/01.mpa.0000226889.86322.9b.

Olive, K. P., M. A. Jacobetz, C. J. Davidson, A. Gopinathan, D. McIntyre, D. Honess, B. Madhu, M. A. Goldgraben, M. E. Caldwell, D. Allard, K. K. Frese, G. Denicola, C. Feig, C. Combs, S. P. Winter, H. Ireland-Zecchini, S. Reichelt, W. J. Howat, A. Chang, M. Dhara, L. Wang, F. Ruckert, R. Grutzmann, C. Pilarsky, K. Izeradjene, S. R. Hingorani, P. Huang, S. E. Davies, W. Plunkett, M. Egorin, R. H. Hruban, N. Whitebread, K. McGovern, J. Adams, C. Iacobuzio-Donahue, J. Griffiths, and D. A. Tuveson. 2009. "Inhibition of Hedgehog signaling enhances delivery of chemotherapy in a mouse model of pancreatic cancer." *Science* 324 (5933):1457-61. doi: 10.1126/science.1171362.

Omary, M. B., A. Lugea, A. W. Lowe, and S. J. Pandol. 2007. "The pancreatic stellate cell: a star on the rise in pancreatic diseases." *J Clin Invest* 117 (1):50-9. doi: 10.1172/JCI30082.

Ozdemir, B. C., T. Pentcheva-Hoang, J. L. Carstens, X. Zheng, C. C. Wu, T. R. Simpson, H. Laklai, H. Sugimoto, C. Kahlert, S. V. Novitskiy, A. De Jesus-Acosta, P. Sharma, P. Heidari, U. Mahmood, L. Chin, H. L. Moses, V. M. Weaver, A. Maitra, J. P. Allison, V. S. LeBleu, and R. Kalluri. 2014. "Depletion of carcinoma-associated fibroblasts and fibrosis induces immunosuppression and accelerates pancreas cancer with reduced survival." *Cancer Cell* 25 (6):719-34. doi: 10.1016/j.ccr.2014.04.005.

Pan, F. C., and C. Wright. 2011. "Pancreas organogenesis: from bud to plexus to gland." *Dev Dyn* 240 (3):530-65. doi: 10.1002/dvdy.22584.

Pasca di Magliano, M., A. V. Biankin, P. W. Heiser, D. A. Cano, P. J. Gutierrez, T. Deramaudt, D. Segara, A. C. Dawson, J. G. Kench, S. M. Henshall, R. L. Sutherland, A. Dlugosz, A. K. Rustgi, and M. Hebrok. 2007. "Common activation of canonical Wnt signaling in pancreatic adenocarcinoma." *PLoS One* 2 (11):e1155. doi: 10.1371/journal.pone.0001155.

Pastor, C. M., M. A. Matthay, and J. L. Frossard. 2003. "Pancreatitis-associated acute lung injury: new insights." *Chest* 124 (6):2341-51.

Pietenpol, J. A., J. T. Holt, R. W. Stein, and H. L. Moses. 1990. "Transforming growth factor beta 1 suppression of c-myc gene transcription: role in inhibition of keratinocyte proliferation." *Proc Natl Acad Sci U S A* 87 (10):3758-62.

Pilarsky, C., O. Ammerpohl, B. Sipos, E. Dahl, A. Hartmann, A. Wellmann, T. Braunschweig, M. Lohr, R. Jesenofsky, H. Friess, M. N. Wente, G. Kristiansen, B. Jahnke, A. Denz, F. Ruckert, H. K. Schackert, G. Kloppel, H. Kalthoff, H. D. Saeger, and R. Grutzmann. 2008. "Activation of Wnt signalling in stroma from pancreatic cancer identified by gene expression profiling." *J Cell Mol Med* 12 (6B):2823-35. doi: 10.1111/j.1582-4934.2008.00289.x.

Polyak, K., J. Y. Kato, M. J. Solomon, C. J. Sherr, J. Massague, J. M. Roberts, and A. Koff. 1994. "p27Kip1, a cyclin-Cdk inhibitor, links transforming growth factor-beta and contact inhibition to cell cycle arrest." *Genes Dev* 8 (1):9-22.

Poplin, E., Y. Feng, J. Berlin, M. L. Rothenberg, H. Hochster, E. Mitchell, S. Alberts, P. O'Dwyer, D. Haller, P. Catalano, D. Cella, and A. B. Benson, 3rd. 2009. "Phase III, randomized study of gemcitabine and oxaliplatin versus gemcitabine (fixed-dose rate infusion) compared with gemcitabine (30-minute infusion) in patients with pancreatic carcinoma E6201: a trial of the Eastern Cooperative Oncology Group." *J Clin Oncol* 27 (23):3778-85. doi: 10.1200/JCO.2008.20.9007.

Raimondi, S., A. B. Lowenfels, A. M. Morselli-Labate, P. Maisonneuve, and R. Pezzilli. 2010. "Pancreatic cancer in chronic pancreatitis; aetiology, incidence, and early detection." *Best Pract Res Clin Gastroenterol* 24 (3):349-58. doi: 10.1016/j.bpg.2010.02.007.

Redston, M. S., C. Caldas, A. B. Seymour, R. H. Hruban, L. da Costa, C. J. Yeo, and S. E. Kern. 1994. "p53 mutations in pancreatic carcinoma and evidence of common involvement of homocopolymer tracts in DNA microdeletions." *Cancer Res* 54 (11):3025-33.

Rhim, A. D., E. T. Mirek, N. M. Aiello, A. Maitra, J. M. Bailey, F. McAllister, M. Reichert, G. L. Beatty, A. K. Rustgi, R. H. Vonderheide, S. D. Leach, and B. Z. Stanger. 2012. "EMT and dissemination precede pancreatic tumor formation." *Cell* 148 (1-2):349-61. doi: 10.1016/j.cell.2011.11.025.

Rhim, A. D., P. E. Oberstein, D. H. Thomas, E. T. Mirek, C. F. Palermo, S. A. Sastra, E. N. Dekleva, T. Saunders, C. P. Becerra, I. W. Tattersall, C. B. Westphalen, J. Kitajewski, M. G. Fernandez-Barrena, M. E. Fernandez-Zapico, C. Iacobuzio-Donahue, K. P. Olive, and B. Z. Stanger. 2014. "Stromal elements act to restrain, rather than support, pancreatic ductal adenocarcinoma." *Cancer Cell* 25 (6):735-47. doi: 10.1016/j.ccr.2014.04.021.

Rhim, A. D., and B. Z. Stanger. 2010. "Molecular biology of pancreatic ductal adenocarcinoma progression: aberrant activation of developmental pathways." *Prog Mol Biol Transl Sci* 97:41-78. doi: 10.1016/B978-0-12-385233-5.00002-7.

Roberts, W. G., E. Ung, P. Whalen, B. Cooper, C. Hulford, C. Autry, D. Richter, E. Emerson, J. Lin, J. Kath, K. Coleman, L. Yao, L. Martinez-Alsina, M. Lorenzen, M. Berliner, M. Luzzio, N. Patel, E. Schmitt, S. LaGreca, J. Jani, M. Wessel, E. Marr, M. Griffor, and F. Vajdos. 2008. "Antitumor activity and pharmacology of a selective focal adhesion kinase inhibitor, PF-562,271." *Cancer Res* 68 (6):1935-44. doi: 10.1158/0008-5472.CAN-07-5155.

Romeo, F., L. Falbo, M. Di Sanzo, R. Misaggi, M. C. Faniello, T. Barni, G. Cuda, G. Viglietto, C. Santoro, B. Quaresima, and F. Costanzo. 2011. "Negative transcriptional regulation of the human periostin gene by YingYang-1 transcription factor." *Gene* 487 (2):129-34. doi: 10.1016/j.gene.2011.07.025.

Rozenblum, E., M. Schutte, M. Goggins, S. A. Hahn, S. Panzer, M. Zahurak, S. N. Goodman, T. A. Sohn, R. H. Hruban, C. J. Yeo, and S. E. Kern. 1997. "Tumor-suppressive pathways in pancreatic carcinoma." *Cancer Res* 57 (9):1731-4.

Sauer, B., and N. Henderson. 1988. "Site-specific DNA recombination in mammalian cells by the Cre recombinase of bacteriophage P1." *Proc Natl Acad Sci U S A* 85 (14):5166-70.

Schmidt, T. T., M. Tauseef, L. Yue, M. G. Bonini, J. Gothert, T. L. Shen, J. L. Guan, S. Predescu, R. Sadikot, and D. Mehta. 2013. "Conditional deletion of FAK in mice endothelium disrupts lung vascular barrier function due to destabilization of RhoA and Rac1 activities." *Am J Physiol Lung Cell Mol Physiol* 305 (4):L291-300. doi: 10.1152/ajplung.00094.2013.

Schramm, A., I. Opitz, S. Thies, B. Seifert, H. Moch, W. Weder, and A. Soltermann. 2010. "Prognostic significance of epithelial-mesenchymal transition in malignant pleural mesothelioma." *Eur J Cardiothorac Surg* 37 (3):566-72. doi: 10.1016/j.ejcts.2009.08.027.

Schultze, A., S. Decker, J. Otten, A. K. Horst, G. Vohwinkel, G. Schuch, C. Bokemeyer, S. Loges, and W. Fiedler. 2010. "TAE226-mediated inhibition of focal adhesion kinase interferes with tumor angiogenesis and vasculogenesis." *Invest New Drugs* 28 (6):825-33. doi: 10.1007/s10637-009-9326-5.

Schutte, M., R. H. Hruban, J. Geradts, R. Maynard, W. Hilgers, S. K. Rabindran, C. A. Moskaluk, S. A. Hahn, I. Schwarte-Waldhoff, W. Schmiegel, S. B. Baylin, S. E. Kern, and J. G. Herman. 1997. "Abrogation of the Rb/p16 tumor-suppressive pathway in virtually all pancreatic carcinomas." *Cancer Res* 57 (15):3126-30.

Shao, R., S. Bao, X. Bai, C. Blanchette, R. M. Anderson, T. Dang, M. L. Gishizky, J. R. Marks, and X. F. Wang. 2004. "Acquired expression of periostin by human breast cancers promotes tumor angiogenesis through up-regulation of vascular endothelial growth factor receptor 2 expression." *Mol Cell Biol* 24 (9):3992-4003.

Sherman, M. H., R. T. Yu, D. D. Engle, N. Ding, A. R. Atkins, H. Tiriac, E. A. Collisson, F. Connor, T. Van Dyke, S. Kozlov, P. Martin, T. W. Tseng, D. W. Dawson, T. R. Donahue, A. Masamune, T. Shimosegawa, M. V. Apte, J. S. Wilson, B. Ng, S. L. Lau, J. E. Gunton, G. M. Wahl, T. Hunter, J. A. Drebin, P. J. O'Dwyer, C. Liddle, D. A. Tuveson, M. Downes, and R. M. Evans. 2014. "Vitamin D receptor-mediated stromal reprogramming suppresses pancreatitis and enhances pancreatic cancer therapy." *Cell* 159 (1):80-93. doi: 10.1016/j.cell.2014.08.007.

Shi, C., R. H. Hruban, and A. P. Klein. 2009. "Familial pancreatic cancer." *Arch Pathol Lab Med* 133 (3):365-74. doi: 10.1043/1543-2165-133.3.365.

Shih, H. P., A. Wang, and M. Sander. 2013. "Pancreas organogenesis: from lineage determination to morphogenesis." *Annu Rev Cell Dev Biol* 29:81-105. doi: 10.1146/annurev-cellbio-101512-122405.

Shikata, K., T. Ninomiya, and Y. Kiyohara. 2013. "Diabetes mellitus and cancer risk: review of the epidemiological evidence." *Cancer Sci* 104 (1):9-14. doi: 10.1111/cas.12043.

Shimazaki, M., K. Nakamura, I. Kii, T. Kashima, N. Amizuka, M. Li, M. Saito, K. Fukuda, T. Nishiyama, S. Kitajima, Y. Saga, M. Fukayama, M. Sata, and A. Kudo. 2008. "Periostin is essential for cardiac healing after acute myocardial infarction." *J Exp Med* 205 (2):295-303. doi: 10.1084/jem.20071297.

Siegel, R. L., K. D. Miller, and A. Jemal. 2015. "Cancer statistics, 2015." *CA Cancer J Clin* 65 (1):5-29. doi: 10.3322/caac.21254.

Siriwardena, B. S., Y. Kudo, I. Ogawa, M. Kitagawa, S. Kitajima, H. Hatano, W. M. Tilakaratne, M. Miyauchi, and T. Takata. 2006. "Periostin is frequently overexpressed and enhances invasion and angiogenesis in oral cancer." *Br J Cancer* 95 (10):1396-403. doi: 10.1038/sj.bjc.6603431.

Smid, J. K., S. Faulkes, and M. A. Rudnicki. 2015. "Periostin induces pancreatic regeneration." *Endocrinology* 156 (3):824-36. doi: 10.1210/en.2014-1637.
Snouwaert, J. N., K. K. Brigman, A. M. Latour, N. N. Malouf, R. C. Boucher, O. Smithies, and B. H. Koller. 1992. "An animal model for cystic fibrosis made by gene targeting." *Science* 257 (5073):1083-8.
Sohn, T. A., C. J. Yeo, J. L. Cameron, R. H. Hruban, N. Fukushima, K. A. Campbell, and K. D. Lillemoe. 2004. "Intraductal papillary mucinous neoplasms of the pancreas: an updated experience." *Ann Surg* 239 (6):788-97; discussion 797-9.
Soltermann, A., V. Tischler, S. Arbogast, J. Braun, N. Probst-Hensch, W. Weder, H. Moch, and G. Kristiansen. 2008. "Prognostic significance of epithelial-mesenchymal and mesenchymal-epithelial transition protein expression in non-small cell lung cancer." *Clin Cancer Res* 14 (22):7430-7. doi: 10.1158/1078-0432.CCR-08-0935.
Sriram, R., V. Lo, B. Pryce, L. Antonova, A. J. Mears, M. Daneshmand, B. McKay, S. J. Conway, W. J. Muller, and L. A. Sabourin. 2015. "Loss of periostin/OSF-2 in ErbB2/Neu-driven tumors results in androgen receptor-positive molecular apocrine-like tumors with reduced Notch1 activity." *Breast Cancer Res* 17:7. doi: 10.1186/s13058-014-0513-8.
Stanger, B. Z., B. Stiles, G. Y. Lauwers, N. Bardeesy, M. Mendoza, Y. Wang, A. Greenwood, K. H. Cheng, M. McLaughlin, D. Brown, R. A. Depinho, H. Wu, D. A. Melton, and Y. Dor. 2005. "Pten constrains centroacinar cell expansion and malignant transformation in the pancreas." *Cancer Cell* 8 (3):185-95. doi: 10.1016/j.ccr.2005.07.015.
Stathopoulos, G. P., K. Syrigos, G. Aravantinos, A. Polyzos, P. Papakotoulas, G. Fountzilas, A. Potamianou, N. Ziras, J. Boukovinas, J. Varthalitis, N. Androulakis, A. Kotsakis, G. Samonis, and V. Georgoulias. 2006. "A multicenter phase III trial comparing irinotecan-gemcitabine (IG) with gemcitabine (G) monotherapy as first-line treatment in patients with locally advanced or metastatic pancreatic cancer." *Br J Cancer* 95 (5):587-92. doi: 10.1038/sj.bjc.6603301.
Stokes, J. B., S. J. Adair, J. K. Slack-Davis, D. M. Walters, R. W. Tilghman, E. D. Hershey, B. Lowrey, K. S. Thomas, A. H. Bouton, R. F. Hwang, E. B. Stelow, J. T. Parsons, and T. W. Bauer. 2011. "Inhibition of focal adhesion kinase by PF-562,271 inhibits the growth and metastasis of pancreatic cancer concomitant with altering the tumor microenvironment." *Mol Cancer Ther* 10 (11):2135-45. doi: 10.1158/1535-7163.MCT-11-0261.
Swift, G. H., Y. Liu, S. D. Rose, L. J. Bischof, S. Steelman, A. M. Buchberg, C. V. Wright, and R. J. MacDonald. 1998. "An endocrine-exocrine switch in the activity of the pancreatic homeodomain protein PDX1 through formation of a trimeric complex with PBX1b and MRG1 (MEIS2)." *Mol Cell Biol* 18 (9):5109-20.
Tai, I. T., M. Dai, and L. B. Chen. 2005. "Periostin induction in tumor cell line explants and inhibition of in vitro cell growth by anti-periostin antibodies." *Carcinogenesis* 26 (5):908-15. doi: 10.1093/carcin/bgi034.
Takeshita, S., R. Kikuno, K. Tezuka, and E. Amann. 1993. "Osteoblast-specific factor 2: cloning of a putative bone adhesion protein with homology with the insect protein fasciclin I." *Biochem J* 294 (Pt 1):271-8.
Tanabe, H., I. Takayama, T. Nishiyama, M. Shimazaki, I. Kii, M. Li, N. Amizuka, K. Katsube, and A. Kudo. 2010. "Periostin associates with Notch1 precursor to maintain Notch1 expression under a stress condition in mouse cells." *PLoS One* 5 (8):e12234. doi: 10.1371/journal.pone.0012234.
Taniguchi, K., K. Arima, M. Masuoka, S. Ohta, H. Shiraishi, K. Ontsuka, S. Suzuki, M. Inamitsu, K. Yamamoto, O. Simmons, S. Toda, S. J. Conway, Y. Hamasaki, and K. Izuhara. 2014. "Periostin controls keratinocyte proliferation and differentiation by

interacting with the paracrine IL-1alpha/IL-6 loop." *J Invest Dermatol* 134 (5):1295-304. doi: 10.1038/jid.2013.500.

Tentler, J. J., A. C. Tan, C. D. Weekes, A. Jimeno, S. Leong, T. M. Pitts, J. J. Arcaroli, W. A. Messersmith, and S. G. Eckhardt. 2012. "Patient-derived tumour xenografts as models for oncology drug development." *Nat Rev Clin Oncol* 9 (6):338-50. doi: 10.1038/nrclinonc.2012.61.

Tian, H., C. A. Callahan, K. J. DuPree, W. C. Darbonne, C. P. Ahn, S. J. Scales, and F. J. de Sauvage. 2009. "Hedgehog signaling is restricted to the stromal compartment during pancreatic carcinogenesis." *Proc Natl Acad Sci U S A* 106 (11):4254-9. doi: 10.1073/pnas.0813203106.

Tian, Y., C. H. Choi, Q. K. Li, F. B. Rahmatpanah, X. Chen, S. R. Kim, R. Veltri, D. Chia, Z. Zhang, D. Mercola, and H. Zhang. 2015. "Overexpression of periostin in stroma positively associated with aggressive prostate cancer." *PLoS One* 10 (3):e0121502. doi: 10.1371/journal.pone.0121502.

Torre, L. A., F. Bray, R. L. Siegel, J. Ferlay, J. Lortet-Tieulent, and A. Jemal. 2015. "Global cancer statistics, 2012." *CA Cancer J Clin* 65 (2):87-108. doi: 10.3322/caac.21262.

Tseng, W. W., D. Winer, J. A. Kenkel, O. Choi, A. H. Shain, J. R. Pollack, R. French, A. M. Lowy, and E. G. Engleman. 2010. "Development of an orthotopic model of invasive pancreatic cancer in an immunocompetent murine host." *Clin Cancer Res* 16 (14):3684-95. doi: 10.1158/1078-0432.CCR-09-2384.

Ueki, T., M. Toyota, T. Sohn, C. J. Yeo, J. P. Issa, R. H. Hruban, and M. Goggins. 2000. "Hypermethylation of multiple genes in pancreatic adenocarcinoma." *Cancer Res* 60 (7):1835-9.

Von Hoff, D. D., R. K. Ramanathan, M. J. Borad, D. A. Laheru, L. S. Smith, T. E. Wood, R. L. Korn, N. Desai, V. Trieu, J. L. Iglesias, H. Zhang, P. Soon-Shiong, T. Shi, N. V. Rajeshkumar, A. Maitra, and M. Hidalgo. 2011. "Gemcitabine plus nab-paclitaxel is an active regimen in patients with advanced pancreatic cancer: a phase I/II trial." *J Clin Oncol* 29 (34):4548-54. doi: 10.1200/JCO.2011.36.5742.

Vonlaufen, A., S. Joshi, C. Qu, P. A. Phillips, Z. Xu, N. R. Parker, C. S. Toi, R. C. Pirola, J. S. Wilson, D. Goldstein, and M. V. Apte. 2008. "Pancreatic stellate cells: partners in crime with pancreatic cancer cells." *Cancer Res* 68 (7):2085-93. doi: 10.1158/0008-5472.CAN-07-2477.

Walsh, C., I. Tanjoni, S. Uryu, A. Tomar, J. O. Nam, H. Luo, A. Phillips, N. Patel, C. Kwok, G. McMahon, D. G. Stupack, and D. D. Schlaepfer. 2010. "Oral delivery of PND-1186 FAK inhibitor decreases tumor growth and spontaneous breast to lung metastasis in pre-clinical models." *Cancer Biol Ther* 9 (10):778-90.

Wang, G. J., C. F. Gao, D. Wei, C. Wang, and S. Q. Ding. 2009. "Acute pancreatitis: etiology and common pathogenesis." *World J Gastroenterol* 15 (12):1427-30.

Watanabe, S., K. Abe, Y. Anbo, and H. Katoh. 1995. "Changes in the mouse exocrine pancreas after pancreatic duct ligation: a qualitative and quantitative histological study." *Arch Histol Cytol* 58 (3):365-74.

Watari, N., Y. Hotta, and Y. Mabuchi. 1982. "Morphological studies on a vitamin A-storing cell and its complex with macrophage observed in mouse pancreatic tissues following excess vitamin A administration." *Okajimas Folia Anat Jpn* 58 (4-6):837-58.

Wendt, M. K., and W. P. Schiemann. 2009. "Therapeutic targeting of the focal adhesion complex prevents oncogenic TGF-beta signaling and metastasis." *Breast Cancer Res* 11 (5):R68. doi: 10.1186/bcr2360.

Westmoreland, J. J., G. Kilic, C. Sartain, S. Sirma, J. Blain, J. Rehg, N. Harvey, and B. Sosa-Pineda. 2012. "Pancreas-specific deletion of Prox1 affects development and disrupts homeostasis of the exocrine pancreas." *Gastroenterology* 142 (4):999-1009 e6. doi: 10.1053/j.gastro.2011.12.007.

Wilde, J., M. Yokozeki, K. Terai, A. Kudo, and K. Moriyama. 2003. "The divergent expression of periostin mRNA in the periodontal ligament during experimental tooth movement." *Cell Tissue Res* 312 (3):345-51. doi: 10.1007/s00441-002-0664-2.

Wilentz, R. E., J. Geradts, R. Maynard, G. J. Offerhaus, M. Kang, M. Goggins, C. J. Yeo, S. E. Kern, and R. H. Hruban. 1998. "Inactivation of the p16 (INK4A) tumor-suppressor gene in pancreatic duct lesions: loss of intranuclear expression." *Cancer Res* 58 (20):4740-4.

Wilentz, R. E., C. A. Iacobuzio-Donahue, P. Argani, D. M. McCarthy, J. L. Parsons, C. J. Yeo, S. E. Kern, and R. H. Hruban. 2000. "Loss of expression of Dpc4 in pancreatic intraepithelial neoplasia: evidence that DPC4 inactivation occurs late in neoplastic progression." *Cancer Res* 60 (7):2002-6.

Wilentz, R. E., G. H. Su, J. L. Dai, A. B. Sparks, P. Argani, T. A. Sohn, C. J. Yeo, S. E. Kern, and R. H. Hruban. 2000. "Immunohistochemical labeling for dpc4 mirrors genetic status in pancreatic adenocarcinomas : a new marker of DPC4 inactivation." *Am J Pathol* 156 (1):37-43. doi: 10.1016/S0002-9440(10)64703-7.

Witt, H., M. V. Apte, V. Keim, and J. S. Wilson. 2007. "Chronic pancreatitis: challenges and advances in pathogenesis, genetics, diagnosis, and therapy." *Gastroenterology* 132 (4):1557-73. doi: 10.1053/j.gastro.2007.03.001.

Wu, J., H. Matthaei, A. Maitra, M. Dal Molin, L. D. Wood, J. R. Eshleman, M. Goggins, M. I. Canto, R. D. Schulick, B. H. Edil, C. L. Wolfgang, A. P. Klein, L. A. Diaz, Jr., P. J. Allen, C. M. Schmidt, K. W. Kinzler, N. Papadopoulos, R. H. Hruban, and B. Vogelstein. 2011. "Recurrent GNAS mutations define an unexpected pathway for pancreatic cyst development." *Sci Transl Med* 3 (92):92ra66. doi: 10.1126/scitranslmed.3002543.

Wu, M. H., E. Ustinova, and H. J. Granger. 2001. "Integrin binding to fibronectin and vitronectin maintains the barrier function of isolated porcine coronary venules." *J Physiol* 532 (Pt 3):785-91.

Yamano, M., H. Fujii, T. Takagaki, N. Kadowaki, H. Watanabe, and T. Shirai. 2000. "Genetic progression and divergence in pancreatic carcinoma." *Am J Pathol* 156 (6):2123-33. doi: 10.1016/S0002-9440(10)65083-3.

Yamashita, O., K. Yoshimura, A. Nagasawa, K. Ueda, N. Morikage, Y. Ikeda, and K. Hamano. 2013. "Periostin links mechanical strain to inflammation in abdominal aortic aneurysm." *PLoS One* 8 (11):e79753. doi: 10.1371/journal.pone.0079753.

Zeng, G., M. Germinaro, A. Micsenyi, N. K. Monga, A. Bell, A. Sood, V. Malhotra, N. Sood, V. Midda, D. K. Monga, D. M. Kokkinakis, and S. P. Monga. 2006. "Aberrant Wnt/beta-catenin signaling in pancreatic adenocarcinoma." *Neoplasia* 8 (4):279-89. doi: 10.1593/neo.05607.

Zhang, H., P. Neuhofer, L. Song, B. Rabe, M. Lesina, M. U. Kurkowski, M. Treiber, T. Wartmann, S. Regner, H. Thorlacius, D. Saur, G. Weirich, A. Yoshimura, W. Halangk, J. P. Mizgerd, R. M. Schmid, S. Rose-John, and H. Algul. 2013. "IL-6 trans-signaling promotes pancreatitis-associated lung injury and lethality." *J Clin Invest* 123 (3):1019-31. doi: 10.1172/JCI64931.

Zhang, Y., G. Zhang, J. Li, Q. Tao, and W. Tang. 2010. "The expression analysis of periostin in human breast cancer." *J Surg Res* 160 (1):102-6. doi: 10.1016/j.jss.2008.12.042.

Zhang, Z., F. Nie, X. Chen, Z. Qin, C. Kang, B. Chen, J. Ma, B. Pan, and Y. Ma. 2015. "Upregulated periostin promotes angiogenesis in keloids through activation of the ERK 1/2 and focal adhesion kinase pathways, as well as the upregulated expression of VEGF and angiopoietin1." *Mol Med Rep* 11 (2):857-64. doi: 10.3892/mmr.2014.2827.

Zhu, L., G. Shi, C. M. Schmidt, R. H. Hruban, and S. F. Konieczny. 2007. "Acinar cells contribute to the molecular heterogeneity of pancreatic intraepithelial neoplasia." *Am J Pathol* 171 (1):263-73. doi: 10.2353/ajpath.2007.061176.

Zhu, M., M. S. Fejzo, L. Anderson, J. Dering, C. Ginther, L. Ramos, J. C. Gasson, B. Y. Karlan, and D. J. Slamon. 2010. "Periostin promotes ovarian cancer angiogenesis and metastasis." *Gynecol Oncol* 119 (2):337-44. doi: 10.1016/j.ygyno.2010.07.008.

Zhu, M., R. E. Saxton, L. Ramos, D. D. Chang, B. Y. Karlan, J. C. Gasson, and D. J. Slamon. 2011. "Neutralizing monoclonal antibody to periostin inhibits ovarian tumor growth and metastasis." *Mol Cancer Ther* 10 (8):1500-8. doi: 10.1158/1535-7163.MCT-11-0046.

7 Appendix

7.1 List of tables

7.2 List of figures

8 Acknowledgments

First of all I would like to express my gratitude to **PD Dr. med. Mert Erkan** for enabling me to do this study in his research group and for the opportunity to work on this interesting topic of the thesis. Furthermore, I want to thank him for his supervision and supporting my attendance at various conferences.

Prof. Dr. Jörg Kleeff for his support and constructive ideas over the past few years, which contributed to the successful completion of this work. Additionally, I want to thank him for taking over the function as first adviser and being part of my Thesis Committee.

A sincere note of thanks goes to **Prof. Dr. Bernhard Küster** for being my second adviser and his helpful comments in the thesis committee meetings.

Dr. rer. biol. hum. Ivonne Regel for being my mentor and friend. I am very thankful for your support, your input and never exhausting will to discuss the results of this project as well as for proof-reading the thesis.

I especially want to thank **Tao Cheng** for performing the orthotopic injections of tumor cells and **Katja Steiger** for helping with the histological analysis of tissue sections.

I want to thank all the people in the lab, past and present, for your support, advice and all the fun we had in and outside the lab: **Dr. rer. nat. Susanne Raulefs**, **Dr. Christoph Michalski**, **Dr. Bo Kong**, **Carsten Jäger, Simone**, **Philipp**, **Nadja**, **Isabell**, **Irina**, **Manja**, **Ziying Jian**, **Miao Lu**, **Lei Liu**, **Chengjia Qian**, **Tamuna, Temesgen** and **Anna**. I would particularly like to thank **Daniela**, **Nadine** and **Kathi**. With you guys, there was always a good atmosphere in the lab and I certainly will miss the chats in between incubation times.

I want to express great gratitude to all my friends for their encouragement, untiring support and love especially throughout the last few years.

In particular I want to thank **Pawel** for always being there for me. Thanks for motivating and cheering me up in times of frustration. Your dedication and enthusiasm for science is contagious. Thanks for inspiring me and especially for being part of my life.

Finally, I want to thank my family, especially my **mom and dad**, my brother **Oliver** and my **grandma** for your immense moral support, never-ending love and always believing in me. Thanks for your continuous encouragement through many ups and downs in the last four and a half years.